The Pennsylvania State University

The Graduate School

Department of Kinesiology

LINKING FOOT AND ANKLE MUSCULOSKELETAL STRUCTURE TO LOCOMOTOR FUNCTION

A Dissertation in

Kinesiology

by

Josh R. Baxter

Submitted in Partial Fulfillment
of the Requirements
for the Degree of

Doctor of Philosophy

December 2012

The Dissertation of Josh R. Baxter was reviewed and approved* by the following:

Stephen J. Piazza
Associate Prefessor of Kinesiology, Mechanical & Nuclear Engineering, and Orthopaedics & Rehabilitation
Dissertation Advisor
Chair of Committee

Jinger S. Gottschall
Assistant Professor of Kinesiology

H. Joseph Sommer III
Professor of Mechanical Engineering

Vladimir Zatsiorsky
Professor of Kinesiology

David E Conroy
Professor of Kinesiology and Human Development & Family Studies
Graduate Program Director

*Signatures are on file in the Graduate School

ABSTRACT

Recent studies have linked plantarflexion moment arm (pfMA) with locomotor function in athletes and elderly adults. Simple biomechanical and computer models suggest that shorter pfMA facilitates energy storage in the Achilles tendon and force generation by the plantarflexors, but no experimental data have been published in support of these modeling results. Though previous investigators found that sprinters possess significantly shorter pfMA than non-sprinters, they did not identify a mechanism responsible for this difference. If sprinters have uniquely shaped joints that provide them with a competitive advantage, this may provide insight to helping individuals with movement disorders. The purpose of this dissertation was to investigate potential mechanisms that link pfMA and locomotor performance.

The first study was designed to identify if ankle joint kinematics differ between sprinters and non-sprinters, and if so, how talocrural geometry affects joint kinematics. Magnetic resonance (MR) images of the foot and ankle in sprinters and non-sprinters were acquired. We found that sprinters have longer forefoot bones and shorter pfMA than non-sprinters. Unlike previous studies that used indirect measurements to link pfMA with function, we identified that the center of rotation (CoR) of the talocrural joint was more posterior in sprinters. These findings are the first to document a difference in ankle joint kinematics in functionally different, but otherwise healthy, adults.

The second study analyzed the three-dimensional geometry of the talocrural joints in sprinters and non-sprinters to determine if CoR differences could be explained by joint structure. We found that sprinters have a less conforming talocrural joint than non-sprinters, which may facilitate muscle force for the task at hand.

The third study investigated the relationship between pfMA and ankle strength in untrained healthy young men. We found that pfMA is positively correlated with ankle strength at all rates of plantarflexion (R^2 = 0.323 – 0.494). Although these findings do not agree with computer simulations that show short pfMA as protective against torque loss at fast speeds, it is possible that musculoskeletal structure in untrained young men is adapted for submaximal activities and not maximal force generation. To our knowledge, this is the first study to link muscle moment arm and joint strength.

The fourth study directly compared several methods for measuring pfMA *in vivo* that have been reported in the literature but have not yet been validated. These measurement techniques can be categorized into two subtypes: geometric methods, which use MR imaging or external measurements; and tendon excursion (TE) methods, which use an ultrasound probe to track the Achilles tendon as it slides during joint rotation. These methods were compared to a highly reliable and commonly used pfMA measurement technique. We found that geometric measures of pfMA have better agreement with the CoR method.

In conclusion, this dissertation is the first study to link pfMA and ankle strength. Previous reports found relationships between pfMA and locomotor performance but were unable to identify a mechanism responsible for differences in function. We also found that shorter pfMA in sprinters are explained by differences in ankle CoR. Three-dimensional analysis of the talocrural joint suggests that a more mobile ankle joint in sprinters may place the foot in a more advantageous position to generate force. While the findings of this dissertation fills some gaps in the literature, they raise further questions about how the musculoskeletal system adapts to geometric constraints and functional demands placed on the system.

TABLE OF CONTENTS

LIST OF FIGURES

LIST OF TABLES

ACKNOWLEDGEMENTS

Throughout my time at Penn State, many people have influenced me, and for that I am sincerely grateful.

This dissertation would not have been possible without the guidance from my advisor, Steve Piazza. I have learned so much from you and will be sad to leave. I would like to thank my committee members, Drs. Gottschall, Sommer, and Zatsiorsky. I would also like to thank all the faculty and staff in the Kinesiology department. This program is great because of you.

I would like to thank my friends and lab mates making me look forward to coming into the lab. I have received unconditional support from my parents, Ken and Jody, and brother, Sean.

Most of all, I would like to thank my wife, Julie, for her love and support.

Chapter 1

Introduction

1.1 Background

Variations in plantarflexor moment arm (pfMA) have been linked to locomotor performance in trained athletes and the elderly. The metabolic cost of running has been correlated with pfMA in distance runners (Scholz et al., 2008; Raichlen et al., 2011), and trained sprinters appear to have shorter pfMA than non-sprinters (Lee and Piazza, 2009). Walking speed in mobility-limited elderly adults is positively correlated with pfMA (Lee and Piazza, 2012). Though these studies document functional differences that are associated with variation in pfMA, the mechanisms responsible for such disparities in pfMA and function have not yet been identified.

The world's fastest running animals, such as the cheetah and greyhound, have relatively long forefeet and short pfMA compared to animals that are primarily adapted for walking and digging (Hildebrand, 1960; Williams et al., 2008). This high 'gear ratio' (ground reaction force moment arm divided by muscle moment arm) allows muscle to contract less quickly during fast joint rotations and is thought to facilitate muscle force (Carrier et al., 1994). The frog musculoskeletal structure appears to be highly adapted for incredible power production during jumping (Lutz and Rome, 1994). Isometric knee strength in frogs is not correlated with muscle moment arm, but instead is mostly explained by peak muscle tension (Lieber and Boakes, 1988). The high joint powers observed in jumping frogs may be explained by a variable gear ratio that allows

for optimal elastic energy storage and release. Running greyhounds also demonstrate a variable gearing mechanism in their hindlimbs during acceleration, which is thought to increase stance time and ground impulses (Williams et al., 2009b).

Computer simulations suggest that ankle work and power are enhanced by variations in musculoskeletal structure. Nagano and Komura (2003, 2007) demonstrated that force-velocity effects of muscle are mitigated by small pfMA and long muscle fibers during fast rates of ankle rotation. These simulations show that the force-velocity effects of shortening muscle have a stronger effect on joint torque that does moment arm. Lee and Piazza (2009) found that computer models with foot proportions that were observed in sprinters increases the amount of time the foot is in contact with the ground and reduces muscle shortening demands, which increases the amount of impulse applied to the ground. Reduced pfMA may also increase elastic energy storage and return by the Achilles tendon during running (Scholz et al., 2008). Although these models demonstrate possible effects of pfMA on ankle strength and running efficiency, experimental data have not validated such models.

Although several studies have found links between pfMA and locomotor function, measurement techniques differ between studies, making it difficult to compare results. Lee and Piazza (2009, 2012) measured the amount of Achilles tendon excursion (TE) during maximal isokinetic contractions. Calcaneal tuberosity length and external measurements of the malleoli were used to estimate pfMA in distance runners (Scholz et al., 2008; Raichlen et al., 2011). While there

is currently no ‘gold standard’ for measuring pfMA, using a modified Reuleaux method to approximate the ankle joint center of rotation (CoR) and measuring the distance to the Achilles line of action has been found to be highly reliable and compares well with cadaveric measurements of pfMA (Rugg et al., 1990; Spoor et al., 1990; Maganaris et al., 1998; Fath et al., 2010; McCullough et al., 2011).

This dissertation will investigate the relationship between pfMA and ankle function, how joint structure might affect leverage, and directly compare previously reported pfMA measurement techniques with values obtained using the CoR method. These studies are important to identify mechanisms that may improve locomotor performance in special populations. To investigate the link between pfMA and locomotor function, we will study the musculoskeletal structure of trained sprinters, and while our focus is not to improve sprint performance, the study of such individuals may provide special insight into how foot and ankle structure affects joint mechanics. These findings may provide insight into populations of clinical significance like elderly adults and individuals with movement disorders. Furthermore, the investigation of pfMA and ankle strength in healthy young men may highlight differences in musculoskeletal adaptations that are specific to functional demands.

1.2 Specific Aims and Hypotheses

Aim 1. To investigate the ankle and foot structure of both trained-sprinters and non-sprinters using magnetic resonance (MR) imaging.

Rationale: Previous research has identified the plantarflexors to be of particular importance in sprint performance (Johnson and Buckley, 2001;

Bezodis et al., 2008), and musculoskeletal adaptations suggest that sprinters are well suited for power generation during a race (Mero et al., 1981; Abe et al., 2000, 2001; Kumagai et al., 2000; Lee and Piazza, 2009). Lee and Piazza (2009) found that sprinters have longer toes and pfMA that are approximately 25% shorter than non-sprinters. However, these measurements of pfMA were obtained using the TE, which is susceptible to tendon compliance artifact. In addition, Lee and Piazza did not locate the ankle joint CoR and were not able to explain the mechanism responsible for differences in pfMA. External measurements of toe length may also be susceptible to soft tissue artifact. In this study, we will use MR imaging to locate the ankle CoR and measure pfMA and forefoot length in sprinters and non-sprinters.

H1. We hypothesize that sprinters will have shorter pfMA and longer first metatarsal and phalange bones than those of non-sprinters.

Aim 2. To investigate talocrural geometry between sprinters and non-sprinters.

Rationale: In Aim 1, we used MR imaging to locate the ankle CoR and found that it was more posterior with respect to the tibia in sprinters than non-sprinters. Simple planar analyses of the talar dome and tibial plafond did not present any explanation for these differences in CoR. There are many factors that contribute to talocrural kinematics, but due to limitations in the MR scanning parameters and the study design from Aim 1, we will

only compare three-dimensional geometry of the talar dome and tibial plafond of sprinters and non-sprinters.

H2. We hypothesize that the differences in talocrural joint CoR between sprinters and non-sprinters that were observed in Aim 1 will be explained by three-dimensional joint geometry.

Aim 3. To investigate the relationship between pfMA and ankle strength during isometric and isokinetic plantarflexion contractions in healthy young men.

Rationale: Computational and mathematical models of muscles and moment arms describe a complex relationship with joint torque and power (Lieber and Fridén, 2000; Nagano and Komura, 2003; Akinori et al., 2007). This framework has been used to explain experimental findings in sprinters, suggesting that sprinters benefit from having longer plantarflexor muscle fascicles (Abe et al., 2000, 2001; Kumagai et al., 2000) and shorter pfMA (Lee and Piazza, 2009). Animal studies have shown that muscle quickly adapts to surgically altered dorsiflexor moment arms, returning the muscle to similar functional status before the surgery (Burkholder and Lieber, 1998; Koh and Herzog, 1998). Plantarflexor volume is strongly correlated with isometric ankle strength (Morse et al., 2004), but a link between muscle moment arm and joint has not yet been published. In this study, we will measure pfMA and ankle strength in healthy young men.

H3. We hypothesize that plantarflexor strength will be positively correlated with pfMA during isometric and slow isokinetic contractions and for this correlation to become less positive during fast isokinetic contractions.

Aim 4. To directly compare methods of measuring plantarflexor moment arm *in vivo*.

Rationale: Plantarflexor moment arm has been linked to locomotor function in athletes and elderly adults (Scholz et al., 2008; Lee and Piazza, 2009, 2012; Raichlen et al., 2011), but these studies used different methods to measure pfMA, making it difficult to compare the results of each study. These measurement techniques can be classified into two groups: geometric and tendon excursion (TE). Geometric methods use direct imaging modalities, like MR, to approximate the distance from the ankle CoR and Achilles tendon line of action (Rugg et al., 1990; Maganaris et al., 1998, 2000; Rosager et al., 2002; Fath et al., 2010; Raichlen et al., 2011). The TE method uses ultrasonography to track the musculotendinous junction (MTJ) during joint rotations to approximate moment arm as the first derivative of the excursion of the MTJ with respect to joint rotation. While no 'gold standard' for measuring pfMA has been reported, a modified Reuleaux method has been described in the literature to reliably identify the talocrural CoR (CoR_{TALUS}), which is used to estimate pfMA (Rugg et al., 1990; Maganaris et al., 1998, 2000). In this

study, we will directly compare methods of measuring pfMA *in vivo* that have been previously reported in the literature.

H4. We hypothesize that geometric measures of pfMA will have good agreement with the CoR_{TALUS} method and TE methods will have poor agreement.

Aim 5. To test a novel method of controlling Achilles tendon force *in vivo* during TE measurements.

Rationale: Fath et al (2010) compared the CoR method to TE measures while subjects were not contracting their plantarflexors and found that these two measures were strongly correlated (R^2 = 0.94). However, the authors reported that ankle torque decreased throughout the plantarflexion rotations. This change in ankle torque was probably the result of a change in tendon tension, violating an important assumption made in the TE method (An et al., 1983). In an attempt to minimize variation in tendon force, Lee and Piazza (2009, 2012) measured TE while subjects maximally plantarflexed. Maximal plantarflexion torque decreases with increased joint angle (Sale et al., 1982), which may result in a similar tendon lengthening artifact. Ito et al (2000) attempted to maintain constant dorsiflexor tendon force *in vivo* during TE excursion measurements. Similar techniques have not been used to test pfMA nor have they been validated with previously reported measures. In this study, we will measure pfMA using TE during several contraction conditions: passive, maximal, and torque matching.

H5. We hypothesize that TE during passive and maximal contraction conditions will produce pfMA values that are significantly smaller than pfMA estimates while subjects control ankle torque to be constant.

Chapter 2

Literature Review

2.1 – Muscle Fiber Composition and Function

The functional unit of muscle, a sarcomere, generates force as a function of its neural excitation and current length and velocity. Assuming muscle fibers are fully activated, the force-length and force-velocity properties of the sarcomere (Figure 2.1.1 and 2.1.2, respectively) dictate force production (Hill, 1938, 1953; Gordon et al., 1966). The force-length curve represents how sarcomere tension relates to sarcomere length (Gordon et al., 1966). Force-velocity properties demonstrate the non-linear dependence of sarcomere force on sarcomere shortening velocity (Hill, 1953). Force-length and -velocity properties of whole muscle are influenced by several factors: the biochemical makeup of muscle, muscle architecture, tendon mechanics, and muscle moment arm. This chapter will provide a review of the literature that addresses the links between musculoskeletal structure and function

2.1.1 – Force-Length Properties

The force-length relationship describes isometric force production as a function of sarcomere length (Gordon et al., 1966). While empirical data describe the force-length behavior of muscles, the concept of the force-length curve is explained by the sliding-filament theory (Huxley and Hanson, 1954; Huxley and Nierdergerke, 1954). Muscle force is developed through the formation of cross-bridges, physical connections between myosin and actin filaments (myosin and actin filaments are often described as the thick

and thin filaments, respectively). During maximal muscle activation, peak isometric force is developed when the thin filaments completely overlap the thick filaments on their own side of the M-line (the midline of a sarcomere). As the sarcomere shortens past this point, thin filaments pass into the opposing half of the M-line and the number of cross-bridges decrease, reducing muscle tension. Likewise, as the H-zone increases (segment of myosin that is not overlapping actin filament) fewer cross-bridges are formed, decreasing the sarcomere tension. In short, muscular force is a function of the cross-bridges formed between the thick and thin filaments.

2.1.2 – Force-Velocity Properties

Force produced by a muscle is also determined by its shortening velocity (Hill, 1953). Sarcomere tension developed by cross-bridges act against the external loads placed on the muscle; therefore, if the internal muscle force is greater than the external load, muscle shortening occurs. Sarcomere shortening is the result of cross-bridges detaching and reattaching. As shortening velocity increases there are fewer cross-bridges, thus resulting in decreased muscle tension (Figure 2.1.2). Since muscle filaments can only produce force directed towards the sarcomere M-lines, muscle lengthening occurs when external loads on the muscle are greater than the internal forces. During lengthening contractions, cross-bridges are stretched and distorted, increasing cross-bridge tension and ultimately, sarcomere force (Joyce et al., 1969). Simply stated, sarcomere tension can be modeled as the number of cross-bridges and the rate at which they are being formed.

2.1.3 – Intrinsic Fiber Properties

Muscle fiber maximal shortening velocity (Vmax) and resistance to fatigue are influenced by the type of myosin isoform and adenosine triphosphate enzymes (ATPase) present in the muscle (Bárány, 1967; Billeter et al., 1980; Schiaffino and Reggiani, 1994). The intrinsic Vmax of fast-twitch fibers is up to 2.5-fold greater than slow-twitch fibers, but these fibers are less resistant to fatigue (Bodine et al., 1982). Muscles of mixed composition have been reported to produce a range of specific tensions, however specific tension values for mammalian muscles is often estimated at approximately 22.5 N/cm^2 (Powell et al., 1984).These authors also found the specific tension of the soleus, a predominantly slow-twitch muscle in the guinea pig, to be 15.4 N/cm^2. This difference of 37% between muscles composed of mixed fibers and muscles predominantly made up of slow-twitch fibers has been documented elsewhere (Witzmann et al., 1983).

2.1.4 – Muscle Fiber Architecture

Muscle architecture has been documented to have strong effects on muscle function (Gans and Bock, 1965; Spector et al., 1980; Bodine et al., 1982; Sacks and Roy, 1982; Powell et al., 1984; Burkholder et al., 1994). The physiological cross sectional area (PCSA) of muscle, which is calculated as equation 2.1 (Powell et al., 1984), is directly proportional to maximal force generated by the muscle (Lieber and Fridén, 2000).

$$PCSA\ (mm^2) = \frac{muscle\ mass\ (g) \cdot \cos(\theta)}{\rho\ (g/mm^3) \cdot fiber\ length\ (mm)} \qquad (2.1)$$

where θ represents the surface pennation of the muscle fascicles and ρ represents the density of skeletal muscle (1.056 g/cm^3,(Lieber and Fridén, 2000)). Equation 2.1 is often

reported in the literature as the ratio between muscle volume and fascicle length (Narici et al., 1992; Fukunaga et al., 2001b; Morse et al., 2005b). PCSA represents the amount of muscle that can to contribute to joint rotation. This concept can be explained with a simple free body diagram of five sarcomeres in parallel (Figure 2.2.1). If each sarcomere produces one unit of force and shortens at a rate of one unit length per unit time, then the muscle would produce 5 units of force and shorten at a rate of 1 unit length per unit time. Muscle fibers that are arranged in parallel increase the amount of force per muscle weight. Cat muscles with high PCSA can produce nearly seven times as much force when normalized to muscle mass than smaller muscles (Sacks and Roy, 1982). The arrangement of muscle fibers in parallel does not affect Vmax or the functional range of muscle but does facilitate greater force generation (Lieber and Fridén, 2000).

Optimal fiber length, the product of sarcomeres in series and optimal sarcomere length, is a strong determinant of Vmax (Gans and Bock, 1965). While the biochemical composition of muscle accounts for a 2.5-fold difference in shortening velocity between slow and fast fiber types (Spector et al., 1980; Sacks and Roy, 1982), fiber lengths in different cat muscles account for as much as a 12.6-fold difference in Vmax (Sacks and Roy, 1982). A simple free body diagram of five sarcomeres in series (Figure 2.2b) demonstrates how rate of sarcomere shortening depends on fiber length. Internal tension developed by each sarcomere is opposed by neighboring sarcomeres, which leaves only one unit of sarcomere force applied to the attachment sites of muscle. The tradeoff of small force output is a large shortening velocity of five units of length per unit time. This arrangement of sarcomeres allows for fast and large joint excursions while maintaining

force output. Muscles that rotate joints through large excursions tend to have long fibers (Spector et al., 1980; Bodine et al., 1982; Sacks and Roy, 1982; Wickiewicz et al., 1984). Longer fibers maintain near-maximal muscle tension through a greater range of muscle lengths, increases Vmax, and permits greater normalized muscle force to be produced at any muscle velocity (Lieber and Fridén, 2000).

2.1.5 Muscle Pennation and Function

While PCSA and optimal fiber length are important determinants of muscle force and shortening velocity, respectively, pennation angle influences muscle force and shortening velocity in complex and not fully understood ways (Burkholder et al., 1994; Azizi et al., 2008). Geometric models of muscle suggest that muscle pennation reduces the amount of muscle-tendon unit (MTU) shortening and fiber force transferred to the tendon (Gans and Bock, 1965). However, a tradeoff between muscle pennation, MTU shortening, and tendon force demonstrates the importance of pennation in observations of muscle. These concepts can be better described with the equation of PCSA, equation 2.1. Maximal fiber tension, which is directly proportional to PCSA, is influenced by fiber pennation angle (θ), optimal fiber length (l_f), and amount of muscle (g). Although increased pennation reduces the proportion of fiber force that is transferred along the axis of the muscle, it allows more muscle fibers to be placed in parallel, thus increasing peak muscle tension. Conversely, muscle with less pennation and long fibers is well suited for large muscle excursions (Lieber and Fridén, 2000). A survey of lower limb muscle structure demonstrates that extensor muscles that do work against the ground have large PCSA and relatively short fibers. Opposing flexor muscles, which move joints through

large excursions and against gravity, tend to have lower PCSA and long fibers (Wickiewicz et al., 1983).

2.1.6 Muscle Fiber Orientation and Gearing

A more contemporary understanding of pennate muscle posits that muscle shortening velocity varies with muscle loading (Brainerd and Azizi, 2005; Azizi et al., 2008). During contraction, muscle dimensions change to maintain constant volume; these changes to muscle thickness and width appear to depend on externally applied loads to muscle. With fiber length change, muscle pennation is modified leading to altered muscle shortening. The ratio of muscle velocity to fiber velocity has been termed a muscle's 'architectural gear ratio' (AGR). Muscle shortening is the result of fiber shortening and pennation change (rotation of the muscle belly). Azizi et al (2008) demonstrated with *in situ* preparations of turkey muscle that AGR dynamically changes as a function of muscle loading. Muscle architecture appears to depend on the external loads placed on the muscle. During shortening contractions of low force muscle pennation increases that causes an increase in pennation, thus an AGR that is greater than 1:1. Shortening contractions at high force outputs maintain near-constant pennation, thus AGR is maintained near 1:1. Muscle models demonstrate that variable gearing may increase muscle shortening to 1.4 times greater than fiber Vmax. Azizi et al (2008) speculated that the intrinsic stiffness of muscle constrain muscle shape. These observations of variable shape changes during loading in pennate muscle suggest that tradeoff between muscle force and velocity is governed by an 'automatic transmission' that is inherent in the muscle structure.

When considering the architectural parameters of muscle, it becomes apparent that the structure of muscle has a complicated relationship with the force-length and force-velocity properties. These architectural parameters suggest that muscles are adapted to either develop large forces or achieve high shortening velocities. Conversely, recent findings suggest muscle may possess an 'automatic transmission', in which muscle shape changes to better satisfy the demands placed on the muscle (Azizi et al., 2008). A general rule of thumb is proposed when describing muscle structure: muscles that work against gravity are better suited for developing large amounts of force, while muscles that flex limbs are better for large joint excursions of high rates (Lieber and Fridén, 2000).

2.2 Influences of joint and limb structure on muscle function

The influence of muscle moment arm on muscle force and joint torque is complex. Linear force and excursion produced by muscle contraction is applied to skeletal levers, resulting in rotational forces and excursions at the joint. The moment arm of a muscle is defined as the shortest distance from the center of joint rotation to the line of action of the muscle-tendon structure, and joint torque is the cross product of moment arm and muscle force (Zajac, 1989). By this definition, muscle acting with a longer moment arm is capable of producing greater torque. However, this relationship is complicated due to force-length and velocity properties of muscle (Lieber and Fridén, 2000). The amount of MTU shortening during joint rotation is governed by joint leverage and is inversely proportional to the mechanical advantage of a joint (Lieber and Fridén, 2000). To visualize this concept, consider two discs of differing radii (Figure 2.3). If both

discs rotate the same amount, the rim of the larger disc will go through a greater excursion than the rim of the smaller disc.

Joint range of motion in which muscular force can be developed is regulated by the ratio of fiber length to moment arm. This property permits joint function to differ from what muscle architecture might suggest. A muscle with large PCSA and short fibers operating with a small moment arm would produce large joint excursions and angular velocities. The same muscle placed with a larger moment arm would result in high moment production through a very small and slow range of joint motion (Lieber and Fridén, 2000). Therefore, careful consideration of both muscle architecture and moment arm is needed to understand joint function.

When considering joint leverage, the ankle joint requires special attention because it interacts with the ground. The distance between the ground reaction force (GRF) and ankle joint center is determined by the length and posture of the forefoot (Hildebrand, 1960). The ratio of GRF moment arm to muscle moment arm is called the 'gear ratio' and is inversely proportional to MTU velocity (Hildebrand, 1960, 1994; Biewener, 1989; Carrier et al., 1994) discusses effective mechanical advantage (EMA), which is the inverse of gear ratio). Lower limb structure imposes a constraint on torque and joint velocity that depends on the dynamically changing GRF moment arm (Carrier et al., 1994). Experimental data supporting this importance is discussed in section 2.2.1.

2.2.1 **Musculoskeletal Architecture and Function in Animals**

Comparative biologists have documented many musculoskeletal adaptations observed in animals that provide functional advantages for specific locomotor tasks. However, no direct links have been made between muscle moment arm and peak joint moment. Lieber and Boakes (1988) found that peak muscle tension explained 77% of knee strength in frogs, but no correlation was found between strength and moment arm. Lutz and Rome (1994) observed that frog muscle generates maximum power during jumping tasks by operating near optimal sarcomere lengths and shortening velocities.

The best animal sprinters, like cheetahs and greyhounds, have very long forefeet and short heel bones, which may be beneficial for generating joint power at high speeds (Hildebrand, 1960). It is widely thought in the comparative morphology literature that gear ratio plays an important role in joint torque during animal locomotion (Hildebrand, 1960, 1994; Alexander et al., 1979; Biewener, 1989; Carrier et al., 1998; Gregersen and Carrier, 2004). These studies suggest that animals with low gear ratios are better suited for slow tasks such as digging and walking that require large amounts of torque, while joints operating with high gear ratios are well adapted for activities like running and jumping (Hildebrand, 1994). During slow joint rotations, force-velocity effects of muscle are likely minimal; therefore increased joint leverage is beneficial for torque production. However, during faster rates of joint rotation, muscle shortening velocity is more important than joint leverage, and poor mechanical advantage yields greater muscle force (Hildebrand, 1994; Nagano and Komura, 2003).

Dogs have been observed to modulate their joint gear ratios during running and jumping tasks (Carrier et al., 1998, 1998). Greyhounds run with larger gear ratios at faster rates of acceleration which has several benefits to performance: increased ground contact time resulting in greater ground impulse during stance, more propulsive forces can be applied to the ground, and greater muscle volume can be recruited (Williams et al., 2009b). Computer simulations of frogs suggest that during jumping, muscle work and power can be increased with a dynamic gear ratio (Roberts and Marsh, 2003). These simulations show that adding compliance to the MTU further increases.

While gear ratio and muscle architecture appear to be linked to locomotor performance in animals, other anatomical features may explain differences in function between animals. Greyhounds have smaller muscle moment arms and greater hind limb musculature compared to the cheetah, but can only run 59% as quickly as the cheetah. Cheetahs have longer hind limb bones and a highly flexible back that allows for longer strides and increased contact with the ground (duty factor), which may facilitate greater propulsive impulse applied to the ground (Hildebrand, 1960; Hudson et al., 2011). Joint structure and limb proportions should carefully be considered during the study of form and function in animals and humans.

2.2.2 Musculoskeletal adaptations to joint leverage

Although comparative biologists suggest that muscle moment arm is an important constraint on animal locomotion that was selected for specific activities (Hildebrand, 1960, 1994; Biewener, 1990), intra-species musculoskeletal variation is not well

understood. Koh and Herzog (1998) surgically increased the dorsiflexor moment arm in rabbits and found that increases in the number of sarcomeres in series and decrease in PCSA preserved joint function. A similar study by Burkholder and Lieber (1998) found that mouse muscle responded to increased dorsiflexor moment arms by remodeling the tibialis anterior muscle to have fewer sarcomeres in series. While these studies suggest that muscle adaptations occur to maintain joint function in mice and rabbits, it is unclear if intra-species variation in muscle moment arm influences function or drives muscle adaptation.

2.3 Plantarflexor structure and locomotor function in humans

Human locomotion is the product of highly coordinated joint rotations, which are constrained by the force generating capacity and mechanical advantage of muscle and the compliance of tendon on which muscle pulls (Zajac, 1989). Though all joints in the body contribute to locomotor function, it has been found that the ankle plantarflexor muscles are of particular importance during walking and running (Jacobs and van Ingen Schenau, 1992; Abe et al., 2000, 2001; Kumagai et al., 2000; Bean et al., 2002). While many muscles aid in ankle plantarflexion, the soleus and lateral and medial gastrocnemius muscles are the main contributors and are often referred to as the triceps surae. The soleus is a uniarticular muscle that originates on the posterior aspect of the tibia and inserts into the Achilles tendon. The lateral and medial gastrocnemii are biarticular muscles that originate on the condyles of the femur and insert into the Achilles tendon (Drake et al., 2009).

Isometric plantarflexor torque is influenced by knee flexion and plantarflexion (Sale et al., 1982; Cresswell et al., 1995; Pinniger et al., 2000; Arampatzis et al., 2006). Due to the biarticular nature of the gastrocnemii, knee flexion increases muscle slack, resulting in muscle fibers operating further from optimal length (Cresswell et al., 1995). Plantarflexor torque also depends on the position of the ankle. Peak isometric plantarflexion is generated around 10º-15º dorsiflexion (Sale et al., 1982). This range of maximal plantarflexor strength coincides with the position of the ankle through much of stance (Perry, 1992). Although the triceps surae are primarily plantarflexors, computer simulations suggest the plantarflexors also contributes to knee flexion during gait (Anderson et al., 2004; Goldberg et al., 2004).

2.3.1 Implications of plantarflexor structure on walking

During normal gait, the plantarflexors absorb and generate substantial amounts of mechanical power to efficiently propel the body forward. At heel strike, the foot goes into a small amount of plantarflexion while the foot rotates onto the ground. During mid-stance, the plantarflexors are absorbing energy while the tibia rotates forward about the ankle. As the foot enters terminal stance, the ankle begins to rapidly plantarflex propelling the leg into swing (Perry, 1992).

Inverse dynamics analyses of the ankle joint during locomotion provide important information for clinicians and researchers (Perry, 1992). However, these analyses may not faithfully represent muscle plantarflexor behavior during walking and running. Studies have used an ultrasound probe to directly image the medial gastrocnemius

fascicles during gait and have documented drastic differences in muscle and tendon behavior (Fukunaga et al., 2001a; Ishikawa et al., 2005). At heel strike, the muscle remains isometric while the tendon shortens as the foot plantarflexes and comes fully in contact with the ground. While the foot is dorsiflexing during midstance, the gastrocnemii fascicles contract isometrically and the Achilles tendon is strained. During this portion of stance, the muscle activation is relatively small, suggesting that tendon loading results from the dynamics of the body moving forward rather than active muscle force. At terminal stance, rapid plantarflexion occurs and the energy stored in the Achilles tendon is quickly released to aid in the initiation of swing. Surprisingly, push-off is preceded by significant reductions in muscle activation (Fukunaga et al., 2001a; Ishikawa et al., 2005, 2007). These findings suggest a 'catapult' like mechanism employed by the plantarflexors to efficiently move the body forward during walking (Ishikawa et al., 2005).

2.3.2 Plantarflexor structure as a determinant in elderly gait

Plantarflexor weakness is a well-documented constraint on walking velocity in the elderly (Bean et al., 2002; Graf et al., 2005). To compensate for reduced plantarflexor strength, elderly adults walk with increased hip flexion to assist the leg in early swing. However, increased hip flexion appears to be an insufficient substitute for plantarflexion, and as a result, elderly adults take shorter and more frequent steps (Winter et al., 1990; Judge et al., 1996; Graf et al., 2005). Judge et al (1996) calculated the joint powers of elderly adults while they walked at their preferred and maximal speeds and found that hip and knee power were both significantly greater during maximal walking, however

plantarflexor power did not change with an increase in speed. Graf et al (2005) found that slower-elderly adults generate greater hip, knee, and ankle power when prompted to walk fast, however they are unable to generate similar ankle powers that are generated by healthy elderly adults.

Lee and Piazza (2012) found that mobility-limited elderly men walk at a speed that is largely explained by pfMA ($R^2 = 0.69$). These findings were found after subjects were grouped into two clusters: 'fast' and 'slow' elderly men. Fast elderly men showed no dependence of walking speed on any musculoskeletal parameter. The slower elderly men were also significantly older (4.5 years) and heavier (10.4 kg) than the faster walking elderly men. The authors suggested that faster walking elderly men had adequate muscle mass and body weight to overcome any disparities in pfMA, while slower adults with small moment arms were unable to generate the necessary joint moments for walking at faster speeds. Although pfMA was linked with walking speed in elderly men, no mechanism was clearly identified. Further study is needed to identify why increased pfMA seems to serve as a protective mechanism against mobility loss in slower elderly men.

2.3.3 – Implications of plantarflexors on running

Human distance running and sprint performance can partly be explained by biomechanical, physiological, and anatomical factors (Costill et al., 1976; Williams and Cavanagh, 1987; Abe et al., 2000, 2001; Kumagai et al., 2000; Anderson et al., 2004; Lee and Piazza, 2009). Distance runners strive to minimize the metabolic cost of running.

Williams and Cavanagh (1987) documented a litany of biomechanical parameters that explain over half of the variation of running economy among experienced runners. One aspect of distance running of particular interest is the role of the plantarflexor muscles and the Achilles tendon. Investigations into Achilles tendon and plantarflexor fascicle behavior during running are not always coupled (Ishikawa and Komi, 2007; Ishikawa et al., 2007), which may minimize muscle shortening and therefore metabolic energy requirements. During the first half of stance, the ankle goes into dorsiflexion, causing an increase in the MTU length of the plantarflexors (Ishikawa et al., 2007). However, fascicle length slowly shortens while rapid loading of the Achilles tendon. Later in stance, as the ankle quickly plantarflexes, the Achilles tendon rapidly shortens and returns stored energy. Some evolutionary biologists propose that modern man evolved to excel at distance running. They suggest that our thick and long Achilles tendons adapted to prolonged distance running that was important during our evolution as a species (Bramble and Lieberman, 2004).

Unlike distance runners who aim to minimize energetic demands, sprinters strive to generate as much energy as possible in an orchestrated manner to quickly accelerate at the start of a race; thus many factors must be considered when investigating the importance of the start of a sprint race (Jacobs and van Ingen Schenau, 1992; Harland and Steele, 1997; Koh and Herzog, 1998; Mero et al., 2006; Slawinski et al., 2010a, 2010b). During the first steps of a race, sprinters position their centers of mass far in front of their feet to minimize breaking impulse(Hunter et al., 2005). To control the large and fast excursions of the lower limbs, the upper body is used to balance the angular momentum

of the sprinter (Slawinski et al., 2010b). Additionally, skilled sprinters benefit from appropriate positioning of the starting blocks, which plays an important role on sprint performance (Harland and Steele, 1997) as improper block locations can reduce the rate of loading and the amount of propulsive impulse.

The plantarflexors appear to play an important role in sprint performance. During the early part of a sprint race, positive muscular work must be done to accelerate the sprinter down the track. The plantarflexor muscles generate a substantial amount of power (Johnson and Buckley, 2001) and are responsible for transferring additional power from the more proximal joints (Jacobs and van Ingen Schenau, 1992). While at maximal running speed, the ankle joint generates more power than the hip and knee, but absorbs roughly the same amount of energy (Bezodis et al., 2008). Sprinters appear to benefit from plantarflexor and ankle musculoskeletal architecture (Abe et al., 2000, 2001; Kumagai et al., 2000; Lee and Piazza, 2009), which will be discussed in depth in section 2.3.4.

2.3.4 – Musculoskeletal adaptations to running and sprinting

Running and sprinting are complex movements that depend on many musculoskeletal parameters. Skeletal muscle biochemical composition and architecture differs between sprinters and distance runners (Costill et al., 1976; Mero et al., 1981; Abe et al., 2000, 2001; Kumagai et al., 2000; Lee and Piazza, 2009). The biochemical makeup of skeletal muscle has strong implications fatigue and shortening rates (Bárány, 1967; Spector et al., 1980; Bodine et al., 1982; Sacks and Roy, 1982). These functional

differences in muscle fibers are shown in the leg muscles of highly trained distance runners and sprinters. Elite distance runners have large proportions of fatigue-resistant fibers (Costill et al., 1976), while trained sprinters tend to have a larger proportion of fast-twitch muscle fibers (Costill et al., 1976; Mero et al., 1981).

Though muscle biochemical composition influences function, muscle architecture potentially has greater influence on whole muscle contractile function (Sacks and Roy, 1982; Burkholder et al., 1994). In trained sprinters, the fascicles of the ankle and knee extensors are both longer and thicker than non-sprinters and distance runners (Abe et al., 2000, 2001; Lee and Piazza, 2009). Longer fascicles increase peak muscle shortening velocities (Sacks and Roy, 1982), critical during fast joint rotations (Akinori et al., 2007; Lee and Piazza, 2009), while larger fascicle cross-sectional area increases peak muscle force (Lieber and Fridén, 2000). Similar differences in fascicle architecture have also been found between elite sprinters (<11s 100m) and good sprinters (<12s 100m) (Kumagai et al., 2000).

Recent investigations of distance runners and sprinters have revealed links between performance and foot and ankle structure (Scholz et al., 2008; Lee and Piazza, 2009; Rolian et al., 2009; Raichlen et al., 2011). Lee and Piazza (2009) document differences in foot and ankle structure between sprinters and non-sprinters as a mechanism for increased muscular work during the start of a sprint race, while others suggeste that pfMA is associated with running economy (Scholz et al., 2008; Rolian et al., 2009; Raichlen et al., 2011).

The foot and ankle structure of sprinters appears to be well adapted for increased muscular work to be done during the start of a sprint race (Lee and Piazza, 2009). Lee and Piazza used an ultrasound probe to measure the TE of the Achilles tendon during plantarflexion. They found sprinters to have pfMA that are ~25% shorter those of non-sprinters. Simple computer simulations suggest that reduced mechanical advantage at the ankle allows for better force-velocity properties of the plantarflexor muscles and increases muscular work (Nagano and Komura, 2003; Lee and Piazza, 2009). Lee and Piazza made external measurements of the foot, finding sprinters to have slightly longer first toes than non-sprinters. Increasing toe length in a simple computer simulation of push-off analogous to sprinting resulted with increased foot contact time with the ground and forward impulse. A study that looked for relationships between sprint performance a myriad of lower leg musculoskeletal parameters in elite sprinters was unable to explain differences in sprint performance (Karamanidis et al., 2011), suggesting that sprinters may possess fundamentally different lower leg musculoskeletal parameters than non-sprinters and small variations within sprinters may not affect performance.

Distance running economy is negatively correlated with pfMA (Scholz et al., 2008; Raichlen et al., 2011). While smaller pfMA in sprinters may allow for greater active muscle force to be generated, simple models suggest that reduced ankle leverage permits greater energy storage in the Achilles tendon (Scholz et al., 2008). The model assumes that runners have similar ankle kinematics and kinetics, so smaller pfMA places greater demands on the muscle to resist the GRF. In addition, plantarflexor fascicles operate at slow velocities during stance so the energy demands to maintain muscle length

and thus increase tendon strain should be minimal (Ishikawa et al., 2007). However, this model does not consider changes in foot and ankle kinematics that are likely to occur with differences in foot and ankle structure. Though experimental data show a strong link between running economy and pfMA, distance runners do not have categorically shorter pfMA than non-distance runners (Rosager et al., 2002).

Some evolutionary biologists argue that modern humans have evolved to excel at distance running in order to chase animals into exhaustion (Bramble and Lieberman, 2004). A caveat should be made when referring to these proposed adaptations; many of these adaptations have not yet been validated with biomechanical analyses, however they have been used to support the idea of our distance running heritage. Modern humans have shorter toes than our bipedal ancestors. Biomechanical analysis of running suggests that shorter toes reduce the GRF moment arm with the metatarsophalangeal joint, decreasing the toe flexor force requirements. Although the toe flexors are small muscles, this reduced muscular work may lower the metabolic cost of running (Rolian et al., 2009). These findings support the importance of toe length in human sprinters (Lee and Piazza, 2009). While distance runners benefit from lowering energetic demands, sprinters profit from increased muscular work. However, reports of reduced pfMA in both sprinters and distance runners with opposite toe structure presents us with a conundrum. Lee and Piazza found that sprinters had longer forefeet and shorter pfMA, but others propose that distance runners benefit from shorter forefeet and shorter pfMA (Bramble and Lieberman, 2004; Rolian et al., 2009; Lieberman et al., 2010). It is unclear if the authors believe that smaller feet would improve running performance, which has yet to be

reported in the literature. Further investigation is needed to obtain a better understanding of foot proportions and running performance.

Although the current literature has investigated possible links between performance and lower limb musculoskeletal architecture, more research is needed to address several limitations: 1 – indirect measurements of pfMA have been unable to identify a mechanism that explains the differences in foot and ankle between athletes and non-athletes (Scholz et al., 2008; Lee and Piazza, 2009; Raichlen et al., 2011), 2 – external measurements of toe length in sprinters and non-sprinters may be the result of soft tissue artifact brought about by sprint training (Lee and Piazza, 2009), and 3 – although computer simulations demonstrate the influence pfMA and toe length has on joint kinetics, experimental data has yet been produced to support these claims.

2.3.5 Computer simulations of pfMA and joint function

Nagano and Komura (2003) developed a simple computer simulation of plantarflexion to demonstrate the effect pfMA has on ankle strength during isometric and isokinetic contractions. At slow speeds, muscle shortening is low and pfMA contributes in a positive way towards ankle strength. However, at increasing rates of plantarflexion, reduced ankle leverage actually serves as a protective mechanism against torque loss by mitigating the effects of the force-velocity properties of muscle (Figure 2.1.2).

A more complex model of a ‘sprinter’ lunging forward demonstrates the effects of pfMA toe length on the work done to the ground. Short pfMA facilitate increased muscle strength via minimizing the rate at which the muscle shortens. Longer toes seem to

increase the amount of time the foot is in contact with the ground, which is important for doing as much work as possible to the ground. Foot and ankle structure in animals like the cheetah and greyhound also suggest that longer forefeet and short heels is partly responsible for fast running speeds (Hildebrand, 1960; Williams et al., 2008; Hudson et al., 2011) as well as human sprinters (Lee and Piazza, 2009)

2.4 Estimates of pfMA and plantarflexor architecture in humans

While the comparative morphology literature is well established, the influence human musculoskeletal variation has on mobility and performance is less understood. One limitation in this area of study is the methodology for measurement of the anatomical structures of interest. Advances in imaging modalities such as ultrasonography and magnetic resonance (MR) imaging allow for direct imaging of the plantarflexor musculature in humans (Narici et al., 1992; Abe et al., 2000, 2001; Kumagai et al., 2000; Fukunaga et al., 2001a, 2001b; Morse et al., 2005b; Lee and Piazza, 2009, 2012). Planar images of muscle made with ultrasonography allow for simple analyses of muscle fascicle length, pennation, and muscle thickness (Abe et al., 2000, 2001; Kumagai et al., 2000; Fukunaga et al., 2001a; Lee and Piazza, 2009). Because muscle fascicles are considered to connect the superficial and deep aponeuroses (Abe et al., 2000, 2001), simple measurements can be made to find muscle length, pennation, and thickness. The pennation angle of the muscle fascicle is measured as the angle between the fascicle and aponeuroses, while muscle thickness is the distance between the superficial and deep aponeuroses (Abe et al., 2000, 2001; Kumagai et al., 2000; Lee and Piazza, 2009). Due to the small imaging area of many ultrasonography probes, fascicle length is often

expressed the muscle thickness divided by the sine of the pennation angle (Abe et al., 2000, 2001). Accurate estimates of muscle volume can be obtained using MR to image the muscle of interest (Fukunaga et al., 1992; Narici et al., 1992).

2.4.1 Geometric identification of the Center of Rotation

These imaging modalities also allow for estimates of *in vivo* pfMA (Rugg et al., 1990; Maganaris et al., 1998, 2000; Rosager et al., 2002; Lee and Piazza, 2009). Rugg et al. (1990) quantified pfMA as the distance from the ankle center of rotation (CoR) to the line of action of the Achilles tendon. To identify the CoR, Reuleaux's method (Reuleaux, 1876) of finding an instantaneous CoR between two bodies was used. Images of the foot and ankle were made in a series of joint postures and the tracings of the tibia and talus, representative of the shank and foot segments, respectively, were treated as the two bodies of interest. Plantarflexor moment arm values increased from ~5.0 to 6.0 (± 0.4) cm as ankle angle increased from 10° dorsiflexion to 40° plantarflexion.

Similar methods were employed by Maganaris et al. in several studies (1998, 2000) to investigate the effects of muscular contraction on pfMA. They found that pfMA estimates were significantly greater at all joint angles during isometric plantarflexion contractions. In agreement with Rugg et al. (1990), Maganaris and colleagues (1998, 2000) found that pfMA increases as a function of plantarflexion angle. During passive measurements, pfMA ranged from 4.4 to 5.5 (± 0.4) cm, at angles of 15° dorsiflexion to 30° plantarflexion, respectively. These values of pfMA are in close agreement with measurements reported by Fath et al (2010). However, during isometric plantarflexion

contractions, they found that pfMA ranged from 5.4 to 7.0 (± 0.4) cm as ankle angle increased from 15° dorsiflexion to 30° plantarflexion.

Interpretation of these results must be taken with caution, the foot and ankle complex is a highly complex system with 26 bones and 33 joints (Drake et al., 2009), yet sagittal plane motion is often modeled as planar rotation between the tibia and talus (referred to as the ankle or talocrural joint). Direct imaging of the ankle complex during constrained plantarflexion suggests that most calcaneal movement is due to talocrural rotation (Sheehan, 2010). *In vivo* imaging of the ankle joint complex during the early part of stance during human walking shows that most ankle motion occurred at the talocrural joint. During mid- and late-stance, most rotation and inversion of the foot occurred at the subtalar joint, however some motion occurred at the talocrural joint, suggesting that the ankle joint is not a truly conforming revolute joint (de Asla et al., 2006). Although sophisticated methods of quantifying pfMA exist, relationships between pfMA and human performance have been made with less advanced measurement techniques (Scholz et al., 2008; Lee and Piazza, 2009, 2012; Raichlen et al., 2011).

Due to the quasi-sagittal behavior of the talocrural joint, 3D quantification of its axis may produce more accurate representations pfMA (Sheehan, 2010; Hashizume et al., 2012). Helical axis decomposition provides an opportunity to identify instant axes of rotation between two bodies (Woltring et al., 1985). Hashizume and colleagues (2012) imaged the foot and ankle in six ankle positions to identify 3D pfMA. Landmarks on the tibia and talus were identified and used to estimate a helical axis for each joint position. The authors found that 2D pfMA estimates were significantly greater than 3D pfMA

values at every ankle position. Three dimensional pfMA estimates also did not display the same dependence on increasing joint angle that has been previously reported with planar analysis (Rugg et al., 1990; Maganaris et al., 1998, 2000). The authors suggest three explanations for these differences between 2D and 3D estimates: 1 – talocrural joint axis 21.4º ± the coronal plane (or the 2D talocrural axis), 2 – sagittal plane selection for 2D analysis was not aligned with the Achilles tendon insertion into the calcaneus, and 3 – bony configuration registration may insert unknown errors into both 2D and 3D estimations. This method also has limitations: the foot and ankle is constrained to rotate about a fixed axis, confining it to a plane of motion; the ankle is unloaded during imaging; and static images are made, which may not capture ankle mechanics during locomotion, though in fairness, few methods capture dynamic data.

Sheehan (2010, 2012) developed a method of identifying the instantaneous helical axis of the talocrural and subtalar joints during dynamic and loaded ankle rotations. Much like the Hashizume et al (2012) results, 3D pfMA magnitudes were significantly smaller than 2D pfMA (Sheehan, 2012). Additionally, 3D pfMA did not increase with plantarflexion angle as has been reported with 2D methods (Rugg et al., 1990; Maganaris et al., 1998, 2000). Differences in pfMA were observed between the sexes, with men having significantly larger moment arms, but when scaled to the width of the distal tibia, no differences between men and women were found (Sheehan, 2012).

2.4.2 – Tendon Excursion measurement techniques

While MR imaging seems to provide reliable measurements of pfMA, both in two and three-dimensions, this modality is quite expensive and not available at all research institutes. Ultrasonography, a less expensive and commonly available imaging technology, can be used to track the amount of Achilles tendon excursion (TE) throughout a known joint rotation (An et al., 1984; Lee and Piazza, 2009; Fath et al., 2010). Storace and Wolf (1979) outline the application of the principle of virtual work for estimating joint moment arms. They consider the joints of interest to be frictionless (workless) and the ligaments to be inextensible. To satisfy the principle of virtual work, the sum of the work done by some externally applied moment and some muscle force must be zero (equation 2.2).

Equation 2.2. $$F_{Muscle} \cdot \delta_L + M_{Ext} \cdot \delta_\theta = 0$$

Rearranging equation 2.2 yields equation 2.3.

Equation 2.3. $$(M_{Ext}/F_{Muscle}) = -1 \cdot (\delta_L/\delta_\theta)$$

Therefore, the joint moment arm (r) can be expressed as (equation 2.3):

Equation 2.4. $$r = (M_{Ext}/F_{Muscle}) \quad \therefore \quad r = -1 \cdot (\delta_L/\delta_\theta)$$

So, the moment arm is calculated as the first derivative of tendon displacement taken with respect to joint displacement. However, a limitation of ultrasonography complicates the TE method. Because the musculo-tendinous junction is the only landmark along the tendon that can be consistently identified length change within the tendon will appear as artifact (Lee and Piazza, 2009, 2012). To compensate for this limitation, it is assumed that *in vivo* tendon force does not change throughout the measurement (An et al., 1984).

While tendon forces are easily controlled for in animal models and cadaveric preparations (Lieber and Boakes, 1988; McCullough et al., 2011), they have yet to be properly controlled for *in vivo* (Lee and Piazza, 2009, 2012; Fath et al., 2010).

Tendon excursion estimates of moment arm in the literature seem to vary based on muscular contraction and research group (Ito et al., 2000; Maganaris et al., 2000; Lee and Piazza, 2009; Fath et al., 2010). Ito and colleagues (2000) measured the tibialis anterior moment arm and found that estimates were significantly greater during any amount of muscular contraction. This difference in moment arm between passive and contracted conditions was hypothesized to be caused by tendon slack in the passive condition. In the plantarflexor muscles, passive joint torque exceeds 25 Nm in dorisflexion and becomes slack in plantarflexion (Riener and Edrich, 1999). Assuming an average pfMA of 5cm, peak passive tendon force could reach upwards of 500 N. Due to this large passive component inherent in the ankle joint, different TE methods have been reported (Lee and Piazza, 2009; Fath et al., 2010).

To date, all *in vivo* TE measurements using ultrasonography underestimate pfMA (Lee and Piazza, 2009; Fath et al., 2010). McCullough et al.(2011) applied constant loads to the Achilles tendon in a cadaver model, resulting in pfMA estimates that are similar to measurements obtained using MR to locate ankle CoR (Rugg et al., 1990; Maganaris et al., 1998; Fath et al., 2010). Maganaris et al. (2000) imaged the Achilles tendon insertion to the calcaneus and applied the TE method to estimate pfMA and produced values that were similar to those obtained with CoR. Ultrasonography based TE has been reported to

correlate well with pfMA obtained with MR (Fath et al., 2010), but the inherent limitations of imaging tendon should be investigated further.

Lee and Piazza (2009) used ultrasonography to measure TE of sprinters and non-sprinters while subjects maximally contracted their plantarflexors. The pfMA estimates at 5° plantarflexion in non-sprinters and sprinters were 4.2 ± 0.6 cm and 3.1 ± 0.4 cm, respectively. Unreported pfMA measurements in non-sprinters were substantially smaller in magnitude when subjects did not contract during the measurements. Tendon slack artifact was considered to be a possible explanation for the pfMA difference between sprinters and non-sprinters. Muscle strength and tendon stiffness differs between sprinters and non-sprinters (Arampatzis et al., 2007a). It is possible that sprinters maintained near peak ankle moment throughout a greater range of motion. This would register as decreased TE and result in smaller pfMA approximations.

Fath et al. (2010) used ultrasonography to measure TE while subjects remained passive and compared these estimates to pfMA from CoR methods. Implementing a finite difference method of ± 15° of neutral position, they found that pfMA correlated very well with TE (R^2 = 0.94). Regardless of differentiation technique, TE estimates were significantly smaller than CoR measurements. Direction of ankle rotation may be important in estimating pfMA as well, Fath et al (2010) found moment arm estimates to be different between plantarflexion and dorsiflexion rotations. Additionally, plantarflexion rotations resulted in stronger correlations between TE and CoR measures ($0.64 \leq R^2 \leq 0.94$) than did dorsiflexion rotations ($0.40 \leq R^2 \leq 0.60$).

While the published results of Fath et al. (2010) appear to be strongly correlated with CoR measurements, their findings should be taken with caution. To guarantee that no tendon strain occurs during measurement, muscle, and therefore tendon, force must remain constant. However, Fath and colleagues (2010) state that no internal forces exist because they instruct subjects to remain passive during the measurements. This statement is misleading for several reasons: first, TE requires no change in *in vivo* tendon force, irrespective of the magnitude of force (An et al., 1984); second, the authors report ankle torque that decreases throughout plantarflexion; third, pfMA dependence on plantarflexion angle would require increased joint torque throughout joint rotation for constant tendon force; and fourth, some reflexive muscle activation is not uncommon during 'passive' joint rotations (Silder et al., 2007). Further investigation is needed to properly control for *in vivo* tendon force.

2.4.3 – Indirect Geometric methods of measuring pfMA

Other investigators have estimated pfMA using bony landmarks. Raichlen et al (2011) compared the fossil remnants of the calcanei of early man and other hominoids with the calcanei of trained distance runners. Due to limitations in the fossil records, calcaneal tuber lengths were used as pfMA estimates. Csapo and colleagues (2010) assumed that the talus rotates about the center of a circle fit to a series of points along the talar dome. Both these measurements do not account for possible variations in the geometries and interactions between the tibia and talus bones.

The axis of the talocrural joint tends to run between the lateral and medial malleoli, but axis orientation and position changes joint motion and individuals (Lundberg et al., 1989). Several studies measured the distance from the lateral and medial malleoli to the posterior border of the Achilles tendon and calculated pfMA as the average of these two distances (Scholz et al., 2008; Ahn et al., 2011). These external measurements have yet to be compared with pfMA measurements made with MR and may be susceptible to soft tissue artifact.

2.5 – Summary

Musculoskeletal structure varies considerably across the animal kingdom, providing animals with adaptations that are well suited for niche tasks (Hildebrand, 1994). The effects of intra-species variability on function are less clear. Recent studies have found links between pfMA and locomotor performance, but they have not yet identified the mechanism responsible. Simple computer simulations suggest that reduced pfMA acts as a protective mechanism against muscle force loss at high speeds, but this has yet to be tested in humans. The relationship between pfMA and function appears to depend on the population of interest. Sprinters and distance runners appear to benefit from reduced pfMA, but mobility-limited elderly men walk at a speed that is highly correlated with pfMA (Lee and Piazza, 2012). To better understand this relationship between joint function and locomotor performance, we first must answer the question: ‘how does muscle moment arm influence joint torque’? At first glance, the answer seems clear, but animal studies suggest that any change in muscle moment arm is quickly compensated for by rapidly adapting muscle structure.

This dissertation investigates several topics of interest that are related to pfMA and function: 1 – what is responsible for pfMA differences between sprinter and non-sprinters, 2 – are these differences explained by talocrural joint geometry, 3 – does reduced pfMA serve as a protective mechanisms during fast isokinetic contractions or do musculoskeletal adaptations occur, which compensate for poor mechanical advantage, and 4 – several authors have linked pfMA to human performance using different pfMA measurement methodologies, how do these values compare to one another and which is the appropriate method to use.

Figure Captions

2.1.1 Force-length properties of muscle. Muscles generate maximal active force when they are near their optimal length. As muscle length deviates from this optimal length, force decay occurs.

2.1.2 Force-velocity properties of muscle. The amount of tension shortening muscle generates is dependent on its rate of shortening. The shortening velocity at which muscle generates no active tension has been termed 'Vmax'.

2.2.1 Simple model of the effects that sarcomere configuration has on muscle force. A muscle consisting of 5 sarcomeres in parallel, generates 5 units of force and shortens at a rate of 1 unit length over the period of 1 unit of time.

2.2.2 Simple model of the effects that sarcomere configuration has on muscle shortening velocity. A muscle consisting of 5 sarcomeres in series, generates 1 units of force and shortens at a rate of 5 unit length over the period of 1 unit of time.

2.3.1 The radii of two discs of varying size demonstrate end point excursions for any given rotation. It is shown that a disc with smaller radius results in less excursion of the rim. This concept can be applied to the more biologically relevant context like the human ankle joint.

2.1.1 - Force-length properties of muscle. Muscles generate maximal active force when they are near their optimal length. As muscle length deviates from this optimal length, force decay occurs.

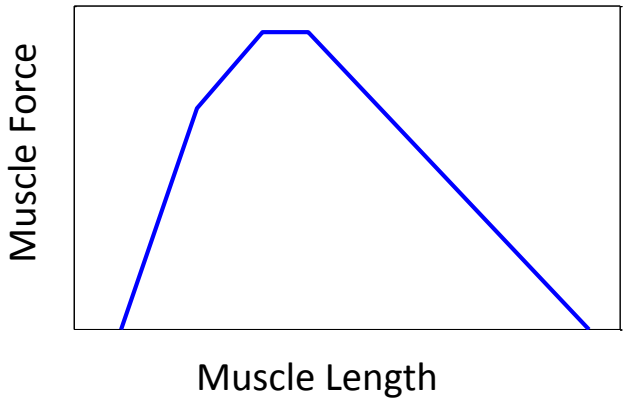

2.1.2 Force-velocity properties of muscle. The amount of tension shortening muscle generates is dependent on its rate of shortening. The shortening velocity at which muscle generates no active tension has been termed 'Vmax'.

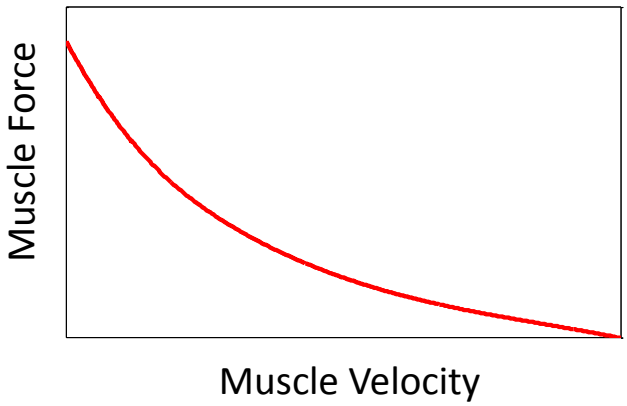

2.2.1 Simple model of the effects that sarcomere configuration has on muscle force.

A muscle consisting of 5 sarcomeres in parallel, generates 5 units of force and shortens at a rate of 1 unit length over the period of 1 unit of time

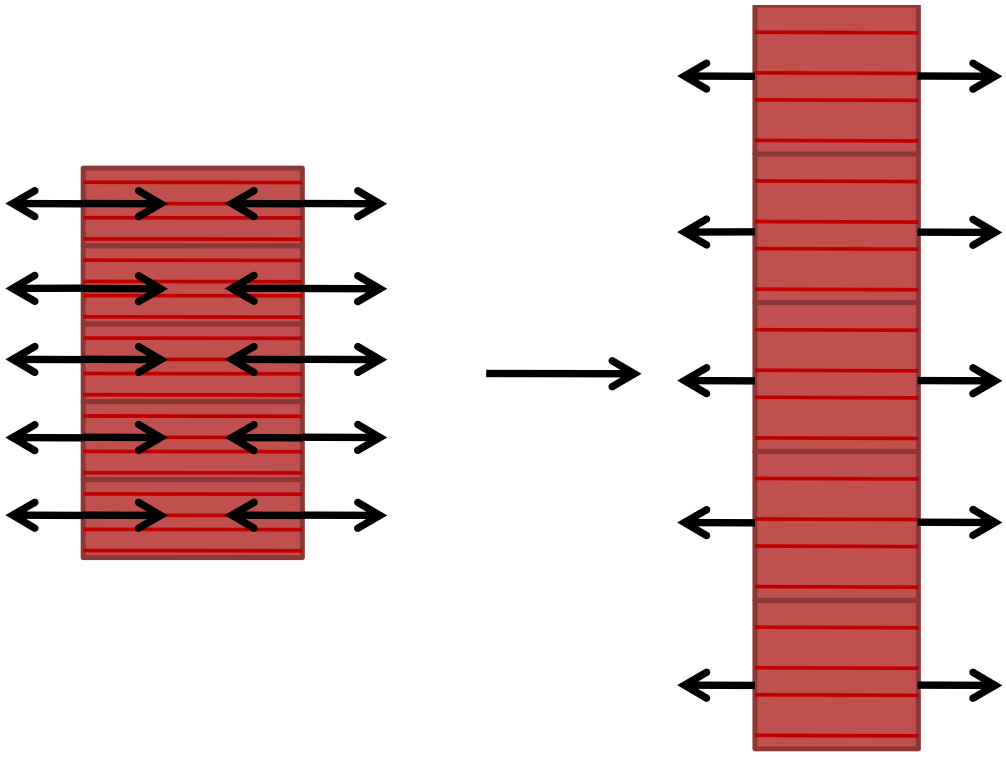

2.2.2 Simple model of the effects that sarcomere configuration has on muscle shortening velocity. A muscle consisting of 5 sarcomeres in series, generates 1 units of force and shortens at a rate of 5 unit length over the period of 1 unit of time.

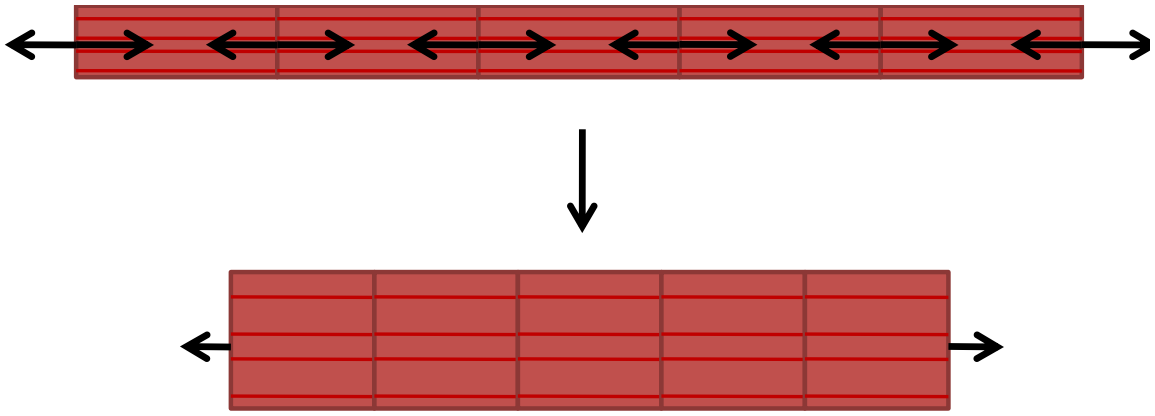

2.3.1 The radii of two discs of varying size demonstrate end point excursions for any given rotation. It is shown that a disc with smaller radius results in less excursion of the rim. This concept can be applied to the more biologically relevant context like the human ankle joint.

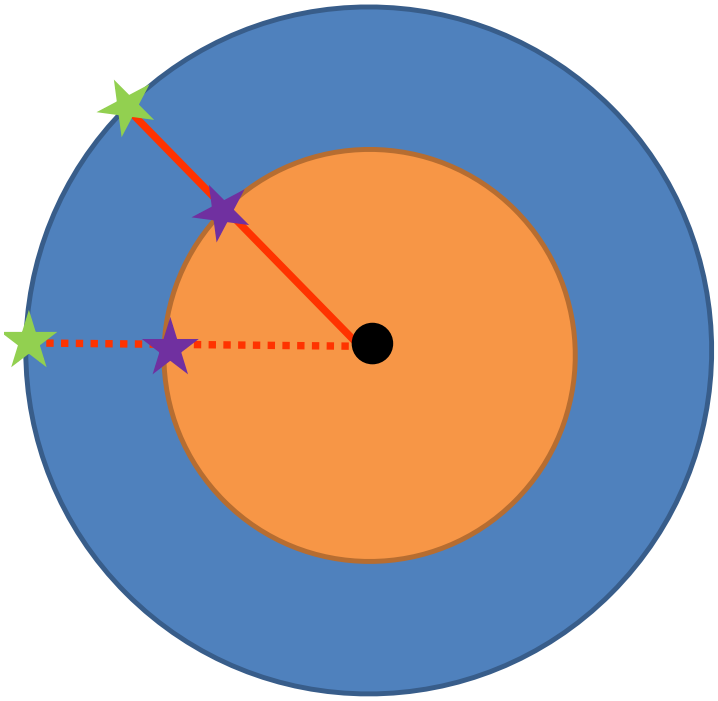

Chapter 3

Ankle Joint Mechanics and Foot Proportions Differ Between Human Sprinters and Non-Sprinters

The study was published in The Proceedings of the Royal Society: B

3.1 - SUMMARY

Recent studies of sprinters and distance runners have suggested that variations in human foot proportions and plantarflexor muscle moment arm correspond to the level of sprint performance or running economy. Less clear, however, is whether differences in muscle moment arm are mediated by altered tendon paths or by variation in the center of ankle joint rotation. Previous measurements of these differences have relied upon assumed joint centers and measurements of bone geometry made externally such that they would be affected by the thickness of overlying soft tissue. Using magnetic resonance imaging, we found that trained sprinters have shorter plantarflexor moment arms ($p = 0.011$) and longer forefoot bones ($p = 0.019$) than non-sprinters. The shorter moment arms of sprinters are attributable to differences in the location of the center of rotation ($p < 0.001$) rather than to differences in the path of the Achilles tendon. A simple computer model suggests that increasing the ratio of forefoot to rearfoot length permits more plantarflexor muscle work during plantarflexion that occurs at rates expected during the acceleration phase following the sprint start.

Keywords: humans, sprinting, plantarflexor, moment arm, center of rotation

3.2 - INTRODUCTION

Human foot and ankle structure is known to vary substantially but the implications of this variation on locomotor function are unclear. The plantarflexor moment arms (pfMA) measured in 21 adult males by Maganaris et al. (Maganaris et al., 2006) were found to range between 4.7 cm and 6.1 cm. The lengths of the metatarsals and phalanges in adult males have been found to exhibit similar variation, with between-subject standard deviations that range from 8% to 17% of their mean values (Dogan et al., 2007). While the influence of such structural variation in the human foot and ankle upon function has not received much attention, variation across species is known to correspond to differences in functional demands. Cursorial animals such as the cheetah and greyhound have long forefeet and short heels, foot proportions that permit rapid joint rotations (Hudson et al., 2011). In contrast, digging animals like the mole have limb structure that permit the large output forces that are needed for digging (Hildebrand, 1994). Within-species variations in joint and skeletal structure may have little connection to function if they are compensated for by muscular and nervous system adaptations, and animal studies have been performed to investigate how muscles adapt to acutely applied variations in muscle moment arm. Koh and Herzog (Koh and Herzog, 1998) found the muscles of rabbits to adapt to retinacular release in such a way that muscle fiber excursion is maintained, but the results of Burkholder and Lieber (Burkholder and Lieber, 1998) suggested that mouse muscles adapt to maintain optimal sarcomere length at a given joint angle. Human muscle has been shown to adapt rapidly to changes in training, loading, and exposure to bed rest (Williams and Goldspink, 1973; LeBlanc et al., 1988;

Dawson et al., 1998), but the relationship between muscle function and constraints due to joint structure are generally not well understood.

Two recent studies have investigated the influence of foot and ankle structure upon human locomotor function in the form of sprinting ability, but with inconsistent results. Lee and Piazza (Lee and Piazza, 2009) found sprinters to have shorter pfMA and longer toes than height-matched non-sprinters. Karamanidis et al. (Karamanidis et al., 2011), however, found no significant differences in pfMA, toe lengths, or midfoot lengths between a group of elite sprinters and a group of slower sprinters. The means used to quantify foot and ankle geometry in these studies were somewhat indirect. In both studies, pfMA were computed from ultrasound images of tendon excursion and measurements of joint angle rather than from the position of the Achilles tendon relative to the center of ankle rotation. Measures of toe and midfoot lengths were made from externally-identified bony landmarks with measuring tapes and without the benefit of medical imaging techniques.

Plantarflexor moment arm has the capacity to influence locomotor performance in complex ways. A long moment arm will result in more plantarflexor moment for a given muscle force, but moment arm also determines the speed at which the plantarflexors shorten during plantarflexion (Nagano and Komura, 2003; Lee and Piazza, 2009). Muscles with longer lever arms will thus shorten more rapidly during the same joint rotation and thus produce less force due to the force-velocity property of muscle. Carrier *et al*. (Carrier et al., 1994) examined the ratio of the lever arm of the ground reaction force to the length of the heel, which they took to represent plantarflexor moment arm, in

human runners. They found this 'gear ratio' to increase in late stance, allowing the plantarflexor muscle fibers to shorten more slowly and maintain force production. It is not currently known, however, whether variation in foot proportions contributes to the ability to generate propulsive muscle forces, perhaps by influencing the gear ratio.

The purpose of the present study was to determine if there are differences in the skeletal structure of the foot and ankle between two groups of humans with different functional abilities and histories: trained sprinters and non-sprinters. In this study we used magnetic resonance imaging to quantify bone lengths directly and to make geometric determination of plantarflexor moment arms. The use of magnetic resonance (MR) imaging permitted identification of the center of ankle rotation that was not possible in previous studies in which ultrasound was used to track tendon excursion, and also facilitated measurement of bony geometry that was unimpeded by soft tissue. We hypothesized that sprinters would have longer forefoot bones and shorter pfMA, which would reduce plantarflexor shortening velocity and increase plantarflexor force during acceleration at the start of a sprint race. It is hoped that characterization of within-species differences in pfMA and toe length that correspond to human sprinting ability will lead to an improved understanding of how joint mechanics and bone geometry affect human and animal locomotor function in general.

3.3 - METHODS

We studied two groups with eight male subjects in each (Table 1). The first group was composed of sprinters who were involved in regular sprint training and competition.

The second group consisted of height-matched individuals who had never trained or competed in sprinting. Inclusion for the sprinter subjects were current engagement in competitive sprinting and at least three years of continuous sprint training. Six sprinter subjects competed in the 100 m dash, with personal best times ranging from 10.5 s to 11.1 s, and two reported 200 m personal best times of 21.4 s and 24.1 s. Subjects were excluded if they had a recent history of lower extremity injuries, joint pain 6 months prior to data collection, or any obvious movement abnormalities. The experimental protocol was approved by the Institutional Review Board of The Pennsylvania State University and participants gave informed consent prior to data collection.

3.3.1 - *Imaging*

Magnetic resonance images of the right foot and ankle of each subject were acquired on a 3.0 T Siemens Trio scanner (Siemens; Erlangen, Germany). Subjects were positioned supine on the scanner bed with both knees flexed to 30° and resting on a foam pad. The right ankle was placed on an MR-compatible ankle positioning device that was constructed from plastic and fastened to the scanner gantry prior to imaging. This device supported the foot while permitting the sagittal-plane ankle position to be set. Images were acquired with the ankle positioned in 15° dorsiflexion, neutral ankle position, and 15° plantarflexion using a Siemens 4-Channel Flex coil placed around the anterior aspect of the ankle and secured using sandbags and Elements 1 to 3 of the Siemens Spine Matrix. Scans were made in each ankle position while subjects remained relaxed. Following these scans, subjects were asked to maximally cocontract their ankle musculature while not moving the foot within the positioning device. The Achilles

tendon and a point midway between the second and third metatarsal heads were palpated and identified using adhesive MR-sensitive external skin markers (Beekley Corp.; Bristol, CT, USA). The high signal intensity registered by these markers provided landmarks for slice positioning and were used to ensure that lateral motion did not occur during scanning. Imaging was performed at the magnet isocenter and verbal communication between the subject and research team was facilitated through the Siemens MR console. T2-weighted two-dimensional True FISP images were acquired with sagittal orientation aligned with the Achilles tendon and a point midway between the second and third metatarsal heads while the subject rested (field of view = 300 mm, 1.2 x 1.2 x 4.0 mm resolution, echo time = 2.2 ms, repetition time = 4.4 ms, flip angle = 50°).

3.3.2 - *Image processing*

Images were post-processed with custom written MATLAB programs (The Mathworks; Natick, MA, USA). Centers of rotation between the tibia and talus were determined from pseudo-sagittal plane (bisecting the length of the Achilles tendon and the second metatarsal bone) images made in dorsiflexion and plantarflexion using a geometric method similar to that of Reuleaux (Reuleaux, 1876) that has previously been described by Maganaris *et al.*(Maganaris et al., 1998). The Achilles tendon line of action was defined as a line drawn down the midline of the tendon on the image taken at neutral ankle position. The pfMA was measured by finding the shortest distance from the tibiotalar center of rotation (CoR) to the Achilles tendon line of action on the neutral-position scan (Figure 3.1). Centers of tibiotalar rotation were located relative to a tibia-fixed coordinate system whose Y-axis was oriented along the long axis of the tibia (with

superior being positive). The origin of this coordinate system was the intersection of the Y-axis and the tibial cortex and the X-axis was directed posterior and perpendicular to the Y-axis (Figure 2). The pfMA of a randomly selected sprinter subject was found 10 times from the same set of images and the coefficient of variation was found to be 3.5%. The standard deviation of the anteroposterior and superior-inferior CoR positions were 1.45 mm and 2.39 mm, respectively. The lengths of the first metatarsal and the proximal and distal phalanges were measure from two-dimensional images recreated from three dimensional MR data using OsiriX software (Pixmeo; Geneva, Switzerland). Lengths of bones were measured along the long axis of the bone between the intersections of the long axis and the cortex at the distal and proximal ends.

3.3.3 - *Statistics*

To test our hypotheses that the forefoot bones of sprinters are longer than those of non-sprinters and that the Achilles tendons of sprinters have smaller pfMA, unpaired, one-tailed t-tests were performed. Differences in stature, body mass, age, foot length and *x*- and *y*-coordinates of the CoR were tested for using unpaired two-tailed t-tests. A paired, two-tailed t-test was performed to compare the pfMA found at resting and contracted states. The level of significance was set at $\alpha = 0.05$ for all tests.

3.3.4 - *Computer simulation*

We developed a simple computer model to investigate the influence of variation in foot proportions on plantarflexor work during an isolated maximal plantarflexion contraction (Figure 3.3). A foot segment with very low mass was confined to planar

rotation with a revolute that represented the ankle joint. To simulate variation in foot proportions across simulations, the revolute joint position relative to the common plantarflexor tendon insertion at the extreme posterior of the foot was changed in 5 mm increments from 45 mm to 70 mm (the range for pfMA measured for our subjects) while the length of the foot was kept constant at 280 mm. The distal end of the foot was connected to a wall by a revolute joint that was permitted to slide without friction along the wall while the revolute constraint force was monitored. Three Hill-type muscle-tendon actuators (Schutte, 1992) representing the soleus and the lateral and medial heads of the gastrocnemius were included in the model and force-generating properties for each muscle (optimal fiber length, tendon slack length, maximum isometric force) were specified according to measurements made in cadaver specimens by Arnold *et al*. (Arnold et al., 2010). These actuators incorporated active and passive muscle force-length behavior, muscle force-velocity relations and tendon force-length curves as specified by Delp *et al*. (Delp et al., 1990). A full description of the details of the model is presented in Appendix A.

During each simulation the plantarflexor actuators were excited maximally as the foot pushed against the wall, which receded at a constant velocity. This velocity was varied across simulations between 0.4 m s^{-1} and 4.0 m s^{-1}, producing a range of ankle joint velocities approximately representative of the velocities occurring during the push-off of walking (Winter, 1983), the start of sprinting (Slawinski et al., 2010b), and maximal speed sprinting (Bezodis et al., 2008). The combined work done by the three muscles between neutral ankle position and the position at which contact between the toe and the

wall was broken (or 50° plantarflexion if this occurred first) was found by trapezoidal integration of the wall reaction force with respect to wall displacement.

3.4 - Results

(**a**) *Structural differences between groups*

Sprinters were found to have shorter pfMA and longer forefoot bones than non-sprinters (Table 3.2). Sprinters had pfMA measured with muscles at rest that were 7.0 mm (12%) shorter than those of non-sprinters ($p = 0.011$). The combined length of the first phalanges was 3.5 mm (6.2%) greater in sprinters ($p = 0.010$). Sprinters' first metatarsals were 2.9 mm (4.3%) longer ($p = 0.050$) and the combined length of the phalanges and metatarsal in sprinters was also significantly longer ($p = 0.019$). Sprinters' CoR were located farther posterior relative to the tibia than the CoR of non-sprinters (Figure 3.2 and Table 3.2; $p < 0.001$).

(**b**) *Contraction state during imaging*

Differences in pfMA between sprinters and non-sprinters were found both from images made with the muscles at rest and from images made with contracted muscles ($p = 0.011$ and $p = 0.021$, respectively). Significant differences in pfMA were not, however, found between resting and contracted states for either sprinters, non-sprinters, or all subjects taken together ($p = 0.133$, $p = 0.887$, and $p = 0.294$, respectively). Similarly, no significant differences in the anteroposterior or superior-inferior positions of the CoR were found between the resting and contracted states for either group or for all subjects (all $p > 0.104$).

(**c**) ***Computer simulation results***

The computer model revealed substantial differences in simulated plantarflexor work as the distance from the ankle to the heel was varied while foot length was held constant. Smaller rearfoot lengths (accompanied by longer forefoot lengths) increased the force applied to the wall by the toe and prolonged toe contact (Figure 3.4a). When the wall retreated at speeds that were consistent with the first steps of a sprint race, the foot configuration with the shortest rearfoot resulted in 3.9 times more muscle work than did the configuration with the longest rearfoot (Figure 3.4b). At slower plantarflexion velocities consistent with walking, a shorter rearfoot also resulted in greater muscle work, but at faster velocities representative of maximal sprinting, the muscles were capable of doing only negligible amounts of work for any prescribed foot geometry.

3.5 - Discussion

The results of the present study show that there are differences in the skeletal structure of the foot and ankle between two groups of healthy human subjects with different levels of locomotor performance and who also vary in the functional demands they place on their limbs. Sprinters were found to have significantly longer forefoot bones and shorter pfMA than those of non-sprinters (Table 3.2), confirming our hypotheses. For the first time, these differences have been documented using measurements made from MR images, and differences in pfMA have been accounted for by a posterior shift of the CoR in sprinters rather than differences in the Achilles tendon path (Figure 3.2). The results of simulations performed using a simple computer model

show that the differences in foot proportions we found experimentally have the capacity to increase plantarflexor work substantially during the acceleration phase of sprinting (Figure 3.4b). Simulations performed with shorter rearfoot lengths were found to increase muscle force by reducing muscular shortening velocities, and to increase the time of contact with the ground (Figure 3.4a).

Our measurements of pfMA were similar to those of previous investigators who have used similar means to quantify Achilles tendon moment arms in healthy subjects. Previous studies report mean values pfMA measured at 0° ankle flexion ranging from 48 mm to 60 mm and with standard deviations of 3.0 mm to 4.3 mm (Maganaris et al., 1998, 2000; Fath et al., 2010). Unlike previous authors, however, we did not find differences between pfMA measured with muscles at rest and those measured with the plantarflexors contracted. Maganaris and colleagues (Maganaris et al., 2000) reported moment arms that were approximately 10 mm to 15 mm greater when subjects maximally contracted. The differences between the present results and those of Maganaris *et al*. (Maganaris et al., 1998) may be due to differences in the ankle strapping technique between the two studies. When we applied a similar technique during pilot tests we found that it reduced the pfMA measured in the passive condition. It is also possible that these differences were due to our subjects' performing co-contractions of the ankle plantarflexors and dorsiflexors rather than plantarflexing against a support.

Our results are similar to those reported by Lee and Piazza (Lee and Piazza, 2009). In that study, external measurements from the tip of the first toe to the first metatarsal head were made to approximate toe length, and an ultrasound probe was used

to track Achilles tendon excursion during plantarflexion. In the current study, MR imaging was used to make direct measurements of the lengths of the first phalanges and first metatarsal. MR-based measurement of pfMA also permitted location of the ankle CoR that permitted insight into the mechanism underlying differences in moment arm. We found smaller differences in pfMA (12% compared to 25%) than those previously reported by Lee and Piazza (Lee and Piazza, 2009) and these disparities may derive from incorrect assumptions related to the tendon excursion method made in the earlier study. Computation of muscle moment arms from tendon excursion is based on the Principle of Virtual Work, which requires that the energy stored in the tendon does not change during the joint rotation (An et al., 1984). However, it is not possible to maintain constant tendon force *in vivo*, thus leading to measurement errors. Also, the mechanical properties of tendons in sprinters differ from non-sprinters (Arampatzis et al., 2007b), complicating the assessment of pfMA differences using tendon excursion. In addition, the subjects studied by Lee and Piazza (Lee and Piazza, 2009) maximally contracted their plantarflexors during measurement of tendon excursion, which may have resulted in additional tendon shortening with plantarflexion among the sprinters that would have been interpreted as a smaller moment arm.

Very few studies have investigated differences in foot and ankle structure and how it relates to functional abilities in humans. Several authors have used indirect measurements to compare foot structure and running economy and sprinting performance, however, none of those investigators who measured plantarflexor moment arms located the ankle CoR (Scholz et al., 2008; Lee and Piazza, 2009; Karamanidis et

al., 2011; Raichlen et al., 2011). The results of the present study reveal differences between sprinters and non-sprinters in the anteroposterior location of the tibiotalar CoR relative to the tibia. This finding raises important questions about whether between-subject variation in muscle moment arm is generally due to differences in CoR location and, if so, whether the CoR location depends on bone shapes or if it is modulated by specific patterns of muscle activity. We examined our sagittal MR images to determine if there were differences in talar dome curvature that might be expected to determine joint kinematics (Leardini et al., 1999), but we did not find any. Further investigation is needed to identify the influence of surface geometry and ligaments on joint kinematics and muscle moment arms in functionally different groups.

The finding that pfMA are shorter and forefoot bones are longer in sprinters suggests that foot proportions may influence the capacity for acceleration. The computer simulation shows that a longer forefoot and shorter pfMA permits the plantarflexors to do more work at certain velocities (Figure 3.4b). At slower velocities, this additional work output is not likely to be of use, because each foot proportion simulated results in muscle work being done that was far greater than the ~26 J necessary for walking (Winter, 1983). At higher speeds consistent with the start of a sprint race, however, the model shows that sprinter-like foot proportions convey a substantial advantage. At speeds consistent with maximal sprinting, our model suggests that plantarflexion occurs at a rate too high for any positive muscular work to be done. The plantarflexors of bipeds such as wild turkeys and wallabies isometrically contract during high speed running and hopping, modulating stiffness and aiding in calcaneal tendon energy storage and return (Roberts et

al., 1997; Biewener et al., 1998). Similarly, horses are able to run at high speeds with very short digital flexor muscles that facilitate energy storage and return from extremely long tendons (Wilson et al., 2001). While we did not measure the ground reaction force moment arms and varying pfMA necessary to compute actual gear ratios, it is reasonable to expect longer forefoot bones coupled with shorter pfMA would result in a larger gear ratio. Larger gear ratios have been found to occur during the late stance phases of accelerating human runners (Carrier et al., 1994) and similar differences in foot proportions have been noted in elite animal sprinters (Hildebrand, 1994; Hudson et al., 2011).

There are many factors known to contribute to elite sprint performance, and the present results do not demonstrate that foot proportions or plantarflexor tendon leverage is a primary determinant of sprinting ability. Muscular strength and the proportion of fast-twitch fibers to slow-twitch fibers are correlated with maximal running velocity (Mero et al., 1981). The muscle fibers of sprinters, especially sprinters' fast twitch fibers, have been reported to have faster fiber conduction velocities than those of distance runners (Sadoyama et al., 1988). The knee extensors and plantarflexors of sprinters are thicker, have smaller pennation angles, and longer muscle fascicles than those of distance runners and non-sprinters (Abe et al., 2000, 2001; Lee and Piazza, 2009). Similar differences in muscle architecture have been documented between highly skilled sprinters and less skilled sprinters (Kumagai et al., 2000), although Karamanidis *et al.* (Karamanidis et al., 2011) failed to identify such differences in a similar study. It is

unknown how any benefits conveyed by foot and ankle structure might compare to those that follow from these characteristics and others.

It is unclear whether differences in foot and ankle skeletal structure are adaptations to sprint training or hereditary, but there is evidence that human skeletal strength and form is altered by certain forms of athletic training. Prolonged participation in activities such as running and gymnastics promote increases in lower leg bone thickness and greater radii cortical areas, respectively (MacDougall et al., 1992; Ward et al., 2005). Athletes involved in sports in which one hand is primarily used, such as bowling and tennis, have thicker and denser humeri and radii on the dominant side (Calbet et al., 1998; Young et al., 2011). Torsion deformation of the humerus has been documented in handball and baseball players (Pieper, 1998; Warden et al., 2009). These adaptations may function as a safety mechanism that corresponds to increased range of motion of the throwing shoulder (Pieper, 1998). Biewener and Bertram (Biewener and Bertram, 1994) documented reductions in tibia length during development when the limbs of chicks were denervated. The authors found no differences in bone length between sedentary and exercised animals, however. Carpenter and Carter (Carpenter and Carter, 2010) used a computer model to simulate straightening of a congenitally bowed tibia in response to repeated loading. It is unknown, however, if human bone lengths or muscle moment arms adapt in similar ways in response to sport training.

Certain limitations affected our study. We were able to perform MR scans of only eight subjects in each group. The sprinters we tested were for the most part club track athletes who may not be classified as ‘elite’ but who were well trained (average

training, 6.5 ± 2.8 years). We measured pfMA only for neutral ankle position and assumed that rotations of the foot relative to the tibia were represented by tibiotalar rotation. Another limitation is that, like those of previous authors (Maganaris et al., 1998) who measured Achilles tendon moment arms, our analysis was two-dimensional. The axis of tibiotalar rotation, however, is known to vary in its location and orientation throughout plantarflexion (de Asla et al., 2006) and rotations out of the sagittal plane could not be accounted for using our planar imaging techniques. The simplified ankle joint and muscle-tendon geometry in our computer model caused pfMA to decrease with plantarflexion; a more complex model might have incorporated a mechanism by which pfMA would remain constant or increase slightly with plantarflexion, behavior that has been reported *in vivo* (Maganaris et al., 1998).

The results of the present study are significant because they are the first indication that variation in the location of the CoR are responsible for differences in joint leverage between functionally different but otherwise healthy groups of humans. Our simple computer simulations show that foot proportions consistent with the pfMA and forefoot bone lengths we measured provide considerable force generating advantages to those with 'sprinter-like' feet. Further research is needed to identify the structural mechanisms that account for differences in CoR and to determine whether differences in CoR and forefoot bone lengths are determined by genetics or are an adaptation to training.

3.6 ACKNOWLEDGMENTS We would like to thank the coaches of the Penn State Track Club, who assisted with the recruiting of participants, and the staff of the Penn State Social, Life, and Engineering Sciences Imaging Center (SLEIC).

Figure Captions

3.1 Magnetic resonance image of a sagittal cross-section of the foot and ankle in neutral position showing measurements of bone lengths and pfMA. Symbols are defined in Table 2.

3.2 Illustration of sprinter and non-sprinter CoR locations with respect to tibia. Sprinters' centers of rotation between the tibia (Ti) and talus (Ta) were located farther posterior relative to the long axis of the tibia than those of non-sprinters.

3.3 Schematic of musculoskeletal model. Foot pushes maximally against a retreating wall of constant velocity. The position of the ankle joint is varied while the foot length is held constant.

3.4 Results of a computer simulation of the foot maximally pushing against a retreating wall as foot proportions (but not foot length) are varied. (a) Simulations performed using this simple model showed that a greater ratio of forefoot length to rearfoot length (R/r) permitted greater force at the toe and extended the time of toe contact. (b) Ankle plantarflexor work for different rates of plantarflexion and different rearfoot lengths. At ankle rotation velocities similar to those reported for the sprint start, the shortest rearfoot length simulated permits the production of 3.5 times more work than the longest rearfoot length. At maximal sprinting plantarflexion speeds, the shortening velocities of the muscle fibers are so great that the muscle cannot do work on the wall.

Table Captions

3.1 Subject characteristics.

3.2 Measurements of foot and ankle structure. * $p \leq 0.05$. L_{DP1} – Length of 1st distal phalanx, L_{PP1} – Length of 1st proximal phalanx, L_{MT1} – Length of 1st metatarsal, $L_{R1} = L_{DP1 +} L_{PP1 + MT1}$ – length of 1st ray, X_{CoR} – anteroposterior position of the center of tibiotalar rotation relative to long axis of tibia. Y_{CoR} – superior-inferior position of the center of tibiotalar rotation.

Figure 3.1 - Magnetic resonance image of a sagittal cross-section of the foot and ankle in neutral position showing measurements of bone lengths and pfMA.

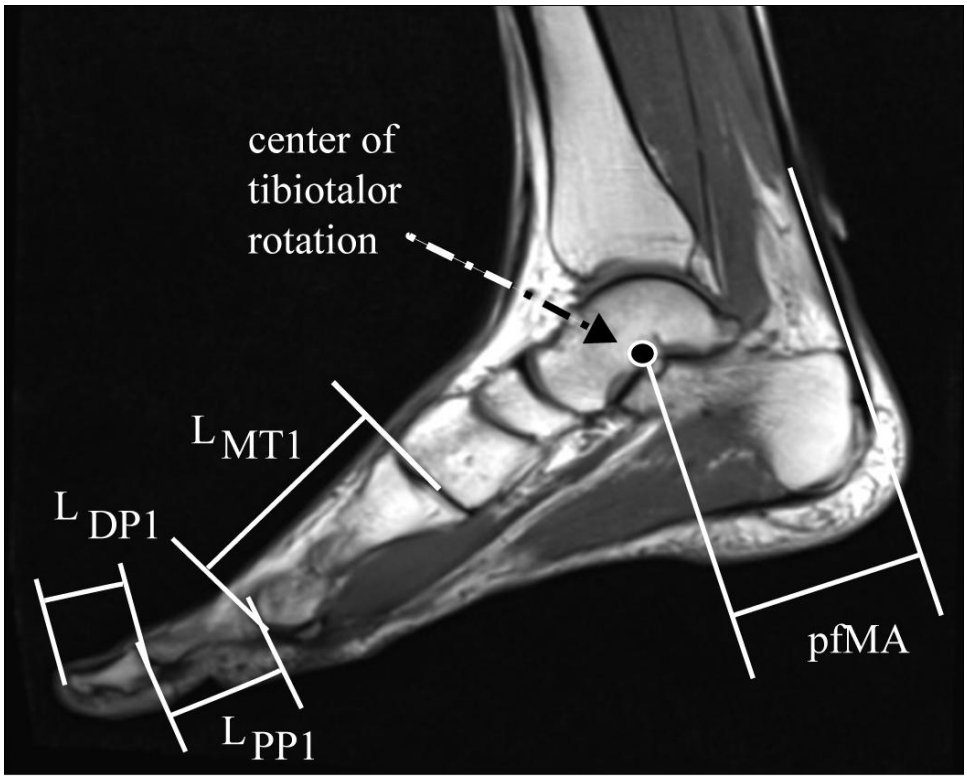

Figure - 3.2 Illustration of sprinter and non-sprinter CoR locations with respect to tibia.

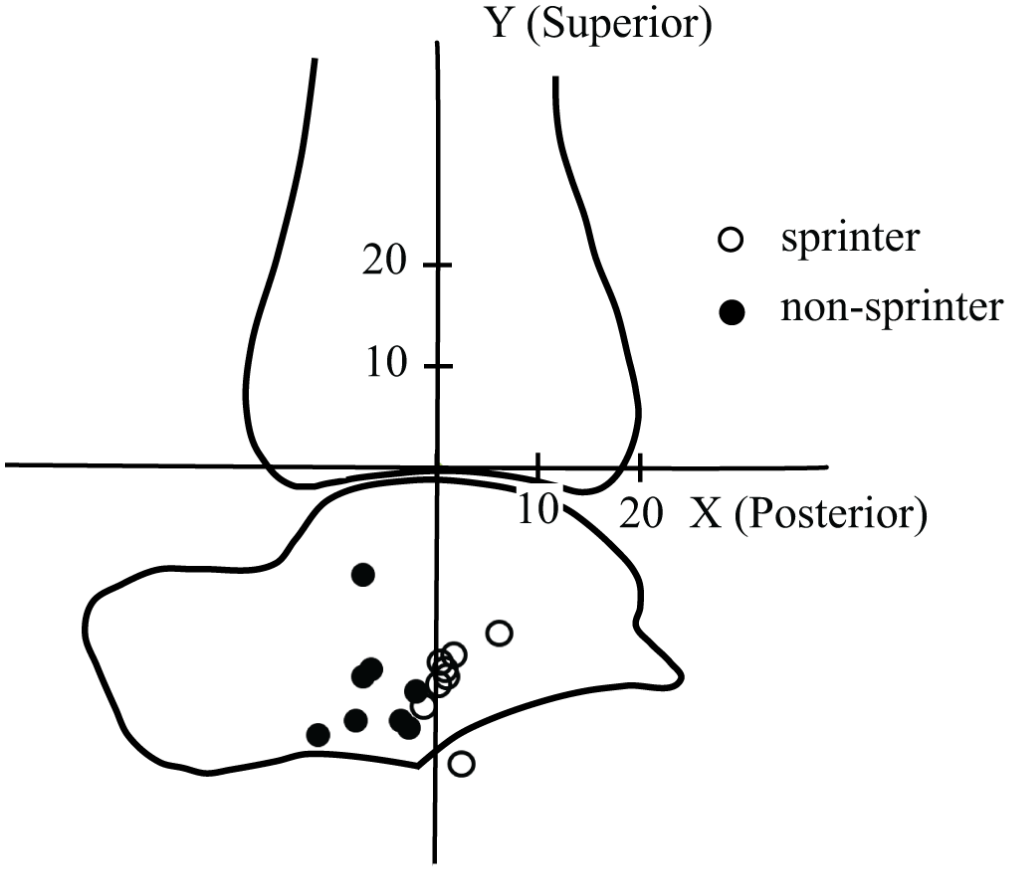

Figure 3.3 - Schematic of musculoskeletal model. Foot pushes maximally against a retreating wall of constant velocity.

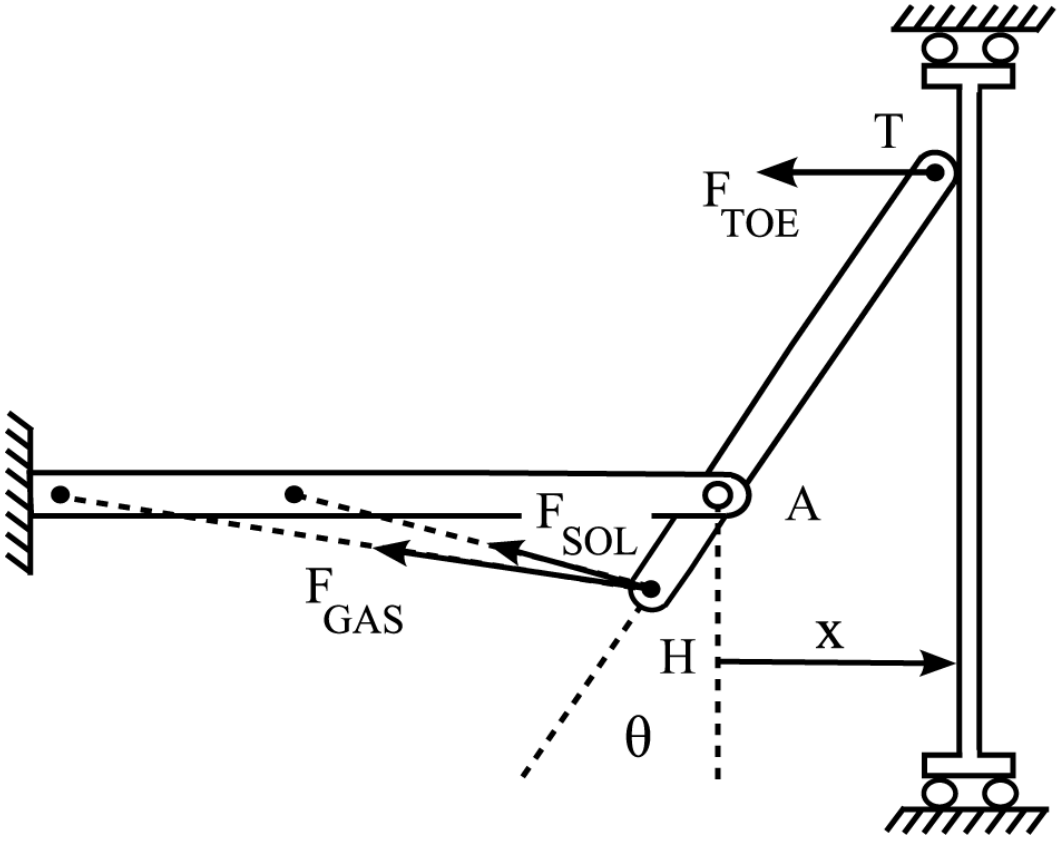

Figure 3.4 - Results of a computer simulation of the foot maximally pushing against a retreating wall as foot proportions (but not foot length) are varied.

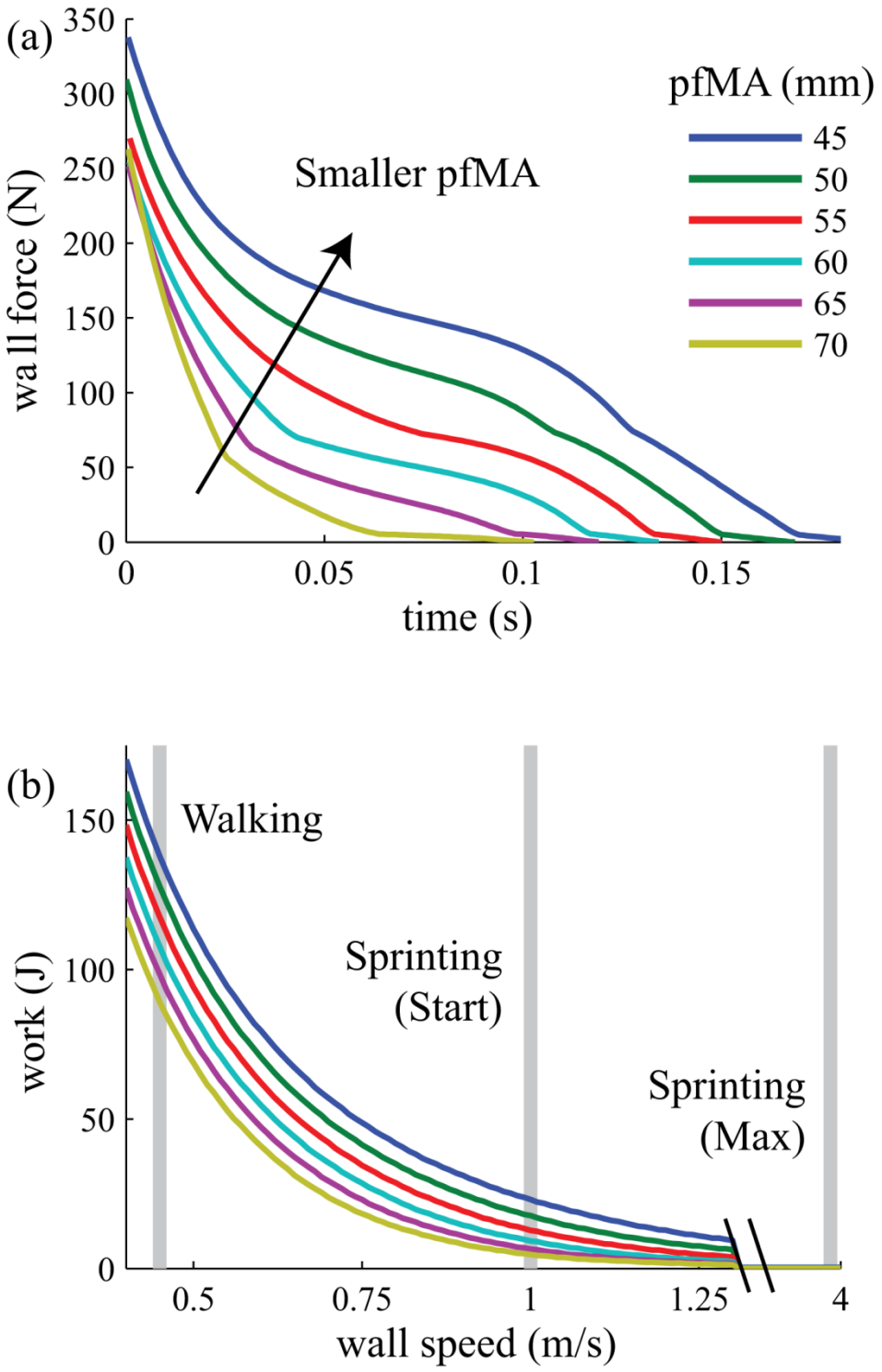

Table 3.1. Subject characteristics.

	Sprinters (n = 8)	non-sprinters (n = 8)	p-value
Stature (cm)	177.4 ± 7.2	177.1 ± 7.0	0.944
Body Mass (kg)	76.3 ± 7.9	82.0 ± 8.9	0.252
Age (y)	21.3 ± 2.5	24.0 ± 2.6	0.051
Foot Length (cm)	27.5 ± 1.2	27.5 ± 0.9	0.946

Table 3.2. Measurements of foot and ankle structure.

	Sprinters (n = 8)	non-sprinters (n = 8)	p-value
L_{DP1} (mm)	26.8 ± 1.2	25.2 ± 2.3	0.052
L_{PP1} (mm)	32.9 ± 1.5	31.0 ± 1.7	0.017*
$L_{DP1} + L_{PP1}$ (mm)	59.7 ± 2.0	56.2 ± 3.2	0.010*
L_{MT1} (mm)	70.1 ± 2.0	67.2 ± 4.2	0.050*
L_{R1} (mm)	129.8 ± 3.7	123.4 ± 7.0	0.019*
$pfMA_{resting}$ (mm)	51.5 ± 3.9	58.5 ± 6.6	0.011*
$pfMA_{contracted}$ (mm)	52.9 ± 4.8	58.7 ± 5.4	0.021*
L_{R1}:$pfMA_{resting}$ (1)	2.5 ± 0.2	2.1 ± 0.2	0.001*
X_{CoR} (mm)	1.2 ± 2.1	-6.0 ± 3.1	< 0.001*
Y_{CoR} (mm)	-21.0 ± 3.9	-21.8 ± 5.1	0.730

CHAPTER 4

Talocrural Geometry Does Not Differ Between Sprinters and Non-Sprinters

This paper is in preparation for submission to Journal of Anatomy

4.1 INTRODUCTION

Several recent studies have linked leverage in the foot and ankle to locomotor function (Scholz et al., 2008; Lee and Piazza, 2009, 2012; Baxter et al., 2011; Raichlen et al., 2011). Trained sprinters have been found to possess shorter plantarflexor moment arms (pfMA) and longer forefoot bones than non-sprinters. Simple computer simulations suggest that these structural differences may increase ankle power generation during the critical acceleration phase of a sprint race (Lee and Piazza, 2009; Baxter et al., 2011).

Our recent work using magnetic resonance (MR) imaging revealed differences in pfMA between sprinters and non-sprinters that could be attributed almost entirely to differences in talocrural joint kinematics. The location of the center of rotation (CoR) of the talus with respect to the tibia in sprinters was on average 7.2 mm posterior to its location in non-sprinters, placing it closer to the Achilles tendon and reducing pfMA (Baxter et al., 2011). This finding raises the question: What are the factors responsible for differences in talocrural mechanics and pfMA between these two populations? One possibility is that the shapes of the tibia and talus are what guides the motions of these bones relative to one another. Analyses of sagittal cross section MR images, however, revealed no significant differences in curvature of the talar dome and tibial plafond between groups (Baxter et al., 2011).

In addition to osseous geometry, talocrural joint kinematics are likely to be influenced by articular cartilage, the orientation and stiffness of ligaments, and active and passive muscle forces. The relative contributions of these factors to ankle joint function, however, are not well understood and have not received a great deal of attention. Movement of the talocrural CoR during passive ankle rotation has been recreated using a simple four-bar linkage with members representing ligaments and articular contact (Leardini et al., 1999). More sophisticated subject specific models of the ankle joint complex that consider bone and ligament variation faithfully predict passive ankle motion (Imhauser et al., 2008).

The purpose of this study was to examine the three-dimensional articular geometry of the talocrural joint to test for differences between sprinters and non-sprinters that might explain the previously observed CoR difference between the two groups. Cylinders fit to the tibial plafond and talar dome were examined for differences in size, orientation, and relative position. We hypothesized that the difference between the tibial radius and talar radius would be greater in sprinters than non-sprinters.

4.2 Methods

4.2.1 *Subjects*:

Two groups of eight subjects were recruited for this study (Table 4.1). The first group consisted of eight male sprinters who were involved in regular sprint training and competition. The second group was composed of eight height-matched control subjects who had never trained or competed in sprint events. Sprinter subjects were currently

engaged in competitive sprinting and had at least 3 years of continuous sprint training (average training: 6.5 ± 2.8 years). Six sprinter subjects recorded personal best times in the 100 m dash ranging from 10.5 to 11.1s, and the other two sprinter subjects reported 200 m personal best times of 21.4 and 24.1 s. Subjects were screened for any recent history of lower extremity injuries, joint pain six months prior to data collection, or any obvious movement abnormalities. Previous analyses of these same subjects found that the sprinter group had significantly shorter pfMA (mean difference of 7.0 mm), and that these differences in joint leverage are explained by a more posterior location of the CoR with respect to the midline of the tibia (7.2 mm) (Baxter et al., 2011).

4.2.2 *Imaging*

MR images of the right foot and ankle were acquired on a 3.0 T Siemens Trio Scanner (Siemens; Erlangen, Germany). Subjects were positioned supine on the scanner bed and both knees rested on a foam wedge that placed the knees at 30° flexion. The right foot was placed on an MR-compatible device that positioned the foot and ankle at neutral ankle position while subjects remained passive. Images were acquired using a Siemens 4-Channel Flex coil placed around the anterior aspect of the ankle and elements 1 to 3 of the Siemens Spine Matrix. T1-weighted images were acquired with a sagittal orientation while the subject rested (field of view = 300mm, 1.2 x 0.9 x 3.0 mm resolution, echo time = 16.0 ms, repetition time = 852 ms).

4.2.3 *Image processing*

MR images were imported into Simpleware ScanIP (Exeter, United Kingdom), a commercially available software suite. Using specialized threshold tools, the tibia and talus were segmented into separate masks using their grayscale values. Manual revisions were made to each slice of the scan using a paint tool to segment the soft tissue from bone. Each mask was left unfiltered and exported as a CAD model. Data were then imported into Avizo, a three-dimensional visual analysis software package (Visualization Sciences Group, Merignac Cedex, France), and the articular surfaces of the talar dome and tibial plafond were identified and exported as a series of points distributed over each surface and expressed in the scanner coordinate system.

4.2.4 *Parameter Optimization*

Cylinders were fit to the articular surface points using a parameter optimization routine implemented in MATLAB (Mathworks, Inc; Natick, MA, USA). The parameters (p) for each fit were the radius of the cylinder (R), the three components of the unit vector along the long axis of the cylinder (u), and the three-dimensional coordinates of a point on the long axis (P). The MATLAB optimization function *fmincon* was used to minimize the objective function J(p), representing the root-mean-squared difference between the points and the surface of the cylinder:

$$J(p) = \sqrt{(\sum_{i=1}^{n}(R - r_i)^2)/n} \tag{4.1}$$

Where $r_i = pt + s \cdot uv$, and s is expressed by

$$s = (x_i - P) \cdot u$$

Where x_i = i^{th} point on bone surface.

During the optimization, an equality constraint was applied to maintain the length of unit vector u:

$$ceq = |u| - 1$$

and an inequality constraint prevented the cylinder radius from taking on negative values:

$$R > 0$$

The ISB ankle joint system was defined for each subject and cylinder axes were transformed to the ankle joint coordinate system (Wu et al., 2002). Parameters reported include the tibia and talus radii (TIBR and TALR, respectively), the skew angle between TIBR and TALR (SKEW), the position of the midpoint of TALR with respect to the ankle joint coordinate system, and the coverage angle, the angle between the two planes that pass through the talus cylinder axis and surround the anterior and posterior borders of the tibial plafond (Figure 4.1).

4.2.5 *Statistics*

Multiple analysis of variance (MANOVA) with post-hoc pairwise comparisons was used to test for talocrural differences between groups. The analysis was performed in IBM SPSS (Version 20, Armonk, New York), and significance levels were set at $\alpha = 0.05$.

4.3 RESULTS

The tibia and talus were well fit by cylinders in all cases. The RMSE values for these fits, given by the value of the objective function, were found to be 0.5 ± 0.1mm (range 0.3 to 0.8) for all tali and 1.2 ±0.2 mm (range 0.8 to 1.6) for all tibiae. There was no significant difference in the quality of these fits between the sprinters and non-sprinters ($p > 0.296$).

Sprinter-nonsprinter comparisons (Table 4.2) yielded a significant difference in coverage angle between groups ($p = 0.016$), but all other differences in cylinder radius and orientation were found to be insignificant ($p > 0.140$). The mean difference in coverage angle between sprinters and non-sprinters was 2.8°. Coverage angle for sprinters was found to be 72.6° ± 2.5° for sprinters and 75.4° ± 1.4° for non-sprinters.

4.4 DISCUSSION

In a previous study, we found that sprinters have smaller pfMA than non-sprinters and that these differences are explained by a posterior shift of talocrural CoR (Baxter et al., 2011). In the current study, we found that while most of the measures of talocrural geometry were not significantly different between sprinters and non-sprinters, the coverage angles of sprinters are significantly smaller than non-sprinters. The results of the present study did not support our hypothesis that the difference between the tibial and talar radii would be larger in sprinters than non-sprinters. Cylinders were found to fit the talar and tibial joint surfaces well.

In the present study, we found TALR (21.3 ± 1.7 mm) was similar with TALR (17.7 ± 1.9 mm) reported in the literature (Frigg et al., 2007). Three-dimensional coverage angles of 73.8 ± 2.0° are substantially smaller than coverage angles measured in two-dimensions (80 – 88.4 ± 6.4°) (Magerkurth et al., 2006; Frigg et al., 2007). These published values were obtained from radiographs instead of three-dimensional data sets. Unlike the planar analyses of coverage angle that measured to the most anterior and posterior boundaries of the bone, three-dimensional coverage angles only encompassed the articulating surface of the tibial plafond.

Patients with excessive joint laxity have been found to have smaller coverage angles and larger talus radii (Frigg et al., 2007). A simple biomechanical model was used by Frigg et al (2007) to show that reduced coverage angles increase the likelihood of joint dislocation. While sprinters would not be expected to benefit from joint dislocation, it may be that sprinters experience enhanced plantarflexor leverage by having more mobile joints. Such joint mobility might facilitate talocrural configurations that place the joint in a more advantageous position for force generation. However, the difference in coverage angle between groups was small and it is likely that CoR location is modulated by other factors as well. Ligaments and active control appear to be likely candidates for influencing joint kinematics (Wu et al., 2002; Imhauser et al., 2008).

There are several limitations that affected this study. MR scanning parameters were not chosen specifically for the purpose of analyzing bone geometry. The slice thickness (3.0 mm) was relatively thick and we were unable to identify ligaments and osteophytes that may influence talocrural mechanics. The number of subjects scanned

was small; we were able to recruit only eight sprinters and eight height-matched controls. Further, the sprinter subjects would not be classified as ‘elite’, although they had participated in sprint training for a number of years.

In conclusion, talocrural CoR differences between sprinters and non-sprinters may be partly explained by reduced coverage angles in sprinters. Increased joint mobility may place the plantarflexors of sprinters in more favorable circumstances to generate force by reducing shortening velocities, and it is unclear if differences in coverage angle are the result of sprint training. The differences in coverage angle we found were small, however, and further investigations that consider muscle control and the roles of other soft tissues are needed.

Figure Captions

4.1 **Three-dimensional representation of the coverage angle.** This angle is computer as the cosine of the dot product of Q and R, where Q is the vector normal to the plane that passes through the talar cylinder axis and intersects the most anterior point on the tibial plafond, and R is the vector normal to the plane that passes through the talar cylinder axis and intersects the most posterior point on the tibial plafond.

Table Captions

4.1 Subject characteristics

4.2 Talocrural geometry parameters. *p-value < 0.05, group means are significantly different.

4.1 - Three-dimensional representation of the coverage angle.

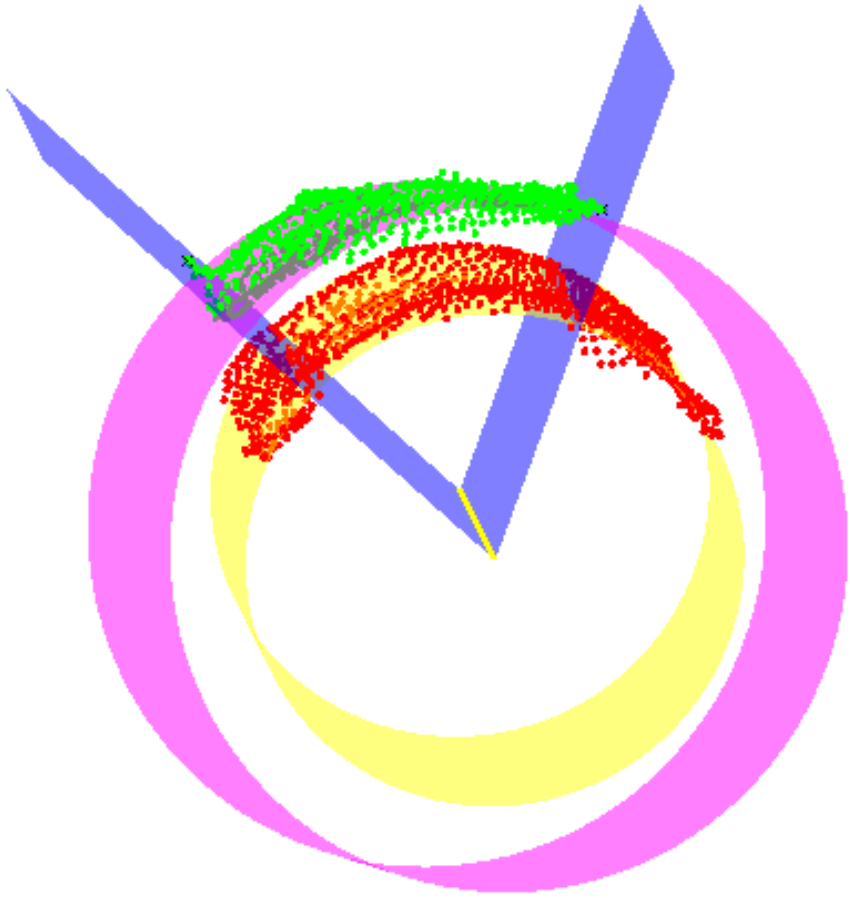

4.1 - Subject characteristics

	Non-Sprinters n = 8	Sprinters n = 8	p-value
Stature (cm)	177.4 ±7.2	177.1 ± 7.0	0.944
Body mass (kg)	76.3 ± 7.9	82.0 ± 8.9	0.252
Age (years)	21.3 ± 2.5	24.0 ± 2.6	0.051
Foot length (cm)	27.5 ± 1.2	27.5 ± 0.9	0.946

4.2 - Talocrural geometry parameters.

	Non-Sprinters n = 8	Sprinters n = 8	p-value
Coverage Angle (°)	75.4 ± 1.4	72.6 ± 2.5	0.016*
TIBR (mm)	34.1 ± 7.8	37.2 ± 14.5	0.583
TALR (mm)	21.9 ± 1.7	20.6 ± 1.7	0.140
TIBR – TALR (mm)	12.1 ± 8.2	16.7 ± 14.4	0.445
TALX (mm)	1.1 ± 3.7	0.7 ± 2.0	0.783
SKEW (°)	12.8 ± 3.7	10.6 ± 4.2	0.294

CHAPTER 5

Correlation Between Ankle Strength and Plantarflexor Moment Arm in Healthy Young Men

This paper is in preparation for submission to Journal of Applied Physiology

5.1 INTRODUCTION

The moment produced by a muscle about a joint is the product of the force carried by the tendon of the muscle and the moment arm of the muscle-tendon unit about the joint. Knowledge of how muscle force and moment arm vary with one another across individuals and how they combine to influence muscle moments is important for understanding limitations on performance. Older adults who walk slowest, for example, tend to be those with decreased capacity for producing muscular plantarflexor torques and powers (Judge et al., 1996; Graf et al., 2005), but little is known about the factors that contribute to their impaired ankle kinetics. Plantarflexor muscle volume (pfVOL) has been correlated with maximal plantarflexor torque in healthy young adults (Fukunaga et al., 2001b; Morse et al., 2004) but similar correlations between maximal plantarflexor torque and plantarflexor moment arm (pfMA) have not been investigated.

Reductions of walking velocity in the elderly has been associated with losses in ankle torque and power (Judge et al., 1996; Graf et al., 2005). Although joint torque is the product of muscle moment arm and muscle force, the relationship between these determinants and joint function are not well understood. Muscle volume is correlated with maximal joint torque in healthy young adults (Fukunaga et al., 2001b; Morse et al.,

2004). However, since ankle strength is not completely explained by muscle volume (Morse et al., 2004), it stands to reason that pfMA should be a predictor of isometric strength, but this has yet to be shown in the literature. Computer simulations and measurements in sprinters suggest that smaller pfMA augments muscle force generation during fast joint rotations in which muscles shorten rapidly (Nagano and Komura, 2003; Lee and Piazza, 2009; Baxter et al., 2011); yet, such effects have not been measured experimentally.

Computer simulations incorporating mathematical models of muscle suggest that smaller pfMA may actually augment plantarflexor force during rapid plantarflexion by reducing plantarflexor shortening velocity (Nagano and Komura, 2003; Lee and Piazza, 2009; Baxter et al., 2011). Nagano and Komura (2003) showed that the force-velocity effects that would reduce plantarflexor force during fast ankle rotations were reduced by assigning small pfMA in their model. These results suggested that torque and power could be maximized by trading leverage for force generation. Lee and Piazza (2009) used a simple model of sprinting to show that long toes and short pfMA increase contact time with the ground and reduce rates of plantarflexor shortening, increasing the propulsive impulse applied as the foot pushes off of the ground. A similar model was used by Baxter et al. (2011) to show that the work performed by ankle muscles increased when pfMA was smaller relative to foot length. In these computer simulations, however, musculoskeletal adaptations to variations in muscle moment arm were not modeled, so it is unclear whether enhanced plantarflexor force production would be evident during *in vivo* isokinetic assessment of maximal plantarflexor torque.

Acute musculoskeletal adaptation has been shown to occur in animal models in response to surgically imposed changes in muscle moment arm. Koh and Herzog (1998) increased the dorsiflexor moment arm in rabbits through retinacular release and found increases in the number of sarcomeres that reduced muscle force and thus preserved muscular joint moment throughout the range of motion. A similar surgery on mice described by Burkholder and Lieber (1998) produced decreases in the number of sarcomeres such that the joint angle at which peak force occurred was maintained. While the results of both of these studies suggest that the muscles of an individual adapt to sudden alterations in moment arm to maintain joint function, it is unclear if natural variation in joint leverage across individuals is accompanied by concomitant variations in muscle structure that preserve joint function.

Links between pfMA and locomotor function in humans have been suggested by the results of several recent investigations (Scholz et al., 2008; Lee and Piazza, 2009, 2012; Baxter et al., 2011; Raichlen et al., 2011). These have included negative correlations between pfMA and running economy (Scholz et al., 2008; Raichlen et al., 2011) and smaller pfMA measured for trained sprinters as compared to control subjects (Lee and Piazza, 2009; Baxter et al., 2011). While the authors of these studies proposed mechanisms by which pfMA influenced ankle kinetics, ankle kinetics were not measured either during locomotion or in a controlled setting using a dynamometer. It may be that there is adaptation of plantarflexor force generating properties to pfMA such that individuals with larger moment arms generate less muscle force, reducing variation in plantarflexor muscle moments across individuals. Ahn et al (2011), for example, found

gastrocnemius thickness to vary inversely with pfMA, perhaps indicating this type of covariation between muscle force and moment arm. Another possibility is that individuals with larger moment arms will be those who have larger and stronger muscles; this was the finding of Sugisaki et al (2010) who found a correlation between muscle volume and moment arm in human elbow extensors.

The purpose of this study was to measure the maximal isometric and isokinetic plantarflexor torque in healthy young males in order to determine if maximal torque is correlated with pfMA and pfVOL. We hypothesized that plantarflexor torque will be positively correlated with both pfMA and pfVOL during isometric and slow isokinetic contractions and that the correlation with pfMA will weaken during fast isokinetic plantarflexions, as subjects with larger pfMA will see force reductions at these higher speeds.

5.2 METHODS

5.2.1 *Subjects.*

Twenty healthy young adult males participated in this study. Subjects had no recent history of musculoskeletal injury to the foot or ankle and all were recreationally active, although none were engaged in competitive sprinting or sprint training. Subject mean (SD) age, height, body mass and foot length were 26.0 (3.5) y, 177.7 (7.7) cm, 76.3 (15.6) kg, and 268.0 (13.0) cm, respectively. All procedures were approved by the Institutional Research Board at The Pennsylvania State University.

5.2.2 *Strength Dynamometer Testing*.

Subjects were seated in an isokinetic dynamometer (System 3, Biodex Medical Systems; Shirley, New York) with the unshod right foot secured to the foot plate with non-elastic straps to prevent foot movement during the study, and with the lateral malleolus aligned with the motor spindle. The right knee was fully extended and the right thigh was strapped to the seat to prevent knee flexion. Neutral ankle position (0°) was defined as occurring when a right angle was formed by the foot plate and the long axis of the shank. Dorsiflexion ankle angles were defined as negative and plantarflexion angles were defined as positive values. To set the ankle range of motion, subjects' ankles were slowly rotated into dorsiflexion until subjects reported slight plantarflexor 'tightness'; this occurred at angles greater than 10º dorsiflexion for all subjects. Maximal plantarflexion was set to 30º for all subjects.

Maximal plantarflexor torques were measured using the following procedures. In isometric tests, subjects were instructed to push against the footplate maximally for at least two seconds as isometric plantarflexor torque was measured at neutral ankle position.. Maximal isometric contractions were performed with rest periods of at least five seconds between each effort. Three maximal contractions were collected for each subject. In isokinetic tests, maximal plantarflexor contractions were performed as the foot plate was rotated in the plantarflexion direction at 30, 120, 210, and $300°\cdot s^{-1}$. Subjects used a handheld switch to manually initiate foot-plate rotation and were instructed to 'simultaneously press the hand switch and press as hard and fast as possible against the foot plate'. To acclimate to the isokinetic trials, subjects performed at least three practice

contractions at each velocity. Subjects then completed a set of five maximal contractions at each of the four plantarflexion speeds. Rest was provided between contractions and the order of speeds was randomized. During each contraction, subjects received verbal encouragement to plantarflex maximally from the same investigator. The torques measured as the ankle passed through the neutral position were those analyzed for all trials. Because five subjects were unable to consistently accelerate the footplate to $300°\cdot s^{-1}$ at neutral position this speed was excluded from subsequent analysis.

5.2.3 Magnetic Resonance Imaging.

To quantify pfMA and pfVOL, magnetic resonance (MR) images of the right leg, foot, and ankle of each subject were acquired with a 3.0 T Siemens Trio scanner (Siemens; Erlangen, Germany) while subjects remained passive. Subjects were positioned supine on the scanner bed with both knees fully extended. The right ankle was placed on an MR-compatible ankle-positioning device that was constructed from plastic and fastened to the scanner bed prior to imaging. This device supported the foot while allowing for manual positioning of the ankle. Non-elastic straps secured the right foot to the ankle-positioning device to minimize movement during scans. MR images were acquired with the ankle positioned at 10° dorsiflexion, neutral ankle position, and 10° plantarflexion (Three dimensional 3D isotropic T1 weighted sequence; TE: 1.31 ms, TR: 3.96 ms, 300 mm field of view, 0.6mm voxel size). The complete volume of the lower leg was acquired at neutral ankle position (3D isotropic T1 weighted; TE: 1.09 ms, TR: 3.96 mm, 500 mm field of view, 0.9mm voxel size).

5.2.4 Image Processing.

MR image data were processed using Osirix software (Pixmeo, Geneva, Switzerland). Quasi-sagittal plane images were reconstructed and printed onto transparent sheets. The center of rotation between the tibia and talus at neutral position were determined using a modified Reuleaux method (Figure 5.1) that has previously been described in detail (Rugg et al., 1990; Maganaris et al., 1998; Fath et al., 2010; Baxter et al., 2011). Plantarflexor moment arm was defined as the shortest distance between the Achilles tendon line of action and the center of tibiotalar rotation. To measure pfVOL, 1 mm thick axial slices of the shank were reconstructed in Osirix viewer and every tenth image was analyzed to approximate 1 cm axial slices (Narici et al., 1992). The margins of the triceps surae were difficult to identify on some images, so the entire posterior compartment of the leg was outlined on each slice with ImageJ (1.45s, NIH, Betheshda, MD, USA). Total pfVOL was found as the product of the summed slice areas and the slice thickness (Figure 5.2). Scans were repeated on a second day for three subjects to assess reliability; the day-to-day differences in pfMA and pfVOL averaged across subjects were 2.7 % and 0.8 %, respectively.

5.2.5 *Statistical Tests*.

Simple and multiple linear regression was performed to test for the correlations between pfVOL and torque and between pfMA and torque. A repeated-measures one-way ANOVA with post-hoc pairwise comparisons was performed to compare the torque values at each velocity condition. To test our hypothesis that pfMA influences ankle

torque, a hierarchical regression analysis was performed with maximal plantarflexor torque as the outcome variable, pfMA as the predictor variable, and pfVOL as a covariate. This analysis, while controlling for pfVOL, tested if the effect of pfMA on plantarflexor torque at each speed (30, 120, and 210°·s^{-1}) differed significantly from the slope found for the isometric regression model. Hierarchical analysis was performed in the R statistical computing environment (Version 2.15.1, R Development Core Team), repeated measures ANOVA was performed using IBM SPSS (Version 20, Armonk, New York), and significance levels were set at $\alpha = 0.05$.

5.3 RESULTS

Maximal isometric plantarflexor torque was moderately correlated with both pfVOL ($R^2 = 0.322$; $p = 0.009$) (Figure 5.3) and pfMA ($R^2 = 0.323$; $p = 0.009$) (Figure 5.4). Maximal plantarflexor torques measured during isokinetic tests were weakly correlated with pfVOL at the three speeds tested: 30°·s^{-1} ($R^2 = 0.226$; $p = 0.034$), 120°·s^{-1} ($R^2 = 0.243$; $p = 0.027$), and 210°·s^{-1} ($R^2 = 0.222$; $p = 0.036$) (Figure 5.3). Stronger correlations between maximal isokinetic torques and pfMA were found at each if the speeds tested: 30°·s^{-1} ($R^2 = 0.479$; $p = 0.001$), 120°·s^{-1} ($R^2 = 0.424$; $p = 0.002$), and 210°·s^{-1} ($R^2 = 0.494$; $p = 0.001$) (Figure 5.4). Multiple regression showed a moderate correlation between maximal torque and pfMA and pfVOL during isometric and isokinetic contractions (Table 1, $R^2 = 0.449 – 0.527$, all $p \leq 0.006$). There was only a weak and insignificant correlation between pfMA and pfVOL ($R^2 = 0.191$, $p = 0.054$) (Figure 5.5).

Plantarflexion velocity had a significant effect on maximal plantarflexor torque, with torque decreasing from 169.4 ± 52.9 Nm during isometric contractions to 76.7 ± 28.1 Nm during isokinetic contractions at $210°\cdot s^{-1}$ (Table 5.2).

The hierarchical regression analysis (Table 5.3) revealed that while pfMA has a significant effect on plantarflexor torque (t-value = 3.252), its influence did not change between any of the three isokinetic conditions and the isometric condition (|t-value| < 1.96).

5.4 DISCUSSION

The results of the present study suggest that maximal plantarflexor torque is positively correlated with pfMA and pfVOL during both isometric and isokinetic contractions (Figure 5.3, 5.4). The results did not support our hypothesis that the association between pfMA and plantarflexor torque would weaken at increasing rates of ankle rotation; we found the opposite to be the case (Table 5.3). No significant correlation between pfMA and pfVOL was found, suggesting that pfMA and pfVOL are independent determinants of plantarflexor torque.

The magnitudes of our strength measurements are similar to previously reported values. Isometric strength of 169 ± 53 Nm at neutral ankle position compared favorably to mean values of 145 ± 9.1 Nm (Miaki et al., 1999) and 171 ± 32 Nm (Morse et al., 2005b) reported in two studies in which similar tests were performed on young male subjects. The mean isokinetic torques we found ranged from 129.6 to 76.7 Nm for speeds of 30 to $210^{o}\cdot s^{-1}$, respectively (Table 5.2), similar to those reported by Thom et al (2005),

who found isokinetic torques of 120 to 57 Nm at speeds of 0 to 250º·s^{-1}. Fugl-Meyer et al (1980) reported peak isokinetic torques in a sedentary population of men and found that at 30º·s^{-1}, peak torque was 145 ± 28 Nm, comparable to our measurement of 129.6 ± 47.5 Nm.

The magnitudes of the pfMA we measured (5.3 ± 0.6 cm) (Table 5.4) were similar to those reported by previous investigators who used the same methods to measure pfMA in healthy young males. These studies report a pfMA at neutral position of 5.2 ± 0.4 cm (Fath et al., 2010) and 5.4 ± 0.3 cm (Rugg et al., 1990). Previous authors have not reported the volume of the posterior compartment, but measurements of lateral and medial gastrocnemius muscle volumes in our subjects compare favorably to those reported in previous studies. The mean lateral and medial gastrocnemius volumes of 167.2 ± 29.8 cm^3 and 304.0 ± 56.7 cm^3, (Table 5.4), are similar to previous reports of lateral and medial gastrocnemius volumes of 144 cm^3 and 244 cm^3, respectively (Fukunaga et al., 1992). The correlation we found between pfVOL and maximal isometric torque (R^2 = 0.322) was much weaker than that previously reported by Morse et al. (2004), who found a correlation with R^2 = 0.80 for young subjects, although those authors reported no such strong correlation (R^2 = 0.06) for older subjects.

To our knowledge, the present study is the first to investigate a possible link between muscle moment arm and maximal joint torque in humans. Lieber and Boakes (1988) found maximal knee flexion torque to be strongly correlated with peak muscle tension in frogs, but torque was not correlated with muscle moment arm. In the present

study we found significant positive correlations between pfMA and maximal isometric and isokinetic plantarflexor torques (Figure 5.3).

The results of the present study suggest that smaller pfMA did not facilitate torque generation at high rates of joint rotation in our subjects; the effect of pfMA on maximal plantarflexor torque seemed instead to be independent of velocity. Previous findings of differences in pfMA between sprinters and non-sprinters (Lee and Piazza, 2009; Baxter et al., 2011) led us to expect that small pfMA might confer a torque-production advantage at high rates of plantarflexion. It may be that the findings for our subjects, who are not regular participants in activities like sprinting that require rapid and forceful joint rotations, do not generalize to sprinters. Adaptations to training among sprinters may place the muscle at different operating points on the force-length and force-velocity curves (Abe et al., 2000, 2001; Kumagai et al., 2000; Lee and Piazza, 2009). A high ratio of muscle fiber length to moment arm, for example, may reduce muscle shortening velocity and enhance force production at faster rates of rotation (Lieber and Fridén, 2000; Nagano and Komura, 2003; Akinori et al., 2007).

Certain limitations affected our study. Plantarflexor moment arm was determined using a two-dimensional analysis conducted in a quasi-sagittal plane. While this method has been employed by several previous investigators (Rugg et al., 1990; Maganaris et al., 1998; Fath et al., 2010; Baxter et al., 2011), rotations out of the plane of the image could not be quantified, and it is possible that more sophisticated three-dimensional determination of pfMA (Sheehan, 2010; Hashizume et al., 2012) would have yielded different results. MR images were acquired the ankles unloaded in this study, and pfMA

measured while the joint was loaded may have greater physiological relevance. Both optimal plantarflexor muscle fiber lengths and Achilles tendon stiffness would be expected to affect peak joint torque but we did not measure either of these quantities. We did not measure electromyographic activity to ensure that subjects gave maximum effort during isometric and isokinetic dynamometer testing, and this variation in effort may have led to our correlations between pfVOL and torque being weaker than those previously reported by Morse et al. (2004). The isokinetic dynamometer constrained the motion of the ankle to a single degree of freedom with the axis of rotation defined by the motor spindle, and while we aligned subjects' lateral malleoli with this axis (Thom et al., 2005), it is possible that this configuration placed some systematic bias on the plantarflexor torque measurements.

In conclusion, maximal isometric and isokinetic plantarflexor torque was found to be correlated with pfMA and pfVOL in healthy young male adults. The correlations between pfMA and torque here have not been reported before for humans. Our results may help to explain the mechanisms behind recently reported correlations between pfMA and locomotor performance.. Further studies that take other factors, such as tendon dynamics and muscle fiber lengths, into account are needed to better understand the determinants of joint kinetic performance in populations such as elderly adults and persons with movement disorders for whom mobility is impaired by compromised joint function.

Figure Captions

5.1 MR image of subject foot and ankle. pfMA was calculated as the shortest distance between the talocrural CoR and Achilles tendon line of action.

5.2 Segmented MR image of the posterior compartment of the lower leg.

5.3 Correlations between pfVOL and ankle strength during isometric and isokinetic plantarflexion contractions.

5.4 Correlations between pfMA and ankle strength during isometric and isokinetic plantarflexion contractions.

5.5 Correlation between pfMA and pfVOL.

Table Captions

5.1 **Multiple regression analysis with pfMA and pfVOL as independent variables and ankle strength during isometric and isokinetic speeds.** *Correlations that are significant at significance of $p < 0.05$.

5.2 **Repeated measures ANOVA comparing maximal voluntary plantarflexor torques across speed conditions**. * p-value < 0.001, Significantly different from all other conditions.

5.3 **Fixed effects of hierarchical regression analysis.** *|t-value| > 1.96 denotes significance of $p < 0.05$

5.4 **Musculoskeletal architecture data**. Lateral gastrocnemius (lgVOL) and medial gastrocnemius (mgVOL).

5.1 MR image of subject foot and ankle.

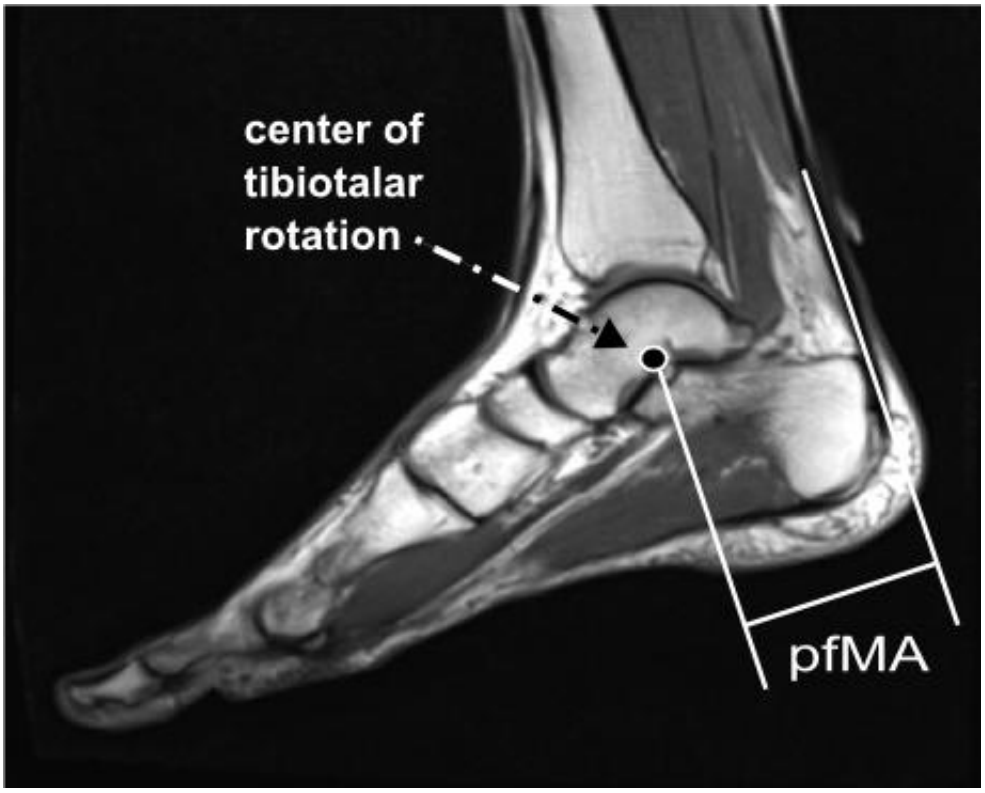

5.2 Segmented MR image of the posterior compartment of the lower leg.

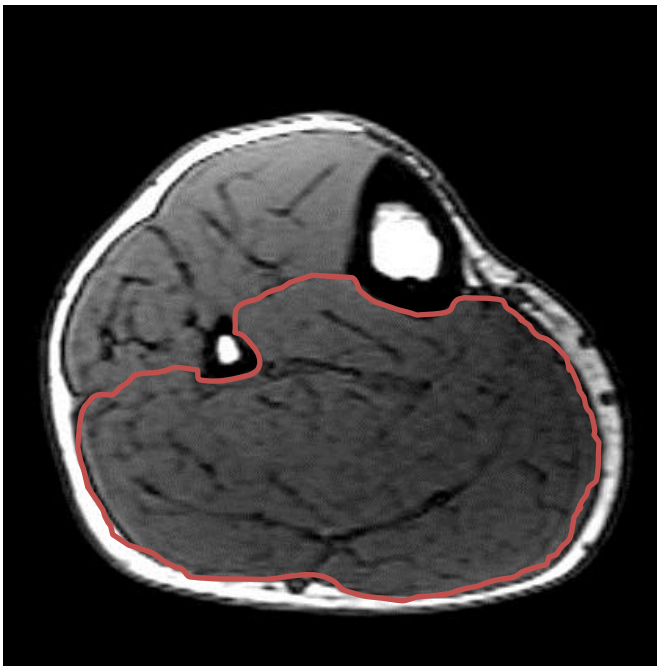

5.3 Correlations between pfVOL and ankle strength during isometric and isokinetic plantarflexion contractions.

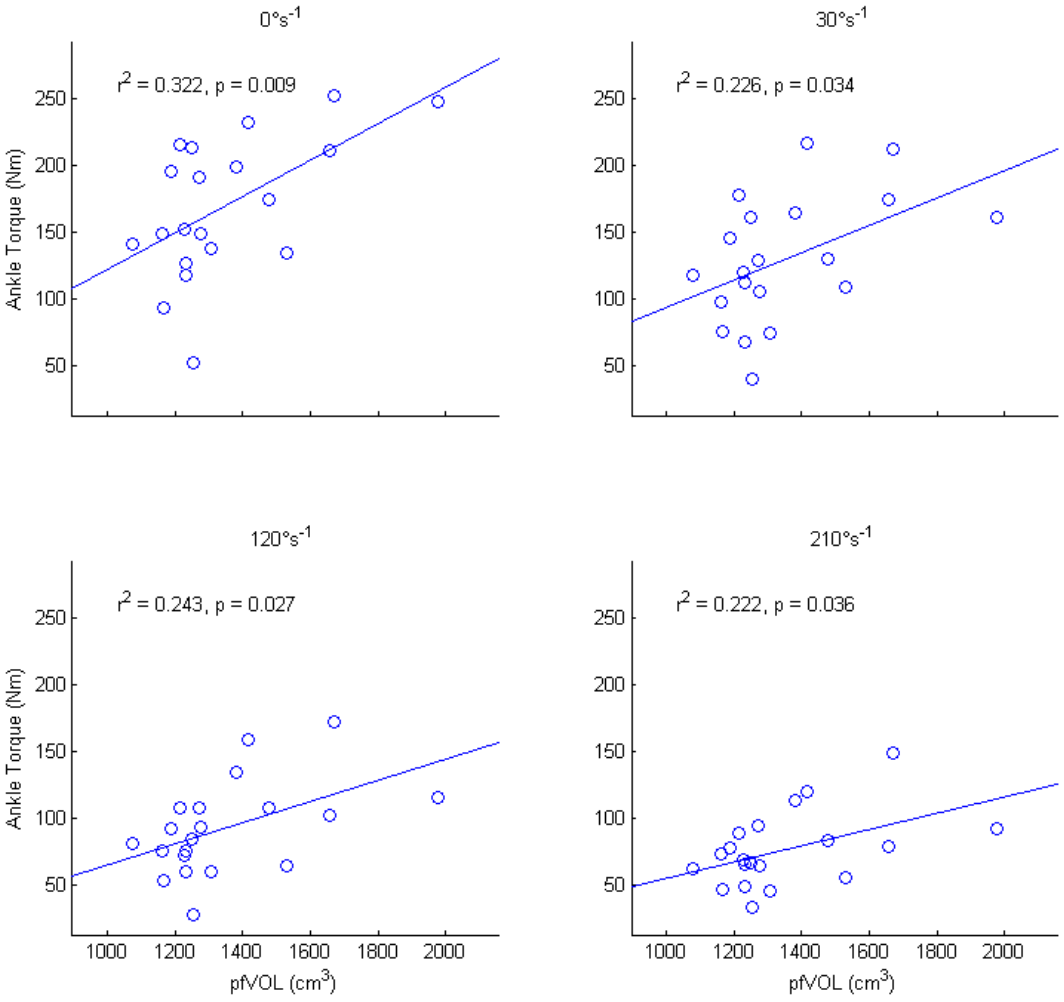

5.4 Correlations between pfMA and ankle strength during isometric and isokinetic plantarflexion contractions.

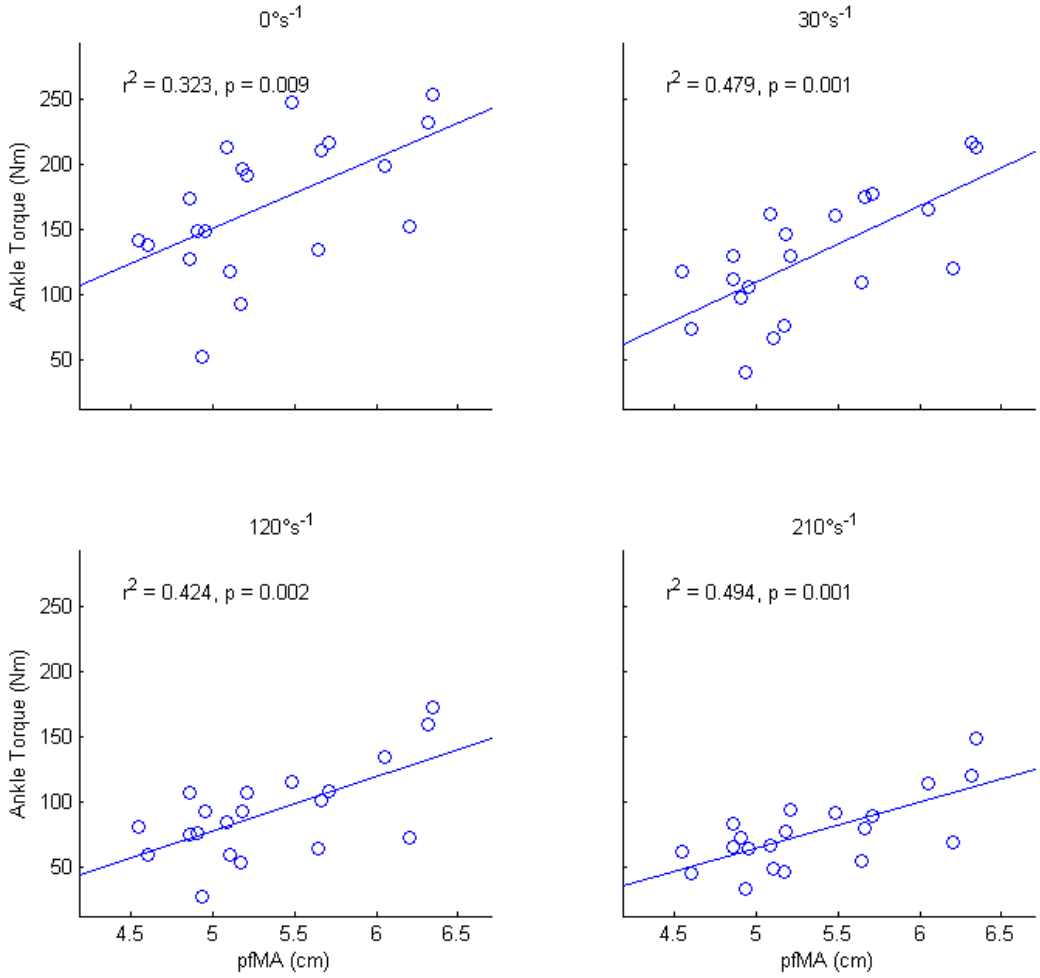

5.5 Correlation between pfMA and pfVOL.

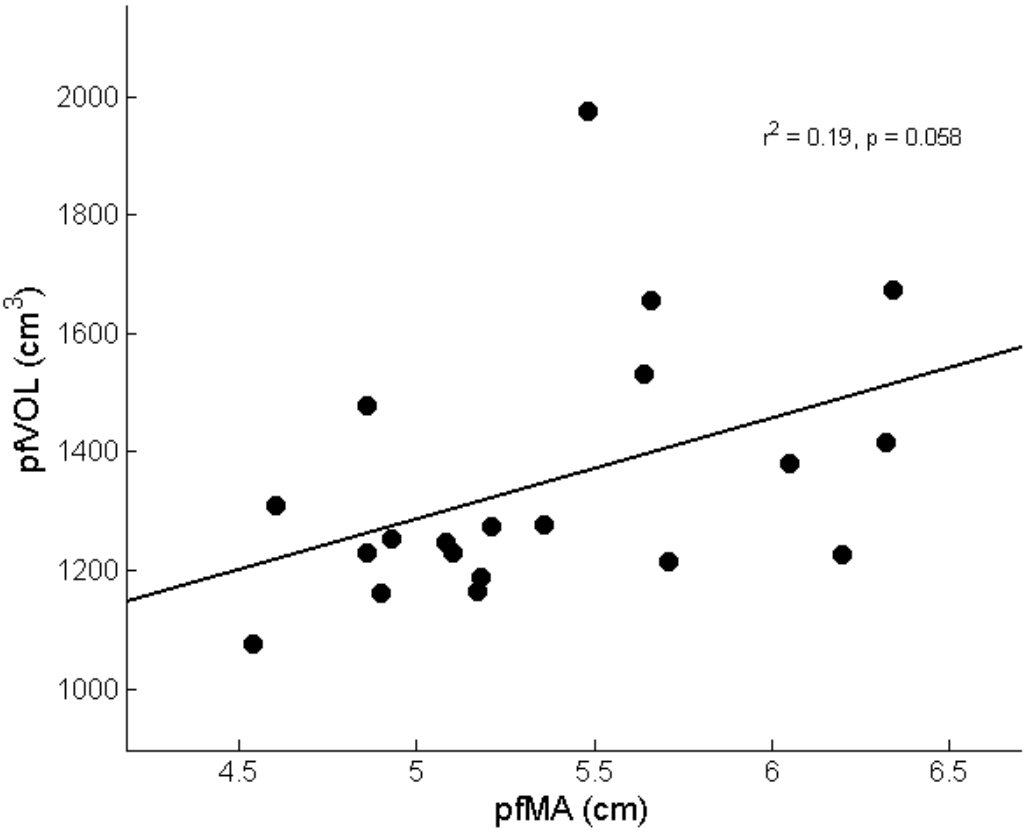

5.1 - Multiple regression analysis with pfMA and pfVOL as independent variables and ankle strength during isometric and isokinetic speeds.

Ankle Speed	R^2	p-value
Isometric: 0°·s^{-1}	0.449	0.006*
Isokinetic: 30°·s^{-1}	0.516	0.002*
Isokinetic: 120°·s^{-1}	0.478	0.004*
Isokinetic: 210°·s^{-1}	0.527	0.002*

5.2 - Repeated measures ANOVA comparing maximal voluntary plantarflexor torques across speed conditions

	Ankle Strength (Nm)
Isometric: 0°·s^{-1}	169.4 ± 52.9*
Isokinetic: 30°·s^{-1}	129.6 ± 47.5*
Isokinetic: 120°·s^{-1}	92.0 ± 35.4*
Isokinetic: 210°·s^{-1}	76.7 ± 28.1*

5.3 - Fixed effects of hierarchical regression analysis. Repeated measures ANOVA

	Estimate	Standard Error	t-value
pfMA	4.965	1.522	3.252*
pfMA:ISOK030	0.511	0.828	0.617
pfMA:ISOK120	-1.248	0.840	-1.485
pfMA:ISOK210	-1.840	1.041	-1.767

5.4 - Musculoskeletal architecture data.

pfMA (cm)	pfVOL (cm^3)	lgVOL (cm^3)	mgVOL (cm^3)
5.3 ± 0.6	1348.2 ± 218.6	167.2 ± 29.8	304.0 ± 56.7

CHAPTER 6

Direct Comparison of Methods for Measuring Plantarflexor Moment Arm *in vivo*

This paper is in preparation for submission to Journal of Biomechanics

6.1 INTRODUCTION

Recent studies have shown that plantarflexor moment arm (pfMA) may be an important determinant of human locomotor performance (Scholz et al., 2008; Lee and Piazza, 2009, 2012; Baxter et al., 2011; Raichlen et al., 2011). However, these studies employed various techniques of approximating pfMA, making it difficult to directly compare findings across studies. Commonly reported measurement techniques of pfMA can be categorized into two types: geometric and tendon excursion methods.

Geometric methods quantify pfMA as the distance from an estimated ankle center of rotation (CoR) to the Achilles tendon line of action. Sagittal magnetic resonance (MR) images are used to estimate CoR between the tibia and talus. pfMA is then calculated as the shortest distance between the tibia-talar CoR to the Achilles tendon line of action (CoR_{TALUS}) (Rugg et al., 1990; Maganaris et al., 1998). This method has been shown to be reliable and produce pfMA estimates comparable to cadaver studies (Spoor et al., 1990; McCullough et al., 2011).

Tendon excursion (TE) eliminates the need to locate the CoR, but requires several assumptions be satisfied.. The principle of virtual work, the underlying assumption of TE, is used to compute pfMA as the first derivative of tendon excursion with respect to joint rotation (An et al., 1983). This assumes that *in vivo* tendon tension remains constant

throughout the measurement. While constant loads can easily be applied to the tendon in cadaveric models (McCullough et al., 2011), its efficacy for *in vivo* testing is less clear. Ultrasonography is an affordable and easily accessible imaging modality that can be used to directly image the musculo-tendon junction (MTJ). However, imaging of the MTJ does not account for changes in tendon force, which can appear as relaxation artifact in the calculation of pfMA.

Direct comparisons between TE and CoR methods demonstrate the importance of imaging modality selection. Fath et al (2010) used ultrasonography to measure TE and found that it underestimates CoR values. However, TE and CoR methods report comparable pfMA values when MR is used (Maganaris et al., 2000). Ito et al (2000) found that ultrasound measurements are significantly influenced by muscle contraction, and that submaximal contractions may minimize changes to *in vivo* tendon loading. If ultrasonography is to be used in future studies, direct comparisons between TE and CoR methods are warranted.

This study has two goals. The first goal is to directly compare previously reported measurements of pfMA with the CoR_{TALUS} method. The second goal is to test if different muscle contraction levels have significant effects on TE measurements. We hypothesize that TE will yield greater pfMA estimates when plantarflexor torque is kept constant when compared to passively acquired pfMA.

6.2 METHODS

6.2.1 Subjects.

Twenty healthy young males volunteered for this study. Subjects had no recent history of musculoskeletal injury to the foot or ankle. Subject mean (SD) age, height, body mass and foot length were 26.0 (3.5) years, 177.7 (7.7) cm, 76.3 (15.6) kg, and 26.8 (1.3) cm, respectively. All procedures were approved by the Institutional Research Board at The Pennsylvania State University.

6.2.2 Ultrasonography.

Subjects were seated in an isokinetic dynamometer (System 3, Biodex Medical Systems) with the unshod right foot secured to the foot plate, the lateral malleolus aligned with the motor spindle, the right knee fully extended, and right thigh strapped securely to the seat. The ankle range of motion was set to 10º dorsiflexion and 20º plantarflexion. Five isometric plantarflexion contractions were performed at neutral position to precondition the muscle-tendon unit (MTU) (2010). Following these contractions, an ultrasound probe (Aloka 1100; transducer: SSD-625, 7.5 MHz and 39mm scan width; Wallingford,CT, USA), secured in a foam cast and to the leg, collected images (10 Hz) of the musculo-tendon junction (MTJ) of the medial gastrocnemius. The dynamometer rotated from peak dorsiflexion to peak plantarflexion at $10°s^{-1}$. During these rotations, subjects were instructed to perform four contraction conditions in the following order: no muscle contraction ($TE_{PASSIVE}$), constant torque matching set at 30% and 60% of voluntary maximal isometric torque measured at neutral ankle position (TE_{30} and TE_{60}, respectively), and finally maximal voluntary plantarflexion throughout the measurement (TE_{MAX}). A computer monitor displayed current and desired torque to the subject, and permitted the subject to produce and maintain specific torque levels throughout

plantarflexion rotations. Each condition was tested three times. Because incomplete data was collected for one subject, nineteen subjects will be included in TE analysis.

Custom written MATLAB (Mathworks, Inc; Natick, MA, USA) routines were used to digitize the excursion of the MTJ as a function of ankle angle. Moment arms were calculated as the first derivative of Achilles tendon excursion with respect to ankle angle using a first order finite difference method over an angular interval of ±10°. This method of differentiation was found to correlate best with CoR derived pfMA (Fath et al., 2010).

6.2.3 Magnetic Resonance Imaging.

Quasi-sagittal images of the right foot and ankle in three postures, 10º dorsiflexion, 0º neutral, and 10º plantarflexion, were acquired with a 3.0 T Siemens Trio scanner (Siemens; Erlangen, Germany). The talocrural CoR was found at 0º and the distance to the Achilles tendon line of action was considered pfMA ($CoR_{TALUS)}$. This method has been described in depth in a previous report (Baxter et al., 2011). Similar procedures were followed to identify the distance between calcaneus-tibia CoR and the Achilles tendon ($CoR_{CALCANEUS}$). Previously reported geometric estimates of pfMA that will be included in the analyses are the average distance from the malleoli to the posterior border of the Achilles tendon, $d_{MALLEOLI}$ (Scholz et al., 2008), the distance between the midpoint of the talus and Achilles tendon, d_{TALUS}, (Csapo et al., 2010), and the calcaneal tuber length, $d_{CALCANEUS}$, (Raichlen et al., 2011).

6.2.4 Statistics.

A repeated measures analysis of variance (ANOVA) with a post-hoc pairwise comparison was performed to test for differences between the four TE methods. The analysis was performed in IBM SPSS (Version 20, Armonk, New York), and significance levels were set at $\alpha = 0.05$.

Bland-Altman plots were used to compare the agreement between CoR_{TALUS} and the other measures of pfMA. This method is appropriate for comparing two measures of the same quantity when no 'gold-standard' is available (Bland and Altman, 1995).

6.3 RESULTS

Moment arms obtained using geometric methods (CoRTALUS, CoRCAL, $d_{MALLEOLI}$, d_{TALUS}, and $d_{CALCANEUS}$) ranged from 53.1-57.8 ± 3.8-5.8 cm (Table 6.1). Smaller values were reported using TE methods ranging from 30.7-42.1 ± 8.5-13.4 cm (Table 6.1). $TE_{PASSIVE}$ and TE_{MAX} values were significantly smaller than TE_{30} and TE_{60} values ($p < 0.05$, Table 6.2). No differences were found between TE_{30} and TE_{60} or $TE_{PASSIVE}$ and TE_{MAX} values ($p > 0.05$). Geometric measurements of pfMA agree better with CoR_{TALUS} (Figure 6.1, average difference: 2.3 mm) than do measurements based on TE (Figure 6.2, average distance: 16.9 mm).

6.4 DISCUSSION

The purpose of this study was to directly compare reported measurements of pfMA with the CoR_{TALUS} method, a frequently reported measurement of pfMA (Rugg et al., 1990; Maganaris et al., 1998). These alternate measures of pfMA can be divided into two groups: TE and geometric measures. While previous authors (Fath et al., 2010) found

that $TE_{PASSIVE}$ was strongly correlated with CoR_{TALUS}, we did not find good agreement between these two methods. Geometric methods of measuring pfMA appear to be adequate substitutes for CoR_{TALUS}.

Our measurements of pfMA using geometric methods are similar to values reported in the literature for young adult males (Table 6.1). Measurements of external malleoli in the current study produced estimates that were approximately 1 cm larger compared to the values reported by Scholz et al. (2008). Csapo et al (2010) measured d_{TALUS} in women and documented substantially smaller pfMA than the current results (47.7 ± 3.6 mm and 54.2 ± 4.1 mm, respectively); however after correcting for sex differences in pfMA (Sheehan 2012), our results were similar to reported values (Table 6.1).

In the current study, $TE_{PASSIVE}$ and TE_{MAX} were smaller than previously reported measures in healthy young adult males (Lee and Piazza, 2009; Fath et al., 2010). The cohort in the current study maximally plantarflexed against an isokinetic dynamometer that rotated at a constant velocity, but Lee and Piazza (Lee and Piazza, 2009) instructed their subjects to maximally contract against the foot plate as it was manually resisted by an investigator. These previous measurements may have been made while subjects generated near-constant torque. Moment arm estimates during TE_{30} and TE_{60} estimates were 39.6 and 42.1 mm compared to 41.6 mm reported by Lee and Piazza (2009).

Several studies have linked pfMA to locomotor function in humans (Scholz et al., 2008; Lee and Piazza, 2009, 2012; Baxter et al., 2011; Raichlen et al., 2011). However,

these studies used methods that have yet been compared experimentally with CoR_{TALUS}. Lee and Piazza (2009, 2012) have found differences in pfMA between sprinters and non-sprinters and a strong correlation between pfMA and slow-walking elderly adults. While they used TE_{MAX} to approximate pfMA, the current study suggests that TE_{MAX} does not have good agreement with CoR_{TALUS}.

Geometric measurements of pfMA show better agreement and less variability than tendon excursion measures (Figure 6.1). It should be noted that geometric and tendon excursion methods measure different phenomena. Geometric methods measure a finite distance between some assumed axis of ankle rotation and the Achilles tendon. Errors in this method are likely due to poorly defined ankle joint axis, which may be due to contraction level, joint non-conformities, or measurement error (Maganaris et al., 1998; Baxter et al., 2011). Tendon excursion measurements are equivalent to the geometric measurements only if all tendon excursion between positions can be attributed to joint rotation, with none attributed to tendon elongation or relaxation (Lee and Piazza, 2009).

Our results do not show the same strong correlation between CoR_{TALUS} and $TE_{PASSIVE}$ that was found by Fath et al. (2010), who reported an R^2 of 0.94. Fath et al. reported changes in ankle joint torque, but made no attempt to control for *in vivo* force. The cohort in the current study was larger (19 versus 9) and likely carried greater intersubject musculoskeletal variation; it is possible that this is the reason we did not find such a correlation. Lee and Piazza (2009) tried to control for tendon slack by asking subjects to maximally contract (TE_{MAX}). Although tendon excursion during forceful

contractions may not have good agreement with CoR_{TALUS}, it may still have important implications for joint function. Tendon excursion is equivalent to the amount of tendon and muscle shortening that occurs proximal of the MTJ and operates with the assumption that the tendon distal of the MTJ does not change length. Computer simulations show that at fast joint rotations, muscle shortening velocity has a stronger effect on ankle strength than variations in pfMA (Nagano and Komura, 2003). Recent reports linking TE_{MAX} with locomotor function suggest that TE_{MAX} is a good measure of muscle function (Lee and Piazza, 2009, 2012), so it may more appropriately be reported as 'muscle shortening'.

This study did not include analysis of three-dimensional pfMA measurements (Sheehan, 2010; Hashizume et al., 2012). Although the talocrural joint is mostly a planar mechanism, this plane is obliquely oriented with respect to the anatomical planes. Movement that deviates from planar or that occurs oblique to the anatomical planes would not have been captured in our two-dimensional analysis. Though CoR_{TALUS} is a reliable measure of pfMA, more sophisticated techniques of reporting moment arm exist. Sheehan (2010) recently developed a method to identify the subtalar and talocrural joint axes during loaded foot rotations in six degrees-of-freedom.

In conclusion, the findings of the current study suggest that geometric measurements of pfMA may be more appropriate when the research question is interested in ankle leverage. Tendon excursion methods underestimated pfMA when compared to CoR_{TALUS} but have been associated with locomotor performance in sprinters and elderly men. While more sophisticated techniques of quantifying pfMA have been reported, CoR and TE techniques have been linked with human locomotor function. Careful

consideration should be given to the choice of such pfMA techniques when designing a study that investigates human function.

Figure Captions

6.1 Comparisons geometric methods with CoR_{TALUS}

6.2 Comparisons of tendon excursion methods with CoR_{TALUS}

Table Captions

6.1 Comparison of pfMA reports in the literature.

a, Rugg et al 1990)
b, Maganaris et al 1998
c, Maganaris et al 2000
d, Fath et al (2010)
e, Raichlen et al (2010)
g, Scholz et al (2008)
h, Csapo et al (2010), corrected for sex differences according to Sheehan 2012.
i, Fath et al (2010)
j, Lee and Piazza (2009), 31.0 mm sprinter values; 41.6 mm non-sprinter values

6.2 Repeated measures ANOVA Post-hoc comparison of means. Tendon excursion measures are reported in mm. Δ difference between measures.

* $p < 0.05$ (Bonferonni corrected level for significance)

Figure 6.1 Comparisons of geometric methods with CoR_{TALUS}

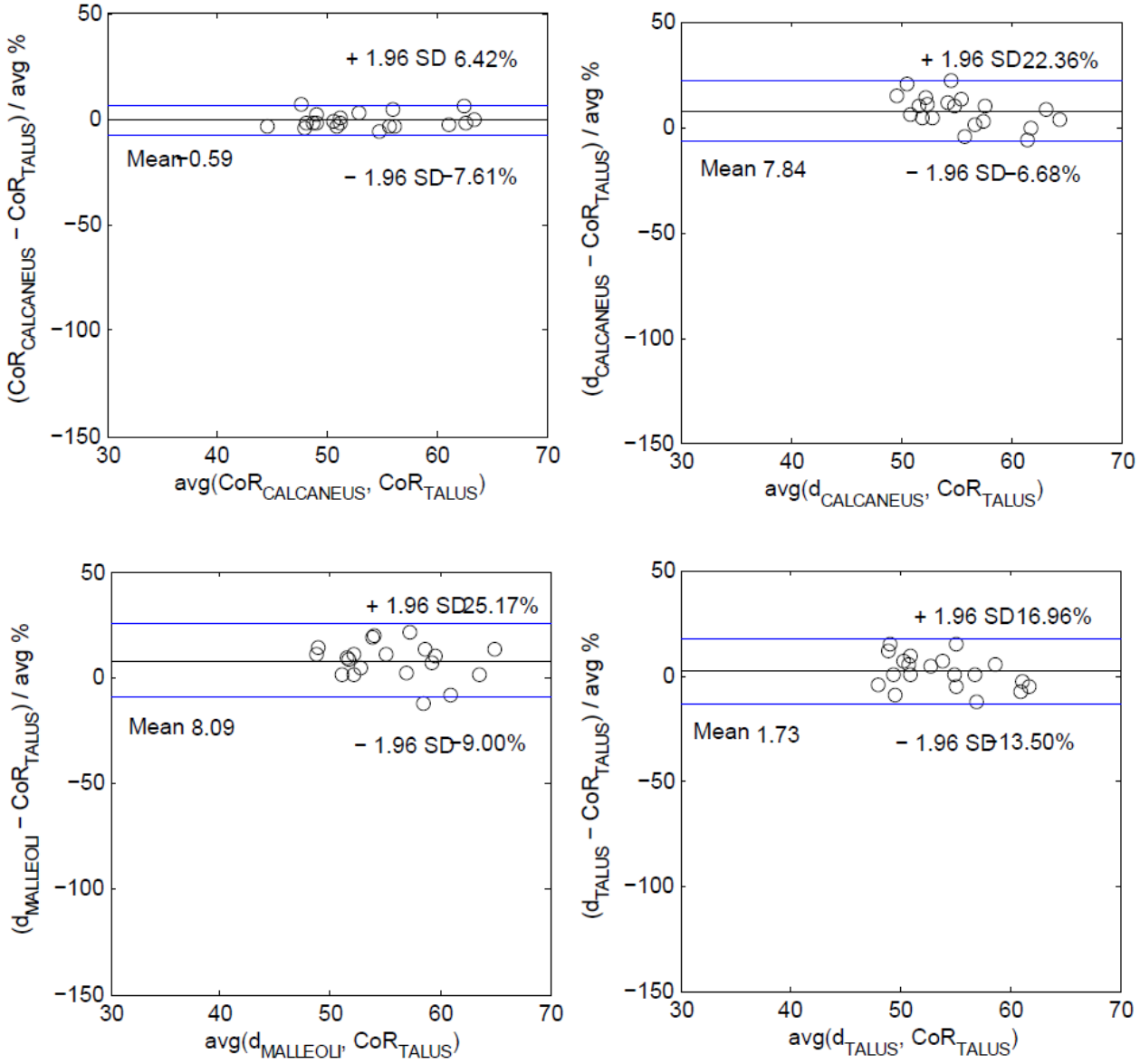

6.2 Comparisons of tendon excursion methods with CoR_{TALUS}

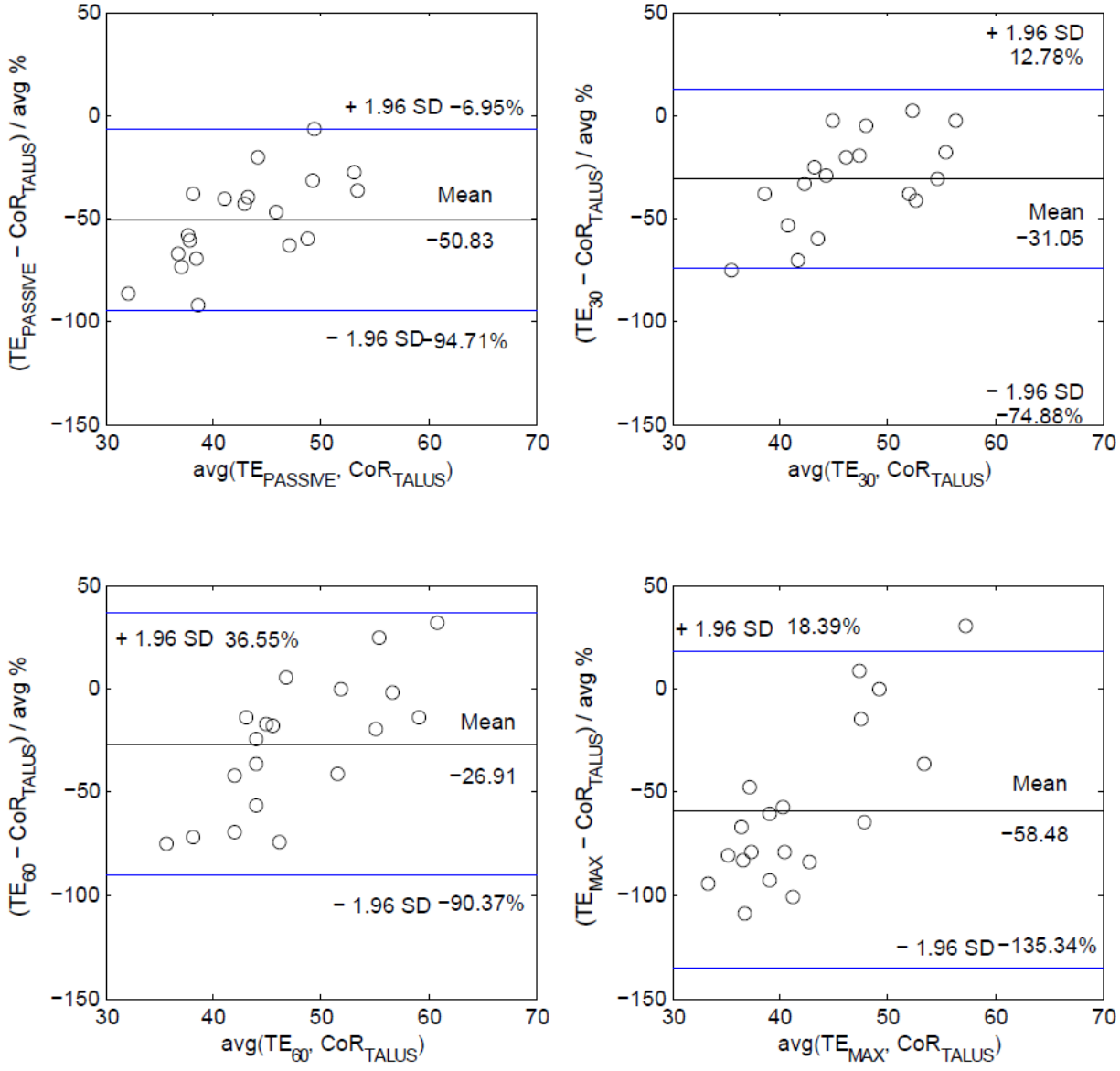

6.1 - Comparison of pfMA reports in the literature.

	Baxter	Literature
CoRT	53.4 ± 5.6	48-60 ± 6.6[a,b,c,d]
CoRC	53.1 ± 5.8	-
CALC	57.6 ± 3.8	54.7 ± 3.1[e]
MALL	57.8 ± 4.9	48.5 ± 3.6[g]
FICT	54.2 ± 4.1	54.9 ± 3.6[h]
TEPV	32.4 ± 8.5	38.2 ± 5.3[i]
TE30	39.6 ± 8.9	-
TE60	42.1 ± 13.1	-
TEMX	30.7 ± 13.4	31.0-41.6 ± 4.4[j]

a, Rugg et al 1990)
b, Maganaris et al 1998
c, Maganaris et al 2000
d, Fath et al (2010)
e, Raichlen et al (2010)
g, Scholz et al (2008)
h, Csapo et al (2010), corrected for sex differences according to Sheehan 2012.
i, Fath et al (2010)
j, Lee and Piazza (2009), 31.0 mm sprinter values; 41.6 mm non-sprinter values

6.2 - Repeated measures ANOVA Post-hoc comparison of means

			TEPV	TE30	TE60
	Average	σ	Δ	Δ	Δ
TEPV	32.4	8.5	-	-	-
TE30	39.6	8.9	7.2*	-	-
TE60	42.1	13.1	9.7*	2.5	-
TEMX	30.7	13.4	1.7	8.9*	11.4*

CHAPTER 7

CONCLUSIONS

7.1 – Summary

The purpose of this dissertation was to investigate the relationship between foot and ankle musculoskeletal structure and function in humans. Previous studies have documented correlations between plantarflexor moment arm (pfMA) and locomotor function in sprinters, distance runners, and mobility-limited elderly men (Scholz et al., 2008; Lee and Piazza, 2009, 2012; Raichlen et al., 2011). These studies failed, however, to specifically characterize differences in joint structure and did not attempt to uncover possible mechanisms behind altered locomotor performance. In addition, measures of pfMA differed among these previous studies, making it difficult to compare the results of one study to another. This dissertation addresses these limitations and reports novel findings on the relationships between joint structure, muscle moment arm, and strength.

Lee and Piazza (2009) found that sprinters have smaller pfMA and longer toes than non-sprinters. However, these findings were made using measurements of tendon excursion that may have been subject to measurement artifact. In the first study presented in this thesis (Chapter 3) we used magnetic resonance (MR) imaging of eight trained sprinters and non-sprinters to directly measure pfMA from the center of tibiotalar rotation and the path of the tendon, and to assess the lengths of forefoot bones. Like Lee and Piazza (2009), we found that sprinters have shorter pfMA than non-sprinters. The use of MR enabled us to determine that forefoot bones were longer in sprinters and that the differences in pfMA were almost entirely attributable to differences in the anteroposterior

location of the talocrural center of rotation (CoR). The ratio of forefoot bone length to pfMA was larger in trained-sprinters and seems to agree with observations of foot structure in some of nature's best sprinters, cheetahs and greyhounds (Hildebrand, 1960; Williams et al., 2008; Hudson et al., 2011). A simple computer simulation of plantarflexion revealed that increasing the ratio of forefoot length to pfMA facilitates greater muscle force and prolonged contact with the ground. In the model, this ratio is inversely proportional to the shortening velocity of muscle and may explain the functional benefits bestowed upon sprinters with these foot and ankle proportions during the first few steps of a race.

The findings of the first study suggest that pfMA differences between trained-sprinters and non-sprinters are explained by talocrural kinematics. Initial planar analyses of the geometry of the talar dome and tibial plafond revealed no difference in talocrural geometry between groups. In the second study presented in this thesis (Chapter 4), a more involved three-dimensional (3D) analysis of the talocrural geometry was performed. Three-dimensional surface models of the talus and tibia were created from MR scans and cylinders were fit to the articulating surfaces of the talar dome and tibial plafond. We found that the coverage angle, the angle between two planes that intersect along the axis of the cylinder and pass through the anterior and posterior margins of the tibial plafond, was significantly smaller in trained-sprinters than non-sprinters, which has been associated with increased joint laxity (Frigg et al., 2007) This difference, while small in magnitude suggests that trained-sprinters may have more mobile talocrural joints, which might permit sprinters to select ankle joint "gearing" that is more favorable for muscle force generation during high speed rotations.

In the third study (Chapter 5), we investigated the possible links between pfMA and ankle strength. Based on computer modeling results (Nagano and Komura, 2003; Baxter et al., 2011) and our previous findings in sprinters, we hypothesized that plantarflexor strength would be positively correlated with pfMA during isometric and slow isokinetic contractions, but at faster isokinetic contractions this correlation would weaken or even become negative. To the contrary, we found that pfMA was positively correlated with ankle strength during isometric and isokinetic contractions at all tested speeds. Hierarchical regression analysis revealed that the effect pfMA on ankle strength is unaffected by plantarflexion velocity. These findings appear to contradict what might be predicted by the results of Lee and Piazza (2009) and the first study (Baxter et al., 2011). It is important, however, to consider that the subjects in this study were untrained young men who would not be expected to possess muscular adaptations to sprint training. Sprinters, on the other hand, possess plantarflexor muscles with longer fascicles and less pennation, which is thought to be an adaptation to sprint training, increasing muscle power at high rates of shortening (Abe et al., 2000, 2001; Kumagai et al., 2000; Lee and Piazza, 2009). These findings suggest that in non-athletic populations, musculoskeletal adaptations occur to efficiently generate submaximal joint torques, which are necessary for locomotion.

In the fourth study (Chapter 6), we compared several methods for measuring pfMA (Scholz et al., 2008; Lee and Piazza, 2009; Csapo et al., 2010; Fath et al., 2010; Baxter et al., 2011; Raichlen et al., 2011) to the talocrural center of rotation (CoR_{TALUS}) method pfMA (Rugg et al., 1990; Fath et al., 2010; Baxter et al., 2011) in the same set of 20 subjects. These measurement techniques were classified as either “geometric” or

"tendon excursion" (TE) methods. We found that geometric methods of quantifying pfMA tend to agree with CoR_{TALUS}, but TE methods tend to produce smaller and more variable pfMA estimates of pfMA. The average distance between the Achilles tendon and malleoli ($d_{MALLEOLI}$) agreed well with CoR_{TALUS} and may serve as a suitable substitute when medical imaging is not available or practical.

7.2 – Implications

Muscle moment arms may be thought of as static constraints in which muscle easily adapts to, without any loss of function. The findings of this dissertation suggest that pfMA is an important constraint on locomotor function and ankle strength. Previous studies of the effects of muscle moment arm on function were limited to acute alterations of moment arm via surgery in animals (Burkholder and Lieber, 1998; Koh and Herzog, 1998). Prior consideration of this question in humans has been limited to simple computer simulations (Nagano and Komura, 2003; Lee and Piazza, 2009; Baxter et al., 2011) in which concomitant muscle adaptations to varied pfMA were not modeled. Because muscle adaptation appears to be highly dependent on the functional demands placed on the organism (Hildebrand, 1960; Mero et al., 1981; Biewener, 1990; Abe et al., 2000, 2001; Kumagai et al., 2000), experimental data were needed to address questions regarding pfMA and ankle function.

Animal studies suggest that muscle architecture adapts to preserve the torques necessary for submaximal locomotion (Burkholder and Lieber, 1998; Koh and Herzog, 1998). While similar adaptation might be expected to occur in healthy individuals who do not participate in activities that require maximal power generation, like sprinting, muscle moment arm may become an important constraint on performance when muscle have

difficulty adapting, or when additional constraints are imposed. For example, elderly adults experience age-related muscle wasting, sarcopenia (Morse et al., 2005a), which reduces muscle force generating capacity. Lee and Piazza (2012) found that slower elderly men walked at speeds that were strongly correlated with pfMA (R^2 = 0.69). Plantarflexor weakness is one of the primary causes of reduced walking velocity in the elderly (Judge et al., 1996; Graf et al., 2005), and the findings of Lee and Piazza (2012) suggest that insufficient ankle leverage, which translates to ankle torque, may be a primary mechanism that limits walking velocity in the elderly, especially older subjects who have increased body mass.

Unlike the studies of sprinters and the elderly, we investigated pfMA and function in untrained healthy young men. Because joint strength is generally not lacking for normal activities in healthy young adults, it is unlikely that insufficient pfMA is a constraint on locomotor ability. However, when these untrained young adults were asked to maximally generate ankle torque, pfMA appeared to be a predictor of performance. To our knowledge, these are the first data showing a relationship between muscle moment arm and joint strength in humans. These findings suggest that musculoskeletal adaptations in untrained healthy adults are in response to submaximal tasks like walking and stair-climbing.

Differences in pfMA between sprinters and non-sprinters were explained by the location of the talocrural CoR. Additionally, we found that the forefoot bones in sprinters are longer than non-sprinters. Computer simulations of a foot pushing against a moving plate show that longer forefeet and shorter pfMA facilitate greater muscular work. These simulations show that the ratio of forefoot to rearfoot length is inversely proportional to

the shortening velocity of the muscle. While these simulations did not model possible adaptations in response to pfMA, they do show that joint leverage would play an important role in joint function if muscle and tendon could not adapt to the loads and demands placed on the system.

To investigate possible mechanisms that are responsible for the differences in talocrural CoR between sprinters and non-sprinters, we analyzed the 3D geometries of thearticulating surfaces of the talocrural joint. We found that sprinters have significantly smaller coverage angles and slightly larger talar radii, although this measure was not significantly different. Increased talar radii and small coverage angles have been associated with ankle instability (Frigg et al., 2007). Frigg et al. developed a simple biomechanical model to demonstrate that a smaller coverage angle reduces the force needed to dislocate the talocrural joint. We are not suggesting that sprinters dislocate their ankles; rather, these observed differences in bone structure may increase the mobility of the joint and give the foot optimal leverage for torque generation for the task at hand, much like an automatic transmission in a car. Azizi et al (2008) found a similar mechanism present in the plantarflexor muscles of wild turkeys.

7.3 – Limitations

Our measurements and experimental design had several limitations. Sample sizes were rather small for the studies of sprinters. The recruitment of male sprinters who were not affiliated with varsity athletics was a serious challenge that restricted the recruitment to only eight subjects.

We did not measure the ankle strength in our sprinter subjects. While we found pfMA group differences, no musculoskeletal parameters correlated with sprint

performance (personal best at 100m or 200m). This was not surprising as it has been previously reported that sprint performance is not correlated with any single musculoskeletal variable (Karamanidis et al., 2011). Also, our sprinter subjects were not 'elite', but rather 'trained', so, while these findings may not represent the mechanisms at play in world-class sprinters, they do demonstrate the possible adaptations that take place to sprint training.

Measurements of pfMA were only planar representations of the talocrural joint CoR. More sophisticated methods of identifying axes of rotation between various bones of the foot exist (Sheehan, 2010; Hashizume et al., 2012), but we were primarily interested in comparing joint leverage across subjects and groups, and CoR_{TALUS} has been shown to be a reliable measure of pfMA (Rugg et al., 1990; Maganaris et al., 1998, 2000). During pilot testing we placed non-elastic straps about the foot and ankle to prevent foot movement during maximal contractions, but the straps seemed to alter the line of Achilles tendon action, so we decided to only report unloaded pfMA. Although we consider the musculoskeletal structure of the ankle joint to consist of muscle, tendon and a moment arm, we did not measure optimal muscle fiber lengths and tendon stiffness.

7.4 – Future Work

This dissertation addressed important gaps in the literature regarding muscle moment arm and function. Our experimental findings suggest that the effects of muscle moment arm on joint function are dependent on the adaptive strategies employed by the organism. From experiments and computer simulations, it appears that human sprinters benefit from reduced pfMA. However, it is unclear as to the influence pfMA has on optimal fiber length. Recent advances in muscle imaging provide the potential for

minimally invasive measurement of muscle sarcomeres in humans (Llewellyn et al., 2008). A logical next step would be to study the effects moment arm has on optimal sarcomere length and muscle function. Two special populations of interest are sprinters and elderly adults. While our goal is not to improve sprint performance, studying humans who operate at the limits of their physiology may provide better insight into how we can help people with movement disorders. Elderly adults are important to study because they operate near their physiological limits during simple tasks like walking and climbing stairs.

Our experimental findings suggest that the talocrural joint of sprinters and non-sprinters are functionally different. Computer and physical models of the talocrural joint would be useful tools to demonstrate how joint non-conformities, observed in trained sprinters, would affect joint function. Variable gearing has been documented at the limb (Williams et al., 2009a) and muscle levels (Azizi et al., 2008), so it is reasonable to think similar mechanisms could be at play at the joint level.

7.5 – Conclusion

This dissertation investigated the relationships between joint structure, leverage and function. Using MR imaging, we identified structural differences in the talocrural joints and forefoot bones of sprinters and non-sprinters. A simple computer simulation demonstrates the possible effects these structural differences have on ankle strength. This dissertation also found correlations between pfMA and ankle strength, which surprisingly have not previously been reported in the literature. Additional study is needed to understand how adaptations to pfMA and functional demands change between groups of differing locomotor capacities.

APPENDIX

A simple planar computer model with one degree of freedom was developed in Simulink (MATLAB) to investigate the influence of foot length proportions on total muscular work performed during forward dynamic simulations of maximal-effort plantarflexion. A foot segment represented by a 28 cm long rigid bar with negligible mass and inertia ($m = 10^{-10}$ kg, $I = 0$ kg m^2) was attached by a revolute joint to a shank segment (which was itself rigidly attached to the ground). The 'toe' of the foot segment was attached by a revolute joint to a slider mounted on wall, permitting the toe to slide without friction along the surface of the wall. This arrangement caused the wall reaction force to be aligned with the long axis of the tibia in a manner similar to way in which a sprinter's ground reaction force is aligned with the tibia during push-off (Kugler and Janshen, 2010). Three Hill-type muscle-tendon actuators, representative of the triceps surae group, applied force to the 'heel' of the foot segment during simulations. The soleus muscle attached to the shank segment 22 cm from the ankle joint and both heads of the gastrocnemius were attached to the shank segment 0.40 m from the ankle joint. Muscle pennation angles, optimal fiber lengths, and peak isometric forces for the muscles in the model were specified according to recent cadaver measurements by Arnold et al. (Arnold et al., 2010) and are given in Table S1. Tendon slack lengths were determined geometrically by subtracting the optimal fiber lengths of each muscle from the distance between the muscle origins and insertion point when the ankle was positioned in 10° plantarflexion.

To represent variation in foot proportions, the ankle joint location with respect to the heel (the most posterior point on the foot segment and the insertion of all three

muscles) ranged from 45 mm to 70 mm, and was varied in 5 mm increments (these were the ranges for pfMA that we measured for our subjects). Static optimization was performed at the beginning of each simulation to find muscle fiber lengths that satisfied the constraint that tendon force and muscle force must be equal for each actuator. During each simulation, the wall was prescribed to recede at a constant speed (0.4 m s^{-1} to 4.0 m s^{-1}), which corresponded to a range of ankle velocities observed during push-off in walking, sprint starts, and maximal speed sprinting (Winter, 1983; Bezodis et al., 2008; Slawinski et al., 2010b). Each muscle was maximally activated throughout the entire trial. Simulations started at 10° dorsiflexion and stopped when the sum of the three active muscle forces became 0 N or when plantarflexion exceeded 50°. Muscle work was derived by taking the integral with respect to time of the product of the wall speed and the force component that was perpendicular to the wall. Variable timestep integration was implemented using the ode45 function in MATLAB with a maximum step size of 10^{-3}.

Table A.1 - Muscle parameters adapted from Arnold et al.(2010).

	Soleus	Lateral Gastrocnemius	Medial Gastrocnemius
Peak Isometric Force (N)	3585.9	606.4	1308.0
Optimal Fiber Length (mm)	44	59	51
Pennation Angle (°)	28.3	12.0	9.9
Origin to Ankle Distance (cm)	22	40	40

BIBLIOGRAPHY

Abe, T., Fukashiro, S., Harada, Y., and Kawamoto, K. (2001). Relationship between sprint performance and muscle fascicle length in female sprinters. J. Physiol. Anthropol. Appl. Human. Sci. *20*, 141–147.

Abe, T., Kumagai, K., and Brechue, W.F. (2000). Fascicle length of leg muscles is greater in sprinters than distance runners. Med. Sci. Sports. Exerc. *32*, 1125–1129.

Ahn, A.N., Kang, J.K., Quitt, M.A., Davidson, B.C., and Nguyen, C.T. (2011). Variability of neural activation during walking in humans: short heels and big calves. Biol. Lett. *7*, 539–542.

Akinori, N., Shinsuke, Y., Taku, K., and Senshi, F. (2007). Influence of the Fascicle Length and Physiological Cross-sectional Area of M. soleus on Ankle Joint Kinetics. International Journal of Sport and Health Science *5*, 98–104.

Alexander, R.M., Jayes, A.S., Maloiy, G.M.O., and Wathuta, E.M. (1979). Allometry of the limb bones of mammals from shrews (Sorex) to elephant (Loxodonta). Journal of Zoology *189*, 305–314.

An, K.N., Takahashi, K., Harrigan, T.P., and Chao, E.Y. (1984). Determination of muscle orientations and moment arms. J. Biomech. Eng. *106*, 280–282.

An, K.N., Ueba, Y., Chao, E.Y., Cooney, W.P., and Linscheid, R.L. (1983). Tendon excursion and moment arm of index finger muscles. Journal of Biomechanics *16*, 419–425.

Anderson, F.C., Goldberg, S.R., Pandy, M.G., and Delp, S.L. (2004). Contributions of muscle forces and toe-off kinematics to peak knee flexion during the swing phase of normal gait: an induced position analysis. J Biomech *37*, 731–737.

Arampatzis, A., Karamanidis, K., and Albracht, K. (2007a). Adaptational responses of the human Achilles tendon by modulation of the applied cyclic strain magnitude. J. Exp. Biol. *210*, 2743–2753.

Arampatzis, A., Karamanidis, K., Morey-Klapsing, G., De Monte, G., and Stafilidis, S. (2007b). Mechanical properties of the triceps surae tendon and aponeurosis in relation to intensity of sport activity. J. Biomech. *40*, 1946–1952.

Arampatzis, A., Karamanidis, K., Stafilidis, S., Morey-Klapsing, G., DeMonte, G., and Brüggemann, G.-P. (2006). Effect of different ankle- and knee-joint positions on gastrocnemius medialis fascicle length and EMG activity during isometric plantar flexion. J Biomech *39*, 1891–1902.

Arnold, E.M., Ward, S.R., Lieber, R.L., and Delp, S.L. (2010). A model of the lower limb for analysis of human movement. Ann. Biomed. Eng. *38*, 269–279.

de Asla, R.J., Wan, L., Rubash, H.E., and Li, G. (2006). Six DOF in vivo kinematics of the ankle joint complex: Application of a combined dual-orthogonal fluoroscopic and magnetic resonance imaging technique. J. Orthop. Res. *24*, 1019–1027.

Azizi, E., Brainerd, E.L., and Roberts, T.J. (2008). Variable gearing in pennate muscles. Proceedings of the National Academy of Sciences *105*, 1745 –1750.

Bárány, M. (1967). ATPase Activity of Myosin Correlated with Speed of Muscle Shortening. The Journal of General Physiology *50*, 197 –218.

Baxter, J.R., Novack, T.A., Van Werkhoven, H., Pennell, D.R., and Piazza, S.J. (2011). Ankle joint mechanics and foot proportions differ between human sprinters and non-sprinters. Proceedings. Biological Sciences / The Royal Society.

Bean, J.F.B., Kiely, D.K., Herman, S., Leveille, S.G., Mizer, K., Frontera, W.R., and Fielding, R.A. (2002). The Relationship Between Leg Power and Physical Performance in Mobility-Limited Older People. Journal of the American Geriatrics Society *50*, 461–467.

Bezodis, I.N., Kerwin, D.G., and Salo, A.I.T. (2008). Lower-limb mechanics during the support phase of maximum-velocity sprint running. Med. Sci. Sports Exerc. *40*, 707–715.

Biewener, A.A. (1989). Scaling body support in mammals: limb posture and muscle mechanics. Science *245*, 45–48.

Biewener, A.A. (1990). Biomechanics of mammalian terrestrial locomotion. Science *250*, 1097–1103.

Biewener, A.A., and Bertram, J.E. (1994). Structural response of growing bone to exercise and disuse. J. Appl. Physiol *76*, 946–955.

Biewener, A.A., Konieczynski, D.D., and Baudinette, R.V. (1998). In vivo muscle force-length behavior during steady-speed hopping in tammar wallabies. J. Exp. Biol. *201*, 1681–1694.

Billeter, R., Weber, H., Lutz, H., Howald, H., Eppenberger, H.M., and Jenny, E. (1980). Myosin types in human skeletal muscle fibers. Histochemistry *65*, 249–259.

Bland, J.M., and Altman, D.G. (1995). Comparing methods of measurement: why plotting difference against standard method is misleading. Lancet *346*, 1085–1087.

Bodine, S.C., Roy, R.R., Meadows, D.A., Zernicke, R.F., Sacks, R.D., Fournier, M., and Edgerton, V.R. (1982). Architectural, histochemical, and contractile characteristics of a unique biarticular muscle: the cat semitendinosus. J. Neurophysiol *48*, 192–201.

Brainerd, E.L., and Azizi, E. (2005). Muscle fiber angle, segment bulging and architectural gear ratio in segmented musculature. J. Exp. Biol. *208*, 3249–3261.

Bramble, D.M., and Lieberman, D.E. (2004). Endurance running and the evolution of Homo. Nature *432*, 345–352.

Burkholder, T.J., Fingado, B., Baron, S., and Lieber, R.L. (1994). Relationship between muscle fiber types and sizes and muscle architectural properties in the mouse hindlimb. J. Morphol *221*, 177–190.

Burkholder, T.J., and Lieber, R.L. (1998). Sarcomere number adaptation after retinaculum transection in adult mice. J. Exp. Biol. *201*, 309–316.

Calbet, J.A., Moysi, J.S., Dorado, C., and Rodríguez, L.P. (1998). Bone mineral content and density in professional tennis players. Calcif. Tissue Int. *62*, 491–496.

Carpenter, R.D., and Carter, D.R. (2010). Computational simulation of spontaneous bone straightening in growing children. Biomech. Model Mechanobiol. *9*, 317–328.

Carrier, D., Heglund, N., and Earls, K. (1994). Variable gearing during locomotion in the human musculoskeletal system. Science *265*, 651–653.

Carrier, D.R., Gregersen, C.S., and Silverton, N.A. (1998). Dynamic gearing in running dogs. J. Exp. Biol *201*, 3185–3195.

Costill, D.L., Daniels, J., Evans, W., Fink, W., Krahenbuhl, G., and Saltin, B. (1976). Skeletal muscle enzymes and fiber composition in male and female track athletes. Journal of Applied Physiology *40*, 149 –154.

Cresswell, A.G., Löscher, W.N., and Thorstensson, A. (1995). Influence of gastrocnemius muscle length on triceps surae torque development and electromyographic activity in man. Exp Brain Res *105*, 283–290.

Csapo, R., Maganaris, C.N., Seynnes, O.R., and Narici, M.V. (2010). On muscle, tendon and high heels. J. Exp. Biol. *213*, 2582–2588.

Dawson, B., Fitzsimons, M., Green, S., Goodman, C., Carey, M., and Cole, K. (1998). Changes in performance, muscle metabolites, enzymes and fibre types after short sprint training. Eur. J. Appl. Physiol. Occup. Physiol. *78*, 163–169.

Delp, S.L., Loan, J.P., Hoy, M.G., Zajac, F.E., Topp, E.L., and Rosen, J.M. (1990). An interactive graphics-based model of the lower extremity to study orthopaedic surgical procedures. IEEE Trans. Biomed. Eng. *37*, 757–767.

Dogan, A., Uslu, M., Aydinlioglu, A., Harman, M., and Akpinar, F. (2007). Morphometric study of the human metatarsals and phalanges. Clin. Anat. *20*, 209–214.

Drake, R.L., Vogl, A.W., and Mitchell, A.W.M. (2009). Gray's Anatomy for Students: With STUDENT CONSULT Online Access, 2e (Churchill Livingstone).

Fath, F., Blazevich, A.J., Waugh, C.M., Miller, S.C., and Korff, T. (2010). Direct comparison of in vivo Achilles tendon moment arms obtained from ultrasound and MR scans. J. Appl. Physiol. *109*, 1644–1652.

Frigg, A., Frigg, R., Hintermann, B., Barg, A., and Valderrabano, V. (2007). The biomechanical influence of tibio-talar containment on stability of the ankle joint. Knee Surg Sports Traumatol Arthrosc *15*, 1355–1362.

Fugl-Meyer, A.R., Gustafsson, L., and Burstedt, Y. (1980). Isokinetic and static plantar flexion characteristics. Eur J Appl Physiol Occup Physiol *45*, 221–234.

Fukunaga, T., Kubo, K., Kawakami, Y., Fukashiro, S., Kanehisa, H., and Maganaris, C.N. (2001a). In vivo behaviour of human muscle tendon during walking. Proc Biol Sci *268*, 229–233.

Fukunaga, T., Miyatani, M., Tachi, M., Kouzaki, M., Kawakami, Y., and Kanehisa, H. (2001b). Muscle volume is a major determinant of joint torque in humans. Acta Physiologica Scandinavica *172*, 249–255.

Fukunaga, T., Roy, R.R., Shellock, F.G., Hodgson, J.A., Day, M.K., Lee, P.L., Kwong-Fu, H., and Edgerton, V.R. (1992). Physiological cross-sectional area of human leg muscles based on magnetic resonance imaging. J. Orthop. Res *10*, 928–934.

Gans, C., and Bock, W.J. (1965). The functional significance of muscle architecture--a theoretical analysis. Ergeb Anat Entwicklungsgesch *38*, 115–142.

Goldberg, S.R., Anderson, F.C., Pandy, M.G., and Delp, S.L. (2004). Muscles that influence knee flexion velocity in double support: implications for stiff-knee gait. J Biomech *37*, 1189–1196.

Gordon, A.M., Huxley, A.F., and Julian, F.J. (1966). The variation in isometric tension with sarcomere length in vertebrate muscle fibres. J. Physiol. (Lond.) *184*, 170–192.

Graf, A., Judge, J.O., Ounpuu, S., and Thelen, D.G. (2005). The effect of walking speed on lower-extremity joint powers among elderly adults who exhibit low physical performance. Arch Phys Med Rehabil *86*, 2177–2183.

Gregersen, C.S., and Carrier, D.R.D.R. (2004). Gear ratios at the limb joints of jumping dogs. Journal of Biomechanics *37*, 1011–1018.

Harland, M.J., and Steele, J.R. (1997). Biomechanics of the sprint start. Sports Med *23*, 11–20.

Hashizume, S., Iwanuma, S., Akagi, R., Kanehisa, H., Kawakami, Y., and Yanai, T. (2012). In vivo determination of the Achilles tendon moment arm in three-dimensions. J Biomech *45*, 409–413.

Hildebrand, M. (1960). How animals run. Sci. Am. *202*, 148–157.

Hildebrand, M. (1994). Analysis of Vertebrate Structure (New York: J. Wiley).

Hill, A.V. (1938). The Heat of Shortening and the Dynamic Constants of Muscle. Proceedings of the Royal Society of London. Series B, Biological Sciences *126*, 136–195.

Hill, A.V. (1953). The mechanics of active muscle. Proc. R. Soc. Lond., B, Biol. Sci *141*, 104–117.

Hudson, P.E., Corr, S.A., Payne-Davis, R.C., Clancy, S.N., Lane, E., and Wilson, A.M. (2011). Functional anatomy of the cheetah (Acinonyx jubatus) hindlimb. J. Anat. *218*, 363–374.

Hunter, J.P., Marshall, R.N., and McNair, P.J. (2005). Relationships between ground reaction force impulse and kinematics of sprint-running acceleration. J Appl Biomech *21*, 31–43.

Huxley, A.F., and Nierdergerke, R. (1954). Structural changes in muscle during contraction; interference microscopy of living muscle fibres. Nature *173*, 971–973.

Huxley, H., and Hanson, J. (1954). Changes in the cross-striations of muscle during contraction and stretch and their structural interpretation. Nature *173*, 973–976.

Imhauser, C.W., Siegler, S., Udupa, J.K., and Toy, J.R. (2008). Subject-specific models of the hindfoot reveal a relationship between morphology and passive mechanical properties. J Biomech *41*, 1341–1349.

Ishikawa, M., and Komi, P.V. (2007). The role of the stretch reflex in the gastrocnemius muscle during human locomotion at various speeds. Journal of Applied Physiology *103*, 1030 –1036.

Ishikawa, M., Komi, P.V., Grey, M.J., Lepola, V., and Bruggemann, G.-P. (2005). Muscle-tendon interaction and elastic energy usage in human walking. J. Appl. Physiol. *99*, 603–608.

Ishikawa, M., Pakaslahti, J., and Komi, P.V. (2007). Medial gastrocnemius muscle behavior during human running and walking. Gait Posture *25*, 380–384.

Ito, M., Akima, H., and Fukunaga, T. (2000). In vivo moment arm determination using B-mode ultrasonography. J. Biomech. *33*, 215–218.

Jacobs, R., and van Ingen Schenau, G.J. (1992). Intermuscular coordination in a sprint push-off. Journal of Biomechanics *25*, 953–965.

Johnson, M.D., and Buckley, J.G. (2001). Muscle power patterns in the mid-acceleration phase of sprinting. J. Sports. Sci. *19*, 263–272.

Joyce, G.C., Rack, P.M., and Westbury, D.R. (1969). The mechanical properties of cat soleus muscle during controlled lengthening and shortening movements. J. Physiol. (Lond.) *204*, 461–474.

Judge, J.O., Davis, R.B., and Ounpuu, S. (1996). Step length reductions in advanced age: the role of ankle and hip kinetics. J. Gerontol. A Biol. Sci. Med. Sci *51*, M303–312.

Karamanidis, K., Albracht, K., Braunstein, B., Moreno Catala, M., Goldmann, J.-P., and Brüggemann, G.-P. (2011). Lower leg musculoskeletal geometry and sprint performance. Gait Posture *34*, 138–141.

Koh, T.J., and Herzog, W. (1998). Increasing the moment arm of the tibialis anterior induces structural and functional adaptation: implications for tendon transfer. J. Biomech. *31*, 593–599.

Kugler, F., and Janshen, L. (2010). Body position determines propulsive forces in accelerated running. J. Biomech. *43*, 343–348.

Kumagai, K., Abe, T., Brechue, W.F., Ryushi, T., Takano, S., and Mizuno, M. (2000). Sprint performance is related to muscle fascicle length in male 100-m sprinters. J. Appl. Physiol. *88*, 811–816.

Leardini, A., O'Connor, J.J., Catani, F., and Giannini, S. (1999). A geometric model of the human ankle joint. J. Biomech. *32*, 585–591.

LeBlanc, A., Gogia, P., Schneider, V., Krebs, J., Schonfeld, E., and Evans, H. (1988). Calf muscle area and strength changes after five weeks of horizontal bed rest. Am. J. Sports Med. *16*, 624–629.

Lee, S.S.M., and Piazza, S.J. (2009). Built for speed: musculoskeletal structure and sprinting ability. J. Exp. Biol. *212*, 3700–3707.

Lee, S.S.M., and Piazza, S.J. (2012). Correlation between plantarflexor moment arm and preferred gait velocity in slower elderly men. Journal of Biomechanics *45*, 1601–1606.

Lieber, R.L., and Boakes, J.L. (1988). Muscle force and moment arm contributions to torque production in frog hindlimb. Am. J. Physiol *254*, C769–772.

Lieber, R.L., and Fridén, J. (2000). Functional and clinical significance of skeletal muscle architecture. Muscle Nerve *23*, 1647–1666.

Lieberman, D.E., Venkadesan, M., Werbel, W.A., Daoud, A.I., D'Andrea, S., Davis, I.S., Mang'eni, R.O., and Pitsiladis, Y. (2010). Foot strike patterns and collision forces in habitually barefoot versus shod runners. Nature *463*, 531–535.

Llewellyn, M.E., Barretto, R.P.J., Delp, S.L., and Schnitzer, M.J. (2008). Minimally invasive high-speed imaging of sarcomere contractile dynamics in mice and humans. Nature *454*, 784–788.

Lundberg, A., Svensson, O.K., Németh, G., and Selvik, G. (1989). The axis of rotation of the ankle joint. J Bone Joint Surg Br *71*, 94–99.

Lutz, G., and Rome, L. (1994). Built for jumping: the design of the frog muscular system. Science *263*, 370–372.

MacDougall, J.D., Webber, C.E., Martin, J., Ormerod, S., Chesley, A., Younglai, E.V., Gordon, C.L., and Blimkie, C.J. (1992). Relationship among running mileage, bone density, and serum testosterone in male runners. J. Appl. Physiol. *73*, 1165–1170.

Maganaris, C.N., Baltzopoulos, V., and Sargeant, A.J. (1998). Changes in Achilles tendon moment arm from rest to maximum isometric plantarflexion: in vivo observations in man. J. Physiol. *510 (Pt 3)*, 977–985.

Maganaris, C.N., Baltzopoulos, V., and Sargeant, A.J. (2000). In vivo measurement-based estimations of the human Achilles tendon moment arm. Eur. J. Appl. Physiol. *83*, 363–369.

Maganaris, C.N., Baltzopoulos, V., and Tsaopoulos, D. (2006). Muscle fibre length-to-moment arm ratios in the human lower limb determined in vivo. J. Biomech. *39*, 1663–1668.

Magerkurth, O., Knupp, M., Ledermann, H., and Hintermann, B. (2006). Evaluation of hindfoot dimensions: a radiological study. Foot Ankle Int *27*, 612–616.

McCullough, M.B.A., Ringleb, S.I., Arai, K., Kitaoka, H.B., and Kaufman, K.R. (2011). Moment Arms of the Ankle Throughout the Range of Motion in Three Planes. Foot Ankle Int. *32*, 300–306.

Mero, A., Kuitunen, S., Harland, M., Kyröläinen, H., and Komi, P.V. (2006). Effects of muscle-tendon length on joint moment and power during sprint starts. J Sports Sci *24*, 165–173.

Mero, A., Luhtanen, P., viitasalo, J., and Komi, P. (1981). Relationships between the maximal running velocity, muscle fiber characteristics, force production and force relaxation of sprinters. Scand. J. Sports Sci. *3*, 16–22.

Miaki, H., Someya, F., and Tachino, K. (1999). A comparison of electrical activity in the triceps surae at maximum isometric contraction with the knee and ankle at various angles. Eur J Appl Physiol Occup Physiol *80*, 185–191.

Morse, C.I., Thom, J.M., Birch, K.M., and Narici, M.V. (2005a). Changes in triceps surae muscle architecture with sarcopenia. Acta Physiol. Scand *183*, 291–298.

Morse, C.I., Thom, J.M., Davis, M.G., Fox, K.R., Birch, K.M., and Narici, M.V. (2004). Reduced plantarflexor specific torque in the elderly is associated with a lower activation capacity. European Journal of Applied Physiology *92*, 219–226.

Morse, C.I., Thom, J.M., Reeves, N.D., Birch, K.M., and Narici, M.V. (2005b). In vivo physiological cross-sectional area and specific force are reduced in the gastrocnemius of elderly men. J. Appl. Physiol. *99*, 1050–1055.

Nagano, A., and Komura, T. (2003). Longer moment arm results in smaller joint moment development, power and work outputs in fast motions. J. Biomech. *36*, 1675–1681.

Narici, M.V., Landoni, L., and Minetti, A.E. (1992). Assessment of human knee extensor muscles stress from in vivo physiological cross-sectional area and strength measurements. Eur J Appl Physiol Occup Physiol *65*, 438–444.

Perry, J. (1992). Gait Analysis: Normal and Pathological Function (Slack Incorporated).

Pieper, H.G. (1998). Humeral torsion in the throwing arm of handball players. Am. J. Sports Med. *26*, 247–253.

Pinniger, G.J., Steele, J.R., Thorstensson, A., and Cresswell, A.G. (2000). Tension regulation during lengthening and shortening actions of the human soleus muscle. Eur. J. Appl. Physiol. *81*, 375–383.

Powell, P.L., Roy, R.R., Kanim, P., Bello, M.A., and Edgerton, V.R. (1984). Predictability of skeletal muscle tension from architectural determinations in guinea pig hindlimbs. J Appl Physiol *57*, 1715–1721.

Raichlen, D.A., Armstrong, H., and Lieberman, D.E. (2011). Calcaneus length determines running economy: implications for endurance running performance in modern humans and Neandertals. J. Hum. Evol. *60*, 299–308.

Reuleaux, F. (1876). The kinematics of machinery: Outlines of a theory of machines (Macmillan).

Riener, R., and Edrich, T. (1999). Identification of passive elastic joint moments in the lower extremities. J Biomech *32*, 539–544.

Roberts, T.J., and Marsh, R.L. (2003). Probing the limits to muscle-powered accelerations: lessons from jumping bullfrogs. Journal of Experimental Biology *206*, 2567 –2580.

Roberts, T.J., Marsh, R.L., Weyand, P.G., and Taylor, C.R. (1997). Muscular force in running turkeys: the economy of minimizing work. Science *275*, 1113–1115.

Rolian, C., Lieberman, D.E., Hamill, J., Scott, J.W., and Werbel, W. (2009). Walking, running and the evolution of short toes in humans. J. Exp. Biol. *212*, 713–721.

Rosager, S., Aagaard, P., Dyhre-Poulsen, P., Neergaard, K., Kjaer, M., and Magnusson, S.P. (2002). Load-displacement properties of the human triceps surae aponeurosis and tendon in runners and non-runners. Scand J Med Sci Sports *12*, 90–98.

Rugg, S.G., Gregor, R.J., Mandelbaum, B.R., and Chiu, L. (1990). In vivo moment arm calculations at the ankle using magnetic resonance imaging (MRI). J. Biomech. *23*, 495–501.

Sacks, R.D., and Roy, R.R. (1982). Architecture of the hind limb muscles of cats: functional significance. J. Morphol *173*, 185–195.

Sadoyama, T., Masuda, T., Miyata, H., and Katsuta, S. (1988). Fibre conduction velocity and fibre composition in human vastus lateralis. Eur. J. Appl. Physiol. Occup. Physiol. *57*, 767–771.

Sale, D., Quinlan, J., Marsh, E., McComas, A.J., and Belanger, A.Y. (1982). Influence of joint position on ankle plantarflexion in humans. J Appl Physiol *52*, 1636–1642.

Schiaffino, S., and Reggiani, C. (1994). Myosin isoforms in mammalian skeletal muscle. J. Appl. Physiol. *77*, 493–501.

Scholz, M.N., Bobbert, M.F., van Soest, A.J., Clark, J.R., and van Heerden, J. (2008). Running biomechanics: shorter heels, better economy. J. Exp. Biol. *211*, 3266–3271.

Schutte, L.M. (1992). Using musculoskeletal models to explore strategies for improving performance in electrical stimulation-induced leg cycle ergometry. Ph.D. Thesis. Stanford University.

Sheehan, F.T. (2010). The instantaneous helical axis of the subtalar and talocrural joints: a non-invasive in vivo dynamic study. J Foot Ankle Res *3*, 13.

Sheehan, F.T. (2012). The 3D in vivo Achilles' tendon moment arm, quantified during active muscle control and compared across sexes. J Biomech *45*, 225–230.

Silder, A., Whittington, B., Heiderscheit, B., and Thelen, D.G. (2007). Identification of passive elastic joint moment-angle relationships in the lower extremity. J Biomech *40*, 2628–2635.

Slawinski, J., Bonnefoy, A., Levêque, J.-M., Ontanon, G., Riquet, A., Dumas, R., and Chèze, L. (2010a). Kinematic and kinetic comparisons of elite and well-trained sprinters during sprint start. J Strength Cond Res *24*, 896–905.

Slawinski, J., Bonnefoy, A., Ontanon, G., Leveque, J.M., Miller, C., Riquet, A., Chèze, L., and Dumas, R. (2010b). Segment-interaction in sprint start: Analysis of 3D angular velocity and kinetic energy in elite sprinters. J. Biomech. *43*, 1494–1502.

Spector, S.A., Gardiner, P.F., Zernicke, R.F., Roy, R.R., and Edgerton, V.R. (1980). Muscle architecture and force-velocity characteristics of cat soleus and medial gastrocnemius: implications for motor control. J. Neurophysiol *44*, 951–960.

Spoor, C.W., van Leeuwen, J.L., Meskers, C.G., Titulaer, A.F., and Huson, A. (1990). Estimation of instantaneous moment arms of lower-leg muscles. J Biomech *23*, 1247–1259.

Storace, A., and Wolf, B. (1979). Functional analysis of the role of the finger tendons. J Biomech *12*, 575–578.

Sugisaki, N., Wakahara, T., Miyamoto, N., Murata, K., Kanehisa, H., Kawakami, Y., and Fukunaga, T. (2010). Influence of muscle anatomical cross-sectional area on the moment arm length of the triceps brachii muscle at the elbow joint. J Biomech *43*, 2844–2847.

Thom, J.M., Morse, C.I., Birch, K.M., and Narici, M.V. (2005). Triceps surae muscle power, volume, and quality in older versus younger healthy men. J. Gerontol. A Biol. Sci. Med. Sci *60*, 1111–1117.

Ward, K.A., Roberts, S.A., Adams, J.E., and Mughal, M.Z. (2005). Bone geometry and density in the skeleton of pre-pubertal gymnasts and school children. Bone *36*, 1012–1018.

Warden, S.J., Bogenschutz, E.D., Smith, H.D., and Gutierrez, A.R. (2009). Throwing induces substantial torsional adaptation within the midshaft humerus of male baseball players. Bone *45*, 931–941.

Wickiewicz, T.L., Roy, R.R., Powell, P.L., and Edgerton, V.R. (1983). Muscle architecture of the human lower limb. Clin. Orthop. Relat. Res 275–283.

Wickiewicz, T.L., Roy, R.R., Powell, P.L., Perrine, J.J., and Edgerton, V.R. (1984). Muscle architecture and force-velocity relationships in humans. J Appl Physiol *57*, 435–443.

Williams, K.R., and Cavanagh, P.R. (1987). Relationship between distance running mechanics, running economy, and performance. J Appl Physiol *63*, 1236–1245.

Williams, P.E., and Goldspink, G. (1973). The effect of immobilization on the longitudinal growth of striated muscle fibres. J. Anat. *116*, 45–55.

Williams, S.B., Tan, H., Usherwood, J.R., and Wilson, A.M. (2009a). Pitch then power: limitations to acceleration in quadrupeds RID E-4960-2010. Biol. Lett. *5*, 610–613.

Williams, S.B., Usherwood, J.R., Jespers, K., Channon, A.J., and Wilson, A.M. (2009b). Exploring the mechanical basis for acceleration: pelvic limb locomotor function during accelerations in racing greyhounds (Canis familiaris). J Exp Biol *212*, 550–565.

Williams, S.B., Wilson, A.M., Daynes, J., Peckham, K., and Payne, R.C. (2008). Functional anatomy and muscle moment arms of the thoracic limb of an elite sprinting athlete: the racing greyhound (Canis familiaris). J. Anat *213*, 373–382.

Wilson, A.M., McGuigan, M.P., Su, A., and van Den Bogert, A.J. (2001). Horses damp the spring in their step. Nature *414*, 895–899.

Winter, D., Patla, A., Frank, J., and Walt, S. (1990). Biomechanical walking pattern changes in the fit and healthy elderly. *70*, 340–347.

Winter, D.A. (1983). Energy generation and absorption at the ankle and knee during fast, natural, and slow cadences. Clin. Orthop. Relat. Res. *175*, 147–154.

Witzmann, F.A., Kim, D.H., and Fitts, R.H. (1983). Effect of hindlimb immobilization on the fatigability of skeletal muscle. Journal of Applied Physiology *54*, 1242 –1248.

Woltring, H.J., Huiskes, R., de Lange, A., and Veldpaus, F.E. (1985). Finite centroid and helical axis estimation from noisy landmark measurements in the study of human joint kinematics. J Biomech *18*, 379–389.

Wu, G., Siegler, S., Allard, P., Kirtley, C., Leardini, A., Rosenbaum, D., Whittle, M., D'Lima, D.D., Cristofolini, L., Witte, H., et al. (2002). ISB recommendation on definitions of joint coordinate systems of various joints for the reporting of human joint motion--part I: ankle, hip, and spine. Journal of Biomechanics *35*, 543–548.

Young, K.C., Sherk, V.D., and Bemben, D.A. (2011). Inter-limb musculoskeletal differences in competitive ten-pin bowlers: A preliminary analysis. J. Musculoskelet. Neuronal Interact. *11*, 21–26.

Zajac, F.E. (1989). Muscle and tendon: properties, models, scaling, and application to biomechanics and motor control. Crit Rev Biomed Eng *17*, 359–411.

Informed Consent Form for Biomedical Research
The Pennsylvania State University

Title of Project:	Ankle structure and human mobility
Principal Investigator:	Stephen J. Piazza, Ph.D.
Address:	Biomechanics Laboratory 29 Recreation Building, University Park, PA 16802
Phone:	814-865-3413
Email:	piazza@psu.edu
Other Investigator(s):	Josh Baxter MS, Huseyin Celik MS, Rebecca Tyrpak, Stephen Jenkins, John Hauber, Brandon Hewitt

1. **Purpose of the study:** The purpose of this research is to understand how the structure and fatigue of the calf muscles and ankle affect mobility and strength in adults.

2. **Procedures to be followed:** You will be asked to perform one or more of the following tasks: a walking test, foot and ankle measurements, ankle strength testing, a series of calf raises that will cause ankle fatigue, measurement of ankle strength, another walking test, and a final measurement of ankle strength. You will be asked to participate in the circled segments below, after reading each segment circled, please initial the corresponding space.

A) Walking Tests - A set of round reflective markers, each about the size of a marble, will be attached to your lower body with skin-safe tape. The location of these markers will be followed using special video cameras as you walk within the lab. On the floor of the gait lab are two force sensitive plates. These force plates record the interaction between the foot and ground. You will be asked to perform a walking test, which is 6 minutes long, twice in this study. You will be asked at a "walk as far as you can" in 6-minutes. A researcher will tell you to stop when the 6 minutes are over. After the 6-minutes of walking, you may be asked to perform several walking trials of approximately 10-30 feet in length. _____

B) Foot and Ankle Measurements: A ruler will be used to make a series of measurements will be made of your leg, foot, and ankle. Digital photographs will be taken of your lower leg and foot. _____

C) Ankle Strength Test: You will be asked to contract your calf muscles as hard as you can, like you are pushing on a gas pedal, while your ankle is rotated through a series of rotations. You will sit upright, with your knee extended and your thigh supported, in a strength testing device that will rotate your ankle through a safe range of motion while measuring the strength of your calf muscles. First we will have you contract your calf muscles at a moderate effort while your ankle moves through a range of motion. Next we will slowly rotate your ankle, causing your toes to point towards you until you feel slight

discomfort. During the study, your ankle will never go past that position. Then we will ask you to relax or contract your calf muscles while the machine you are seated in slowly rotates your ankle. A computer display will give you feedback as to how hard you are pushing against the footplate and you will be asked to match a given value on the screen. Next, you will perform a series of trials in which we will ask you to contract your calf muscles while the foot platform either stays motionless or rotates your ankle at varying speeds. After each speed, you will be given time to rest.

During these tests of ankle strength, we will take images of your lower leg with an ultrasound probe. The ultrasound probe takes images of the tissues beneath the skin and does not damage any tissues. To do this we will apply a water-based gel that allows a clear image to be recorded by the probe. To prevent the probe from moving during these tests, we will use skin-safe tape to secure the probe to your leg. _____

D) Fatigue Test: Next, you will perform a single series of calf muscle contractions with both feet until you are only able of pushing against the foot plate with a fraction of your maximal strength. Immediately following this series of calf contractions, you will be asked to perform the second, and final, 6-minute walking test. _____

3. **Discomforts and risks:** There are only minimal risks associated with this study. During a muscle contraction it is possible that you may experience a muscle cramp or injury. You will be given time to rest between each contraction and water will be available for the duration of the study. Mild muscle soreness may result from the ankle fatigue protocol that may last for several days.

4. **Benefits:** There is no direct benefit to you for participating in this research. There is an indirect benefit of contributing to the research in the fields of biomechanics and rehabilitation. The results of this study will contribute to a better understanding of how foot and ankle structure affects movement in groups of people who are.

5. **Duration/time of the procedures and study:** Your visit to The Biomechanics Lab will last approximately 1.5-2 hours.

6. **Alternative procedures that could be utilized:** The procedures used in this study were designed to obtain the highly reliable and accurate images of the calf muscles and Achilles tendon. Other forms of muscle imaging are available, but they offer no safety benefit and cannot be implemented alongside strength testing. There are no other means of testing your ankle strength while controlling the speed of ankle rotation. You may choose not to participate in this research.

7. **Statement of confidentiality:** Any data collected in this experiment will remain confidential. The data will be located within a file cabinet in a part of The Biomechanics Lab that has limited access and will remain under the supervision of Dr. Stephen Piazza.

   Any identifiers, such as your name or personal information, will be kept separate from the actual data. All data will be destroyed within 3 years following the completion of the study.

You will be provided with a private changing area and a locker to store any of your possessions. The tests will take place in the Biomechanics Lab which is secured and off limits to the public.

All records associated with your participation in the study will be subject to the usual confidentiality standards applicable to medical records (e.g., such as records maintained by physicians, hospitals, etc.). In the event of any publication resulting from the research, no personally identifiable information will be disclosed.

The Office of Human Research Protections in the U.S. Department of Health and Human Services, the U.S. Food and Drug Administration (FDA), the Office for Research Protections at Penn State and the Institutional Review Board may review records related to this project.

8. **Right to ask questions:** You can ask questions about this research. Please contact Dr. Stephen Piazza at (814) 865-3413 with questions. You can also call this number if you have complaints or concerns about the research. If you have any questions, concerns, problems about your rights as a research participant or would like to offer input, please contact The Pennsylvania State University's Office for Research Protections (ORP) at (814) 865-1775. The ORP cannot answer questions about research procedures. Questions about research procedures can be answered by the research team.

9. **Permission for future use of records:** May the researchers make and retain your video and photo records for future use, education, or presentation? No identifiable markings on any of the images will be present. (Please circle two choices)

    1. I agree that segments of the recordings made of my participation in this research may be used for conference presentations.

    2. I do not want segments of the recordings made of my participation in this research to be used for conference presentations. Recordings will be destroyed by 2017

    3. I agree that segments of the recordings made of my participation in this research may be used for education and training of future researchers/practitioners.

    4. I do not want segments of the recordings made of my participation in this research to be used for education and training of future researchers/practitioners. Recordings will be destroyed by 2017

10. **Payment for participation:** You will receive no payment for participation in this portion of the study.

11. **Voluntary participation:** Your decision to be in this research is voluntary. You can stop at any time. You do not have to answer any questions you do not want to answer. Refusal

to take part in or withdrawing from this study will involve no penalty or loss of benefits you would receive otherwise.

12. **Injury Clause:** In the unlikely event you become injured as a result of your participation in this study, medical care is available. It is the policy of this institution to provide neither financial compensation nor free medical treatment for research-related injury. By signing this document, you are not waiving any rights that you have against The Pennsylvania State University for injury resulting from negligence of the University or its investigators.

13. **Abnormal Test Results:** In the event that abnormal test results are obtained, you will be made aware of the results in 3 days and recommended to contact your private medical provider for follow-up.

You must be 18 years of age or older to take part in this research study. If you agree to take part in this research study and the information outlined above, please sign your name and indicate the date below.

You will be given a copy of this signed and dated consent form for your records.

_____ _____

Participant Signature Date

_____ _____

Person Obtaining Consent Date

Informed Consent Form for Biomedical Research
The Pennsylvania State University

Title of Project:	Ankle structure and human mobility
Principal Investigator:	Stephen J. Piazza, Ph.D.
Address:	Biomechanics Laboratory 29 Recreation Building, University Park, PA 16802
Phone:	814-865-3413
Email:	piazza@psu.edu
Other Investigator(s):	Josh Baxter MS, Thomas Novack, David Pennell MS, Huseyin Celik MS

1. **Purpose of the study:** The purpose of this research is to understand how the structure of the ankle and foot affect the ability to walk and run.

   If you agree to participate in the study, magnetic resonance imaging (MRI) scans will be taken. The MRI scans will assist us in understanding the structure and function of different parts of the body. There are two types of scans that may be done. Anatomy scans are used to determine the structure of the body. Scans of function are used to determine areas of activity when you perform different tasks.

   NONE of the scans done during this study are designed to detect or evaluate any medical condition you may have. They are intended solely for research purposes.

2. **Procedures to be followed:** To date, 150 million patients have undergone MRI examinations around the world. We will be following standard MRI procedures and safety guidelines. MRI has been shown to be extremely safe as long as proper safety precautions are taken. MRI uses strong magnetic fields and radio waves to make pictures of the body. There is no exposure to x-rays or radioactivity during an MRI scan. Levels of energy used are within FDA safety limits. This study will use a 3.0 Tesla MRI scanner.

   You will be asked to leave metal objects and personal belongings in lockers provided in the prep room of the MRI center. You will also be asked to remove any articles of clothing with metal inserts or clasps before entering the MRI room. Please ask the experimenter if you are unsure about any items.

   You will be asked to lie on a bed that slides into the long tube of the scanner. You will be given earphones and/or earplugs for hearing protection since the MRI scanner makes loud noises during normal operation. You will be asked to remain very still at these times. You will be able to talk to the MRI technologist by an intercom, and he/she will be able to see you and hear you at all times. You will also be given a squeeze-ball signaling device. If at any time you would like to discontinue the study, you can tell the investigators over the intercom or press the squeeze-ball signaling device and you will be removed immediately from the scanner. You can discontinue the study at any time without penalty.

This study consists of a series MRI scans of your leg and foot. Two small adhesive gel-caps will be placed on your foot and lower leg. These gel-caps will help with orientating the scanning equipment. You will then be asked to lay on a bed with your knees slightly bent and supported by a foam block. Your right foot will be strapped to an apparatus and you will have handles to grasp which will prevent your foot and body from moving, respectively. During the scans, your right foot will be placed in three positions; slightly pointed toward the body, slightly pointed away from the body, and neutrally positioned. In the first two positions several scans will be taken: a short series of scans will be used to orientate the scanning equipment, one scan with the foot relaxed and another scan with the foot undergoing a maximal toe-pointing of 4 seconds, much like pressing down on a gas pedal. These scans will only last a few seconds to help ensure a maximal effort is possible. When your foot is in the third position several more scans will be taken; the short series of orientating scans and the two scans previously described for the other positions, one scan of the entire foot and one scan of the lower leg during which you will asked to relax and remain motionless. These last two scans will last between 1-3 minutes each. If your foot moves during a scan we will reattempt the scan.

3. **Discomforts and risks of the MRI:** Risk of injury is very low during an MRI scan. However, MRI is not safe for everyone. It may not be safe for you to have an MRI scan if you have any metal containing iron in or on your body. This is because metal containing iron can pose a safety risk when in the presence of strong magnetic fields. Radiowaves may also heat the body and metallic objects within or on the body, possibly resulting in burns. Before you are allowed in the scanner room, you will be asked a set of questions to determine if it is safe for you to have an MRI scan at this time. For example, it may not be safe to have an MRI scan if you have a cardiac pacemaker, aneurysm clips, an intrauterine device (IUD), etc. For your safety, it is very important that you answer all questions truthfully.

   It is possible that you may feel uncomfortable or confined once inside the scanner. This feeling usually passes within a few minutes as the experimenters talk with you and the study begins. You might experience dizziness, mild nausea, or tiny flashing lights in your field of vision. These sensations are mostly due to movement while inside the magnet and can be minimized by holding still. All of these sensations should stop shortly after you leave the magnet.

4. **Other discomforts and risks:** You may experience some skin irritation due to the foot straps or adhesive gel-caps used during the scans. These are both necessary to make sure accurate scans are made. You may also experience some muscle soreness resulting from the maximal muscle efforts you will perform during the study. As with any maximal muscle effort there is a possibility of injury to the muscle.

5. **Benefits:** There are no benefits to you for participating in this study.

   The benefits to society include an increased understanding of how the structure of the ankle joint affects mobility.

6. **Duration/time of the procedures and study:** A number of MRI scans will be performed with the entire procedure lasting up to 45 minutes. You will be asked to lie still for up to 10 minutes at a time.

The time you will spend participating in this research will take not longer than 1 hour. This time includes all necessary paperwork, measurements, and MRI scans.

7. **Alternative procedures that could be utilized:** Ultrasound scans and external measurements have been used to measure important aspects of ankle joint structure; however, these results may not be as accurate as MRI scans.

8. **Statement of confidentiality:** Your participation in this research is confidential. All possible steps have been taken to assure your privacy. For the MRI, you will be assigned a code number that will be used throughout the scan. Only this code (and never your name) will be used when analyzing or reporting the data. Any identifying information will be kept in a locked location and password protected electronic files located on computers in Chandlee lab as well as the Biomechanics Lab in Rec Hall. All study data on the Kinesiology network will be deleted following the conclusion of the study. Confidential data will be destroyed 3 years after the conclusion of the study.

   The Pennsylvania State University's Office for Research Protections, the Institutional Review Board, and the Office for Human Research Protections in the Department of Health and Human Services may review records related to this research study.

   In the event of any publication or presentation resulting from the research, no personally identifiable information will be shared. The results of the research, including but not limited to your images, may be published and presented at lectures and professional meetings, but you will not be identified in any such publication or presentation.

   After the scans are made, your data will be paired with a code number and will be stored in secure cabinets and computers which only the investigators of this study have access to. During the analysis and presentation of your data, no identifying information will be present.

   The MRI scans will take place in a secure facility where only authorized individuals are allowed to enter. The facility has secure lockers and a private area to change clothes if needed and secure possessions during the scans.

9. **Right to ask questions:** You can ask questions about this research. Please contact Dr. Stephen Piazza at (814) 865-3413 with questions. You can also call this number if you have complaints or concerns about the research. If you have any questions, concerns, problems about your rights as a research participant or would like to offer input, please contact The Pennsylvania State University's Office for Research Protections (ORP) at (814) 865-1775. The ORP cannot answer questions about research procedures. Questions about research procedures can be answered by the research team.

10. **Permission for future use of records:** May the researcher make and retain your video and photo records for future use, education, or presentation? No identifiable markings on any of the images will be present. (Please circle two choices)

    1. I agree that segments of the recordings made of my participation in this research may be used for conference presentations.

2. I do not want segments of the recordings made of my participation in this research to be used for conference presentations. Recordings will be destroyed by 2017

3. I agree that segments of the recordings made of my participation in this research may be used for education and training of future researchers/practitioners.

4. I do not want segments of the recordings made of my participation in this research to be used for education and training of future researchers/practitioners. Recordings will be destroyed by 2017

11. **Payment for participation:** You will receive $15 for participation in this portion of the study. If you withdraw from the study before completion you will be compensated for the time you participated to the ½ hour (i.e., ½ hour = $7.50).

12. **Voluntary participation:** Your decision to be in this research is voluntary. You can stop at any time. In order to participate you must answer all Participant Safety and Screening questions accurately; however, you do not have to answer any other questions that you do not want to answer. Refusal to take part in or withdrawing from this study will involve no penalty or loss of benefits you would otherwise receive.

13. **Injury Clause:** In the unlikely event you become injured as a result of your participation in this study, medical care is available. It is the policy of this institution to provide neither financial compensation nor free medical treatment for research-related injury. By signing this document, you are not waiving any rights that you have against The Pennsylvania State University for injury resulting from negligence of the University or its investigators.

14. **Incidental findings:** The investigators for this project are not trained to perform medical diagnosis, and the scans to be performed in the study are not optimized to find abnormalities. On occasion, a member of the research team may notice a finding on a scan that seems abnormal. When a finding is noticed, the investigator or designate may consult a physician specialist, such as a radiologist or neurologist, as to whether the finding merits further investigation. If the specialist recommends further follow-up, the investigator or another designate will contact you within **48 hours** of the recommendation and suggest that you contact your private medical provider for follow-up. To facilitate follow-up care, you may be given a copy of your images upon written request. Being told about a finding may cause anxiety as well as suggest the need for additional tests and financial costs. Medical insurance may be affected whether or not the finding is ultimately proved to be of clinical significance. Costs for clinical follow-up are not budgeted in the cost of research. The decision as to whether to proceed with further examination or treatment lies with you.

15. **Abnormal test results:**

    In the event that abnormal test results are obtained, you will be made aware of the results in ***3*** days and recommended to contact your private medical provider for follow-up.

    Please provide contact information so that you can be reached in the event of an incidental finding and/or abnormal test results.

Address_____

Phone_____

By consenting to participate, you agree to:

- Answer the SLEIC 3T MRI Participant Safety & Screening questions accurately,
- Tell the investigators about all metallic devices in/on your body, and
- Not bring any metal devices (e.g., pens, coins, keys, credit cards) into the scanning room without staff approval.

You must be 18 years of age or older to take part in this research study. If you agree to take part in this research study and the information outlined above, please sign your name and indicate the date below.

You will be given a copy of this signed and dated consent form for your records.

_____	_____	
Participant Signature	Printed Name	Date
_____	_____	
Person Obtaining Consent	Printed Name	Date

Curriculum Vitae

Josh R. Baxter

Education

2012 The Pennsylvania State University, University Park, PA
PhD, Kinesiology, Concentration - Biomechanics
Thesis Topic: 'Linking foot and ankle musculoskeletal structure to locomotor function'
Advisor: Stephen Piazza, Ph.D.

2009 Oregon State University, Corvallis, OR
MS, Exercise and Sport Science, Concentration - Biomechanics
Thesis Topic: 'The effects of voluntary step-training on slip recovery'
Advisor: Michael Pavol, Ph.D.

2007 Central Washington University, Ellensburg, WA
BS, Exercise Science
Minor, Mathematics

Professional Experience

2010-present The Pennsylvania State University, University Park, PA
Graduate Research Assistant
Department of Kinesiology, Biomechanics Laboratory

2007-2009 Oregon State University, Corvallis, OR
Graduate Research Assistant
Department of Nutrition and Exercise Sciences, Biomechanics Laboratory

Refereed Articles

Baxter JR, Novack TA, Van Werkhoven H, Pennell D, and Piazza SJ (2011) Ankle joint mechanics and foot proportions differ between human sprinters and non-sprinters. Proceedings of the Royal Society B, epub ahead of print

Media Mentions

Print Media

"Kings of the track share traits with speedy cats", *The New York Times*, 12/27/2011

Television & Radio

"Quirks and Quarks", *CBC Radio*, 2/4/2012